

Deconstruction of Polymers through Olefin Metathesis

Published as part of Chemical Reviews virtual special issue "The Future of Plastics Sustainability".

Devavrat Sathe, Seiyoung Yoon, Zeyu Wang, Hanlin Chen, and Junpeng Wang*



Cite This: <https://doi.org/10.1021/acs.chemrev.3c00748>



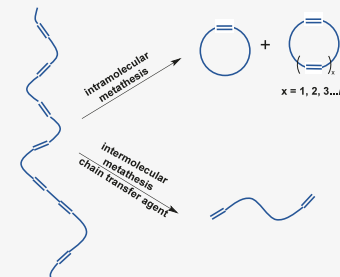
[Read Online](#)

ACCESS |

Metrics & More

Article Recommendations

ABSTRACT: The consumption of synthetic polymers has ballooned; so has the amount of post-consumer waste generated. The current polymer economy, however, is largely linear with most of the post-consumer waste being either landfilled or incinerated. The lack of recycling, together with the sizable carbon footprint of the polymer industry, has led to major negative environmental impacts. Over the past few years, chemical recycling technologies have gained significant traction as a possible technological route to tackle these challenges. In this regard, olefin metathesis, with its versatility and ease of operation, has emerged as an attractive tool. Here, we discuss the developments in olefin-metathesis-based chemical recycling technologies, including the development of new materials and the application of olefin metathesis to the recycling of commercial materials. We delve into structure–reactivity relationships in the context of polymerization–depolymerization behavior, how experimental conditions influence deconstruction outcomes, and the reaction pathways underlying these approaches. We also look at the current hurdles in adopting these technologies and relevant future directions for the field.



CONTENTS

1. Introduction
2. Olefin-Metathesis-Based Depolymerizable Polymers
 - 2.1. General Mechanisms of Olefin Metathesis
 - 2.2. Thermodynamics of Ring-Opening Metathesis Polymerization
 - 2.3. Depolymerizable ROMP Polymers
 - 2.3.1. Cyclopentene
 - 2.3.2. Cycloheptene
 - 2.3.3. Cyclooctene
 - 2.3.4. Bridged Bicyclic Olefins
 - 2.4. Depolymerizable Polymers via Cascade Metathesis Reactions
 - 2.5. Other Olefin-Metathesis Based Chemically Recyclable Polymers
3. Metathesis-Based Degradation of Commercial Polymers
 - 3.1. Metathesis-Based Degradation of Polyolefins
 - 3.2. Metathesis-Based Degradation of Other Commercial Polymers
4. Effects of Experimental Conditions on Metathesis-Based Deconstruction
 - 4.1. Effects of Experimental Conditions on RCM-Based Depolymerization/Degradation
 - 4.1.1. Concentration Effects
 - 4.1.2. Temperature Effects

	4.1.3. Effects of Catalysts and Catalyst Loading	Y
B	4.2. Effects of Experimental Conditions on Cross-Metathesis-Based Degradation	Z
D	4.2.1. Concentration Effects	Z
D	4.2.2. Effects of Catalysts and Catalyst Loading	Z
E	4.2.3. Effects of Chain-Transfer Agents and Their Loading	ZA
G	4.2.4. Influence of Metathesis Catalyst on Tandem Dehydrogenation and Olefin	AA
K	Cross-Metathesis Degradation	AB
L	4.2.5. Influence of Short-Length Alkane on Tandem Dehydrogenation and Olefin	AB
Q	Cross-Metathesis Degradation	AB
S	4.2.6. Influence of Dehydrogenation Catalyst on Tandem Dehydrogenation and Olefin	AB
S	Cross-Metathesis Degradation	AB
U	5. Mechanisms of Olefin-Metathesis-Based Deconstruction	AC
U	5.1. Fragmentation Degradation	AC
X	5.1.1. Alkenolysis	AC

Received: October 12, 2023

Revised: May 10, 2024

Accepted: May 14, 2024

5.1.2. Alkane Metathesis	AD
5.2. Fragmentation Followed by Continuous Depolymerization	AD
5.3. End-to-End Continuous Depolymerization	AE
6. Conclusion and Outlook	AF
Author Information	AG
Corresponding Author	AG
Authors	AG
Notes	AG
Biographies	AG
Acknowledgments	AG
Abbreviations	AG
References	AH

1. INTRODUCTION

The present status of the linear plastics economy has major implications for the fate of post-consumer waste. According to recent statistics (Organization for Economic Co-operation and Development or OECD, 2019),¹ 68% of post-consumer plastic waste was either landfilled or incinerated, and 22% was mismanaged and escaped into the environment; only 9% of the plastic waste was recycled. These facts, together with the consistent growth in plastic waste generation (which almost doubled from ~156 million tonnes in 2000 to ~353 million tonnes in 2019), make improved approaches to plastic waste management desirable and urgent (Figure 1a). From a technological standpoint, one of the routes toward reducing the amount of plastic waste is the development of better approaches for its utilization (Figure 1b). At present, the majority of recycled plastic waste is recycled via mechanical methods (i.e., melt reprocessing).² However, this approach has significant drawbacks. First and foremost, mechanical recycling is typically applicable only to thermoplastics. Also, it requires expensive sorting and cleaning operations since plastic waste often consists of mixtures of different plastics, which cannot be processed together. Finally, when subjected to multiple reprocessing cycles, recycled polymers suffer from loss in material properties due to the mechanical degradation that causes molecular weight reduction.³ An alternative is chemical recycling, which can be realized in the form of two distinct processes: chemical recycling to monomers and chemical recycling to other small molecules. Chemical recycling has the potential to enable a circular economy and overcome some of the challenges associated with mechanical recycling. Conversion of polymers back to pristine monomers could enable manufacturing of high-quality polymer materials, essentially converting post-consumer waste to high-quality monomer feedstock. At the same time, other chemical recycling approaches can open avenues toward the conversion of cheap polymer waste into high-value small molecules for applications beyond the polymer industry.

The realization of the imperativeness of a circular polymer economy has brought with it a steadily increasing interest in chemical recycling within the polymer research community. Progress has come in the form of both new methods for the chemical recycling of commercial polymers as well as the development of new chemically recyclable polymers. Within commercial polymers, much of the attention has been on depolymerization of polyesters via transesterification,³ conversion of polyolefins into small molecules via dehydrogenation and degradation methods, functionalization strategies to convert polyolefin wastes into value-added materials,^{4–8} and

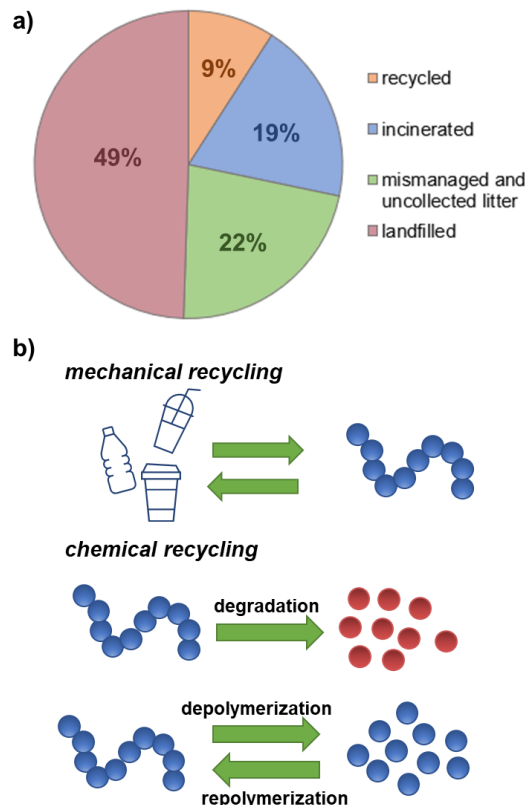


Figure 1. Polymer economy and approaches to close the loop of the polymer economy. a) A chart showing the fate of post-consumer plastic waste (using the data from ref 1). b) Approaches to post-consumer waste utilization including mechanical recycling and chemical recycling; the latter includes degradation to small molecule building block and depolymerization to monomer.

approaches for selective degradation of other vinyl polymers into monomers and other small molecules.^{5,9–15}

As far as newly developed chemically recyclable polymers are concerned, these approaches have involved both step-growth and chain-growth, and the latter has largely focused on ring-opening polymerizations (ROPs).^{16,17} The ROP approach is particularly useful for the design of depolymerizable polymers since the thermodynamics of polymerization can be readily tuned via the size of the cyclic monomers and the functional groups on them.¹⁸ Both approaches have utilized a gamut of chemistries, forming various polymers including polyesters,^{19–21} polythioesters,^{22–24} polyacetals,^{25,26} polysulfides,²⁷ and polyalkenamers,^{28–30} to name a few.

Chemistries based on olefin metathesis stand out, having certain key advantages. For one, olefin metathesis allows the preparation of polymers with all-hydrocarbon backbones that are unsusceptible to hydrolytic degradation. Further, olefin metathesis can be performed under mild conditions in the presence of appropriate metathesis catalysts while being kinetically unfavorable in the absence of a catalyst.³¹ As a result, undesirable metathesis reactions and depolymerization at elevated temperatures can be avoided, provided that the catalyst is removed judiciously. Olefin metathesis catalysts are also often compatible with a wide variety of functional groups, enabling the synthesis of polymers with diverse properties. Figure 2 shows some important metathesis catalysts used in the studies discussed in this review (for discussions on the

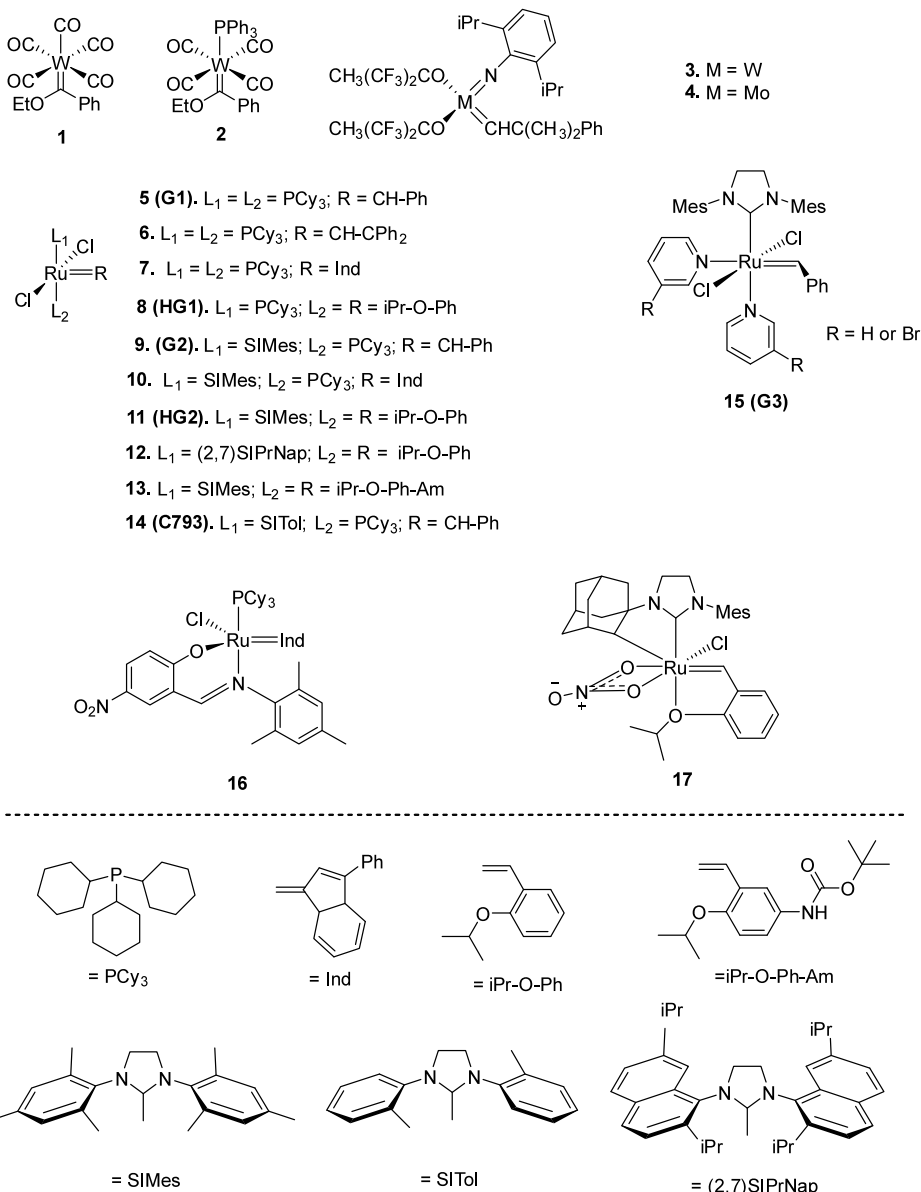


Figure 2. Olefin metathesis catalysts used for the metathesis reactions discussed in this review.

evolution of olefin metathesis catalysts and structures of some common metathesis catalysts, see refs 31, 32). Finally, a number of important commercially available polymers consist of olefinic backbones, including neoprene, polyisoprene, and polybutadiene. As a result, metathesis chemistry has also been explored as an avenue for the chemical recycling of these commercially important synthetic polymers.

This review aims to cover important advances in the utilization of olefin metathesis in the chemical recycling of polymers. The **second section** discusses the development of new polymers that have been designed to undergo depolymerization or degradation via the metathesis processes. The **third section** discusses the application of olefin metathesis to the degradation of commercially relevant polymers. The **final two sections** delve deeper into the effects of experimental conditions (temperature, concentration, pressure, catalysts, and chain transfer agents) and depolymerization mechanisms in the aforementioned studies.

Before beginning the next sections, we must note the following. In this review, we adopt the recommended IUPAC definition for depolymerization: “the process of converting a polymer into a monomer or a mixture of monomers”.³³ All other metathesis-based fragmentation of polymers is termed degradation (both falling within the scope of chemical recycling). While depolymerization has been used in some literature to mean fragmentation to monomer, oligomers, and other small molecules, we stay with the standard definition for clarity purpose. Note that this review is distinct from an important earlier review by Gianneschi and co-workers.³⁴ In their review, the authors delve into olefin-metathesis-based polymers that can be degraded via different stimuli. On the other hand, the present review focuses on deconstruction of polymers (both commercial and newly designed) by olefin metathesis chemistry, irrespective of the chemistry used to synthesize the polymers.

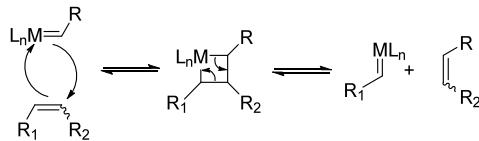
2. OLEFIN-METATHESIS-BASED DEPOLYMERIZABLE POLYMERS

The depolymerization and degradation of polymers via olefin metathesis involve a combination of cross-metathesis (CM) and ring-closing metathesis (RCM) reactions. Before embarking on an exploration of the different newly developed metathesis-based depolymerizable and degradable polymers in the literature, we discuss the thermodynamics involved in these processes as well as the mechanisms involved in metathesis reactions.

2.1. General Mechanisms of Olefin Metathesis

To advance metathesis-based technologies for the chemical recycling of polymers and for developing new chemically recyclable polymers, it is important to understand the mechanism through which polymers are metathetically synthesized and deconstructed. A typical olefin metathesis reaction involves the exchange of substituents between different olefins—a transalkylideneation process, resembling the transesterification process during deconstruction of polyesters.^{35,36} Hérisson and Chauvin proposed the generally accepted mechanism of transition metal olefin metathesis reactions,³⁷ which involves a series of [2+2] cycloaddition/cycloreversion reactions (Scheme 1). A metallacyclobutane

Scheme 1. Chauvin Mechanism of Olefin Metathesis



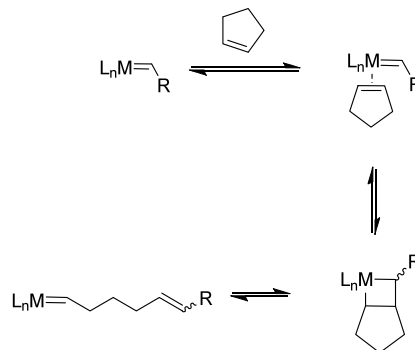
intermediate is first generated from the [2+2] cycloaddition between an olefin and a metathesis catalyst, i.e., a transition metal alkylidene. The metallacyclobutane can then undergo cycloreversion to give a new olefin and a metal alkylidene. It should be noted that all steps are reversible.

Olefin metathesis includes cross-metathesis (CM), ring-closing metathesis (RCM), ring-opening metathesis polymerization (ROMP), and acyclic diene metathesis (ADMET). Taking advantage of the excellent functional group tolerance, ROMP (chain-growth) and ADMET (step-growth) have been widely implemented as powerful tools for polymer syntheses. The main types of olefin metathesis reactions that are involved in olefin metathesis depolymerization are CM (where the intermolecular transalkylideneation of two different olefins generates two new olefins) and RCM (where dienes react intramolecularly to produce cyclic olefins).

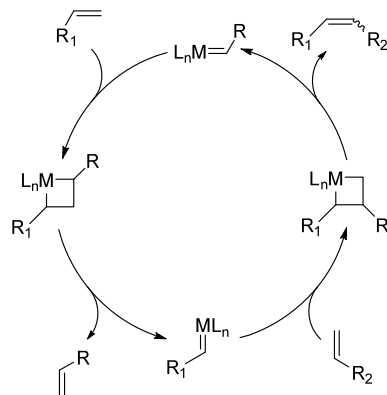
The ROMP reaction is typically initiated by the insertion of the cyclic olefin into the metal–alkylidene bond to form a metallacyclobutane, which undergoes reversible ring-opening to form a new alkylidene propagating chain end.³⁸ Further propagation occurs by similar ring opening events via a cross-metathesis-type reaction with the cyclic olefin monomer (Scheme 2). The reaction is driven in the forward direction as a result of the thermodynamic favorability of the ring-opened state (discussed further in this section).

A productive CM reaction typically involves the transalkylideneation of two terminal olefins to generate an internal olefin with the release of volatile ethylene (Scheme 3).³⁹ In the context of metathesis-based polymer deconstruction, CM occurs between internal olefins (e.g., those in the unsaturated polymer backbone) and terminal olefins (small molecules or

Scheme 2. Monomer Insertion during ROMP



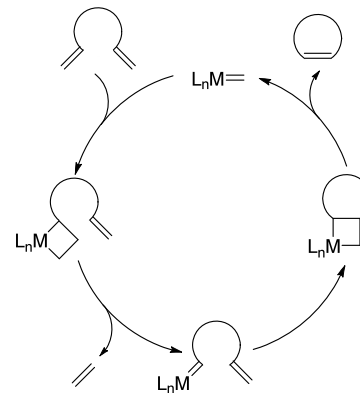
Scheme 3. Catalytic Cycle of a Cross-Metathesis Reaction



polymer chain end) and causes chain scission and scrambling of the molecular weight distribution. Polymerization via ADMET typically involves similar cross-metathesis events, where propagation involves cross-metathesis between terminal alkenes along with the expulsion of an ethylene molecule.

RCM is widely used in organic chemistry to synthesize cyclic olefins via the intramolecular metathesis of terminal dienes, driven by the formation of volatile ethylene (Scheme 4). In the

Scheme 4. Catalytic Cycle of a Ring-Closing Metathesis Reaction



context of depolymerization, the RCM involves the intramolecular transalkylideneation of a terminal olefin (e.g., the polymer chain end) and a neighboring internal olefin to generate cyclic olefins and new polymer chains. This process is favored entropically, forming nonstrained cyclic products, i.e., nonstrained macrocycles and/or 5–7-membered cyclic olefins

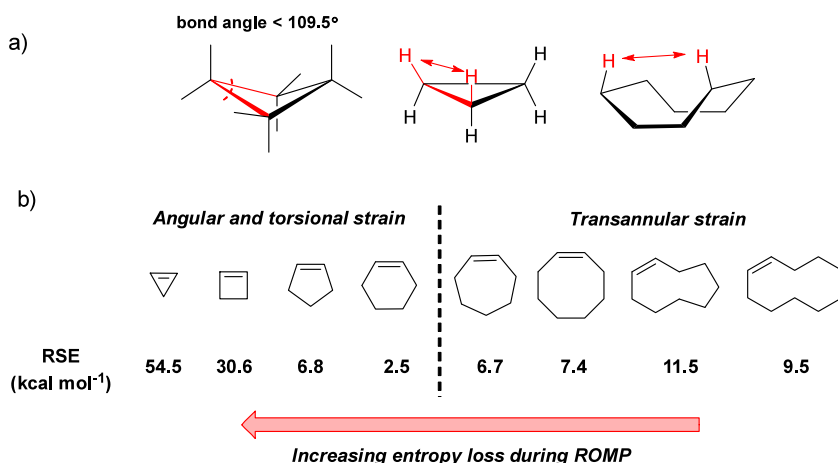


Figure 3. Ring strain in cyclic compounds. a) Components of ring strain in simple cycloalkanes. From left to right: angle strain in cyclobutane due to distorted bond angles $<109.5^\circ$ (dashed curve indicates the angle), torsional strain due to the interactions between eclipsed hydrogen atoms in cyclopropane, transannular strain due to proximity between nonadjacent hydrogen atoms in the boat-conformation. b) Ring strain energies (RSEs) of cycloalkenes of different sizes. RSEs were obtained from ref 44. RSE for *cis*-cyclododecene was calculated using the enthalpy of formation obtained in ref 45 and Schleyer's single conformer group increment method described in ref 44.

(the latter of which can be small molecules or the original monomers), depending on the concentration of the reaction.

2.2. Thermodynamics of Ring-Opening Metathesis Polymerization

The present section discusses the thermodynamics of ROMP and its relation to monomer size/geometry. Understanding this is crucial to comprehending the effects of polymer structure and reaction conditions on the depolymerization and degradation behaviors. Ultimately, the nature of the depolymerization products formed, whether monomers or other cyclic and linear olefins, depends on the relative stability of these species. A significant portion of our discussion in this section will deal with metathesis-based depolymerization to monomers or cyclic oligomers. Here, the reversibility of polymerization can be understood in terms of the free energy change, which is in turn related to the enthalpy and entropy⁴⁰ change of polymerization given by the following expression:⁴⁰

$$\Delta G_p = \Delta G_p^0 - T \Delta S_p$$

For depolymerization to be feasible, the enthalpy change of polymerization must be small enough and/or the entropy loss large enough so that the reaction is reversible under practical conditions. In the context of ring-opening polymerizations in general, the enthalpy change of polymerization arises primarily from the release of ring strain as a cyclic monomer is opened up and incorporated into the polymer chain as a linear repeat unit. The entropy of polymerization is understood to have contributions from multiple degrees of freedom including translational, rotational, and vibrational entropy.⁴¹ Typically, a loss of translational entropy is expected as the monomer unit is incorporated into the polymer chain while a gain of rotational entropy is expected as the bonds in the polymer repeat units have more degrees of rotational freedom compared to the cyclic monomer (in a typical polymerization, ΔS_p is dominated by the loss of translational entropy, thus being negative).^{40,42}

In practical terms, thermodynamics can be leveraged for depolymerization via control of the temperature and concentration. In most cases where $\Delta H_p < 0$ and $\Delta S_p < 0$, there will be a temperature above which $\Delta G > 0$ and polymerization is not feasible. This temperature is called the

ceiling temperature (T_c). T_c relates to the enthalpy, entropy change, and monomer concentration ($[M]$) as follows:

$$T_c = \frac{\Delta H_p}{\Delta S_p} = \frac{\Delta G_p^0}{\Delta S_p^0 + RT \ln[M]}$$

The above discussion, for the sake of simplicity, considers the monomer and growing polymer chains as the only two types of species involved in the reversible polymerization reaction. However, in the presence of a metathesis catalyst, the system would exist in a ring–chain equilibrium with cyclic and linear chains of different sizes. The distribution of these species is governed by the factors discussed above, such as the ring strain (enthalpic) and concentration (entropic).

Grubbs and Kornfield have developed theoretical models to predict the concentration of cyclic and linear species during equilibrium polymerization of 4-, 6-, 8- and 12-carbon cyclic olefins.⁴³ To obtain free energies of the reversible cyclization reactions, entropic contributions were derived from the Jacobson–Stockmayer theory, while enthalpic terms were derived in the form of ring strain calculated by molecular mechanics methods. It was found that for the 4-, 8- and 12-carbon monomers, there were practically no monomers present as part of the ring–chain equilibrium, but higher cyclic oligomers were abundant; in fact, in the case of cyclobutene, even the dimer was only present in trace amounts. For cyclohexene, on the other hand, the monomer was the most abundant species, reflecting the difficulty in polymerizing cyclohexene due to its low ring strain. Further, they determined that the concentration of cyclic species increases with initial monomer concentration, reaching a maximum limiting value defined as the critical monomer concentration—any excess amount of monomer exclusively contributes to the formation of linear species.

Clearly, the ring size of cyclic olefins has a major impact on the reversibility of ring-opening metathesis polymerization (ROMP) and on the distribution of products in the ring–chain equilibrium. For cyclic olefins below a certain size (≤ 12 member rings), the enthalpic contribution in the form of ring strain is especially important (Figure 3).⁴² For high-strain olefins such as cyclopropene and cyclobutene, depolymeriza-

Table 1. Thermodynamics Parameters for Different Cyclopentene Analogues

Monomer	Monomer Structure	ΔH_p (kcal mol ⁻¹)	ΔS_p (cal mol ⁻¹ K ⁻¹)	T_c @ 1 M (°C)	Reference
M1		-4.4	-14.9	22	53
M1		-5.6	-18.9	23	57
M1		-4.5	-14.5	35	60
M4^a		-4.5	-18.4	-30	60
M5		-3.8	-15.0	-15	60
M6		-3.2	-9.8	49	60
M7		-5.2	-17.2	31	60
M8		-3.8	-14.7	-14	60
M9		-3.6	-15.0	-35	60
M10		-3.9	-15.9	-25	60
M11		-4.8	-18.7	-15	60
M14		-3.0	-11.9	-20	63
M15		-5.1	-19.2	-8	63
M16		-1.6	-7.2	-45	63
M18		-5.0	-19.4	-15	29

^aThe slope and intercept for the van 't Hoff plot of entry 10 in ref 60 are incorrect; the values here were obtained by replotted the raw $\ln[M]_e$ vs $1/T$ data from the SI of ref 60.

tion of polymers to monomers is unfavorable, with larger cyclic oligomers being formed at sufficiently low monomer concentrations. Five- and six-carbon cycloolefins are fairly

low in strain (with cyclohexene being nearly strainless and being nonpolymerizable).^{42,46} Cyclopentene, in particular, strikes a balance between its enthalpy and entropy of

polymerization such that under certain conditions (elevated temperature and/or low concentration), polypentenamer can be depolymerized into monomer quantitatively. In these smaller cycloolefins, the major contributor to strain is the angular and torsional strain (also called Bayer and Pitzer strain, respectively, Figure 3a).^{42,47} For larger cycloolefins (7–12-carbon), the strain is usually moderate, rendering these monomers polymerizable but not necessarily selectively depolymerizable; at the same time, they can be degraded into cyclic oligomers under appropriate conditions.⁴² Here, the major contributor to strain is transannular strain (also known as Prelog strain, arising from steric repulsion between hydrogens on nonadjacent carbons, Figure 3a). Larger rings are often low-strain or practically strainless as bond angles and dihedral angles are close to what is seen in their linear analogues, and minimal steric crowding is formed from the hydrogen atoms.^{42,48} In addition, the entropic penalty of polymerization decreases with an increase in ring size. For example, in contrast to cyclopentene, the irreversible polymerization of cyclooctene can be attributed to the combination of higher ring strain and lower entropic penalty of polymerization.^{42,49} This is because in larger cyclic olefins, the loss in translational entropy during polymerization becomes less significant and can be countered by the gain in rotational entropy—for very large rings, this can even manifest in a net entropy gain during polymerization, leading to what is known as entropy-driven ROMP.^{40,48,50}

In addition to the ring size, the presence of substituents and their position can also alter the polymerizability of cyclic olefins.⁴² The presence of bulky substituents can lead to increased steric crowding and, thus, strain energy. At the same time, this can reduce the rotational entropy per repeat unit in the polymer chain, known as the Thorpe–Ingold effect.^{51,52} The more significant effect would determine the polymerizability of a monomer. The several monomer designs that lead to depolymerizable ROMP polymers often do so by exploiting one or more of these structural features.

The rest of this section is devoted to a discussion of the literature describing different polymers capable of undergoing metathesis-based depolymerization. The majority of this discussion revolves around different ROMP polymers capable of undergoing depolymerization into monomers organized by the ring size of the cyclic olefin monomers. We will also discuss polymers prepared by enyne metathesis and other approaches that can undergo metathesis-based depolymerization and/or degradation. The focus of the discussion will be the effect of monomer structure on polymerization thermodynamics, depolymerizability, and material properties.

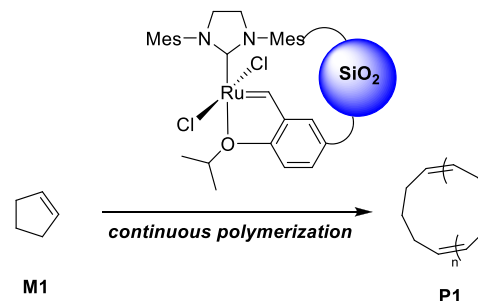
2.3. Depolymerizable ROMP Polymers

2.3.1. Cyclopentene. For reasons discussed above, cyclopentene has been the most common motif for developing depolymerizable ROMP polymers. The reversible nature of the polymerization of cyclopentene was realized quite early, with Ofstead and Calderon determining its enthalpy and entropy of polymerization ($-4.4 \text{ kcal mol}^{-1}$ and $-14.9 \text{ cal mol}^{-1} \text{ K}^{-1}$, respectively, Table 1, M1) in the presence of a tungsten-carbene metathesis catalyst in 1972.⁵³ Around the same time, Kranz and Beck reported the enthalpy of polymerization of liquid cyclopentene to solid *trans*-, *cis*-, and 65% *trans*-polypentenamer (determined calorimetrically). Interestingly, polymerization to *cis*-polypentenamers had the smallest enthalpy change ($\sim -3.2 \text{ kcal mol}^{-1}$), while the enthalpy

changes of polymerization to 100% and 65% *trans*-polypentenamer were found to be ~ -4.2 and $\sim -4.5 \text{ kcal mol}^{-1}$, respectively (Table 1).⁵⁴ This difference in the enthalpy change of polymerization could be attributed to the relatively higher stability of the *trans*-alkene compared to its *cis* counterpart. The mechanism of depolymerization of polypentenamers was investigated by Korshak et al.⁵⁵ and Badamshina et al.⁵⁶ via the study of molecular weight and molecular weight distribution profiles over the course of depolymerization and will be discussed in Section 5.

More recently, Tuba and Grubbs investigated the equilibrium polymerization of cyclopentene in the presence of well-defined *N*-heterocyclic carbene-coordinated ruthenium benzylidene catalyst (G2, Figure 2).⁵⁷ While the cyclopentene conversions obtained were slightly higher than that was reported by Ofstead and Calderon, a decrease of conversion with increase in temperature was observed with $\Delta H_p = -5.6 \text{ kcal mol}^{-1}$ and $\Delta S_p = -18.9 \text{ cal mol}^{-1}$ (Table 1, M1). In an interesting development, Grubbs, Choi, Tuba, and co-workers demonstrated continuous synthesis of cyclic polypentenamer using a supported ruthenium benzylidene catalyst (Scheme 5)

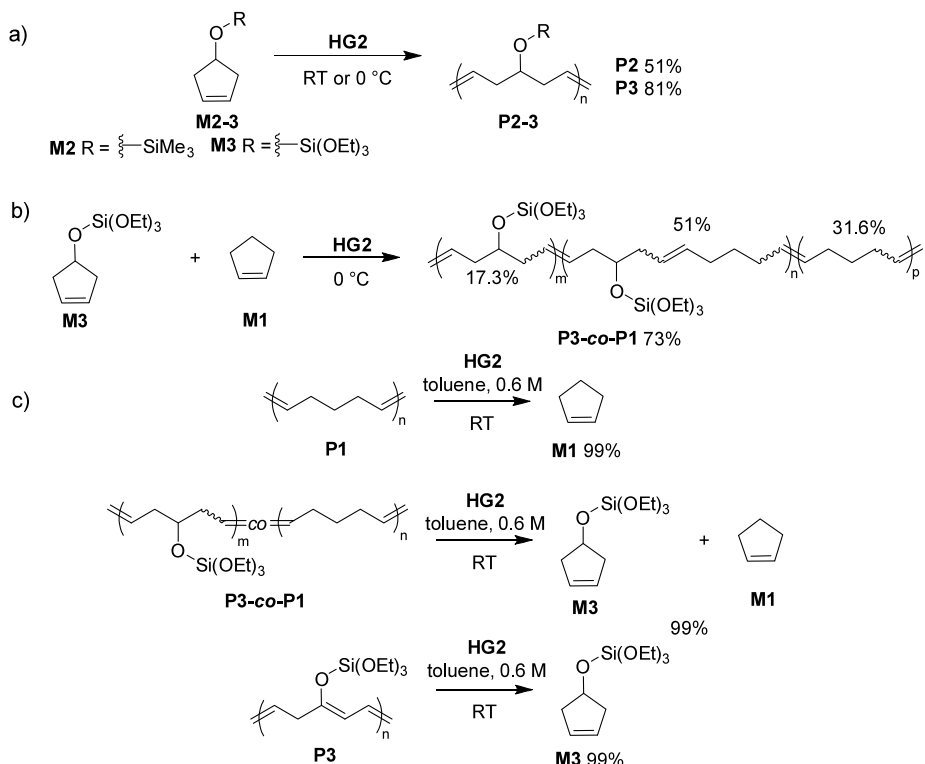
Scheme 5. Synthesis of Cyclic Polypentenamers Using a Heterogeneous Hoveyda–Grubbs Type Catalyst (Ref 58)



and compared the depolymerization of cyclic and linear topologies in the presence of G1 catalyst.⁵⁸ These cyclic polymers could be depolymerized, just like their linear counterparts. However, at similar degrees of polymerization (DP), the cyclic polymer could be depolymerized faster than the linear polymer. It was hypothesized that upon random scission of an internal olefin in the cyclic polymer, a single linear chain is generated, which can undergo cyclization to yield monomers. This is in contrast to the depolymerization mechanism in linear polycyclopentene, where the metathesis results in the formation of two chains: an active chain with the catalyst at one end that is ready for cyclization and an inactive chain that needs to coordinate to another catalyst center before it can undergo cyclization reactions (discussed further in Section 5).

A significant portion of new work with polypentenamers has involved functionalized cyclopentene monomers. This is borne out of a need for diversifying materials properties, e.g., tuning the glass transition temperature (T_g). Here, it is important to understand the effects of adding different functional groups on the thermodynamics of polymerization. Any drastic effects on the thermodynamics can render either the polymerization difficult under ambient conditions or the depolymerization inefficient.

With the aim to develop chemically recyclable tire additives, Tuba, Al-Hashimi, Bazzi, and co-workers performed density functional theory (DFT) calculations to screen multiple siloxy-

Scheme 6. Synthesis and Depolymerization of Recyclable Tire Additives (Ref 59)^a

^a a) Homopolymerization of 4-(trimethylsilyloxy) cyclopentene (M2) and 4-triethoxysilyloxy cyclopentene (M3). b) Copolymerization of 4-triethoxysilyloxy cyclopentene (M3) with cyclopentene. c) Depolymerization of polymers P1, P1-*co*-P1, and P3.

functionalized cyclopentene derivatives based on their ring strain. They further studied homo- and copolymerization of (cyclopent-3-enyl-1-oxy)trimethylsilane and (cyclopent-3-enyl-1-oxy)triethoxysilane (M2, M3; Scheme 6) as well as the depolymerization of the resulting polymers.⁵⁹ As a result of the low ring strain, M2 could only be polymerized to ~51% yield even in bulk at 0 °C while M3 could be polymerized to ~81% yield as a solution in toluene ([M]₀ = ~4.8 M at 0 °C) (Scheme 6a). M3 could also be copolymerized with cyclopentene (M1) (~32.5% yield), with ~51.0% alternating dyads and ~17.3% and 31.6% homo dyads of M3 and M1, respectively (Scheme 1b). Both the homopolymer of M3 (P3) and the copolymer underwent quantitative depolymerization (~99%) in the presence of the HG2 catalyst in toluene at room temperature within 75 and 180 min, respectively (Scheme 6c). Depolymerization of the homopolymer was performed at [olefin]₀ = ~0.25 M with 3 mol % HG2, while for the copolymer, [olefin]₀ = ~0.22 M with ~3.6 mol % of HG2. Moore and co-workers exploited the depolymerizability of polypentenamers to develop dissociative covalent adaptive networks (Figure 4a).⁶⁰ To determine the most suitable monomer designs for the networks, different functionalized cyclopentene derivatives were synthesized (M4–M11), and their ceiling temperatures were obtained by determining the equilibrium monomer concentrations at different temperatures (using variable temperature NMR or VT-NMR). Depolymerization temperature under bulk polymerization conditions could also be characterized with differential scanning calorimetry (DSC); these temperatures correlated well with the *T*_c calculated for neat polymerization, found by using VT-NMR. It was found that the polymerizability generally declined when bulky substituents were used (Table 1, entries M4–

M11). Typically, increasing the size of the R group within the same set of functional groups led to a monotonic decrease in *T*_c (calculated for neat monomer concentration) and polymerization conversion of the neat monomer. Additionally, it was seen that these trends in *T*_c and bulk conversion did not strictly follow the *T*_c calculated for [M]₀ = 1 M. This is likely because different monomers have different concentrations under neat conditions, and thus the trends in *T*_c calculated under bulk polymerization conditions correspond to different monomer concentrations and different trends emerge when *T*_c is compared for the same concentration across all monomers. While the authors did not compare the entropy of polymerization for the monomers, these can be obtained from the reported van 't Hoff plots (shown in Table 1). Further, to prepare the polymer networks, bifunctional and trifunctional cyclopentene monomers were prepared, and it was seen that polymerizability increased from monofunctional to bifunctional and from bifunctional to trifunctional. This may be because in the case of cross-linked networks formed by the bi- and trifunctional monomers, the conversion was calculated by measuring the amount of unreacted monomer using solution-phase NMR spectroscopy. It is possible that there were monomers that were incorporated into the network but had one or more unreacted cyclopentene rings (which would not be seen in solution NMR). In such a case, the amount of unreacted cyclopentene rings would be underestimated (and the polymerizability of the monomers would be overestimated). The reversibility of polymerization could be utilized to cycle between states of low and high monomer conversion, as seen with the COOBn-functionalized cyclopentene (M11) by cycling the temperature between 25 and 50 °C for a mixture of monomer and 0.22 mol % G2 catalyst and

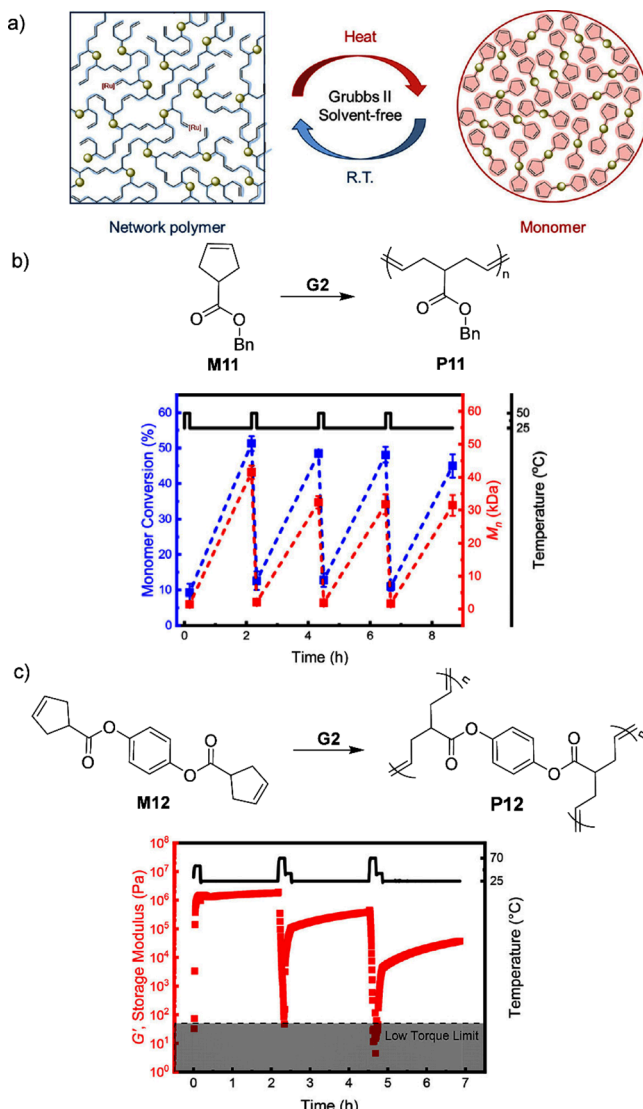


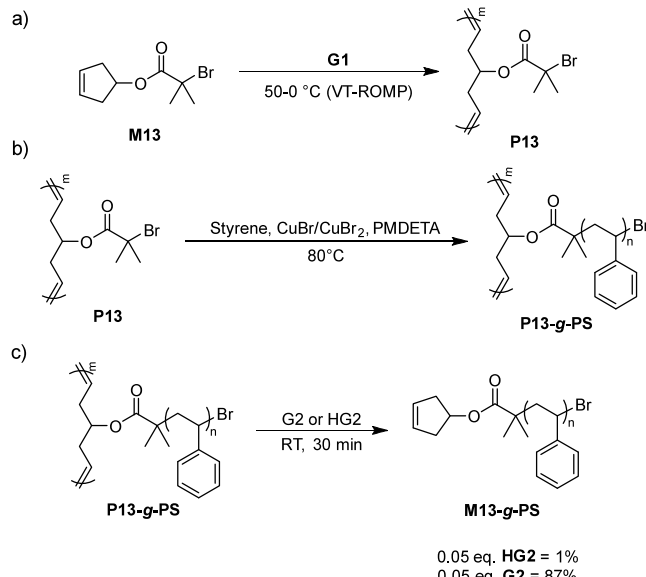
Figure 4. Olefin-metathesis-based dynamic covalent networks. a) Schematic of polymerization and depolymerization of cyclopentene-based networks in the presence of G2. b) Consecutive bulk polymerization and depolymerization of benzyl cyclopent-3-ene carboxylate (M11) as indicated by monomer conversion and number-average molecular weight. c) Bulk polymerization of a bifunctional cyclopentene monomer (M12) monitored based on changes in storage modulus. Reproduced from ref 60. Copyright 2018 American Chemical Society.

following the reaction with NMR and GPC (Figure 4b). This behavior was further exploited with the polymer networks (P12) where cycling the temperature resulted in a change in the storage modulus G' of the network, with high G' and solid-like behavior at low temperatures and low G' and viscous liquid-like behavior at high temperatures. Interestingly, the maximum modulus achievable decreased with cycling, possibly due to the decomposition of the catalyst, highlighting a potential limitation of the system (Figure 4c).

In the past few years, the Kennemur group has also made strides in establishing structure–activity relationships in the polymerization of functionalized cyclopentenes. In 2019, Kennemur and co-workers demonstrated the depolymerization of bottlebrush polymers comprising a polypentenamer backbone and polystyrene (PS) side chains.²⁸ The bottlebrush

polymer was prepared using the grafting-from method: A polypentenamer with α -bromo isobutyrate pendant group on each repeat unit was made, and from each bromoisobutyrate (P13) group was grown a polymer chain via the atom transfer radical polymerization of styrene, thereby forming a bottlebrush polymer with a polypentenamer backbone and PS side chains (P13-g-PS, Scheme 7b).⁶¹ The backbone itself was

Scheme 7. Synthesis of Bottlebrush Polymers with Polystyrene Side Chains and a Polypentenamer Backbone (Ref 28)^a



^aa) Synthesis of α -bromo isobutyrate functionalized polypentenamers (P13) via VT-ROMP. b) Polymerization of styrene by ATRP, initiated by α -bromo isobutyrate functional groups on the polypentenamer backbone to yield bottlebrush polymers (P13-g-PS). c) Depolymerization of the bottlebrush polymers.

prepared via variable temperature ROMP in the presence of a G1 catalyst, where the polymerization was first carried out at 50 °C (to ensure fast initiation) and continued at 0 °C to achieve a high degree of polymerization while minimizing chain transfer to afford narrow-dispersion polymers (Scheme 7a).^{61,62} The bottlebrush polymers could be readily depolymerized to give PS-functionalized cyclopentene in the presence of different ruthenium metathesis catalysts, with up to ~92% conversion to monomer achieved (Scheme 7c). At the same time, kinetic studies revealed that backbone length had no significant effects on the rate of depolymerization while the length of the side chains had only a small effect on the rate (the rate slowing at longer times for the bottlebrush with longer side chains).

Although this work did not explore the thermodynamics of depolymerization of such a system (or hypothesize how the bottlebrush architecture may affect it), we lay out the following scenario for the reader to consider. One could expect that the presence of sterically crowded side chains in the bottlebrush might decrease the rotational degrees of freedom available as compared to the product of the depolymerization, PS-functionalized cyclopentene, which possesses a less crowded linear architecture. In addition, due to the large size of the macromonomer and the bottlebrush, little change in translational freedom is expected for the depolymerization. As a

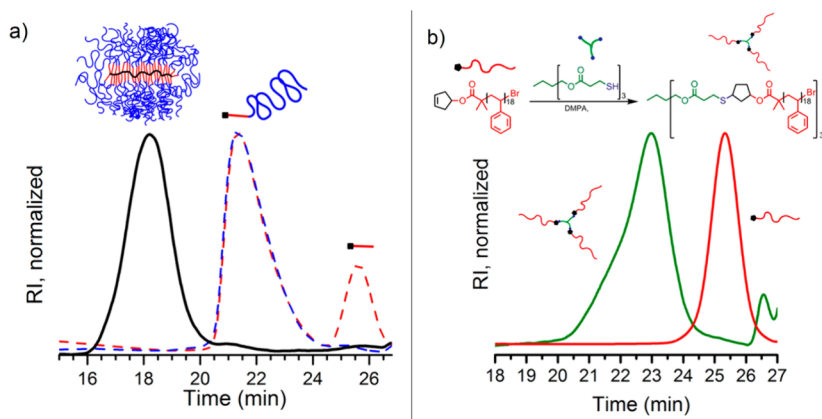


Figure 5. Depolymerization induced the topological transformation of polypentenamer bottlebrush polymers. a) Depolymerization of a core–shell bottlebrush polymer with PS-*b*-PMMA grafts yields a mixture of PS-*b*-PMMA diblock copolymers and a small amount of the PS block. b) Depolymerized PS-graft polypentenamer bottlebrush polymer, upon thiol–ene addition with a trifunctional thiol, yields a polystyrene star polymer. Reproduced from ref 28. Copyright 2019 American Chemical Society.

result, the total entropy change in the depolymerization of the bottlebrush polymer should be much lower than that in the linear polypentenamer.

The depolymerization was also leveraged to bring about topological transformations within these bottlebrush polymers. This was demonstrated via two approaches. In the first approach, core–shell bottlebrush polymers were prepared with a polypentenamer backbone and poly(methyl methacrylate) (PMMA) and PS diblock copolymer side chains. Upon depolymerization, the topology could be transformed from the core–shell bottlebrush polymer into a PMMA–PS linear diblock copolymer with a cyclopentene end group (Figure 5a). In the second approach, depolymerized polystyrene grafted bottlebrush copolymers were reacted with a trifunctional thiol under UV-irradiation to form a PS star polymer (Figure 5b).

The Kennemur group also explored the thermodynamics of polymerization for a range of substituted cyclopentenes, providing additional insights into monomer development for depolymerizable ROMP polymers. In a study with several allylic-substituted trialkylsiloxy–cyclopentene monomers, thermodynamic studies revealed that increasing alkyl substituent size resulted in the decrease in polymerizability (Table 1): methyl (M14) > ethyl (M15) > isopropyl (M16). Notably, the triisopropylsiloxy-functionalized cyclopentene (M17) could not be polymerized even at a relatively low temperature of 10 °C. In addition, dimethyltertbutylsiloxy-functionalized cyclopentene showed the lowest loss in enthalpy and entropy and the highest T_c for bulk polymerization (Table 1, entry M14). The authors concluded that the size of the substituents affected both entropy and enthalpy in a similar manner, leading to the aggregate effects observed.⁶³

While the examples above are restricted to polymers with hydrocarbon backbones, the work by Feist and Xia provides a rare example of a depolymerizable poly(enol ether). This work was especially notable for being the first example of a cyclic enol ether (2,3-dihydrofuran) (P18) being polymerized by ROMP (Figure 6).²⁹ Typically, vinyl/enol ethers are used to quench metathesis reactions due to their tendency to form very stable Fischer carbenes with the active catalyst;^{64,65} thus, polymerization of vinyl ethers was not considered possible heretofore. Additionally, both enthalpy and entropy changes of polymerization for 2,3-dihydrofuran are very close to those of cyclopentene (Table 1, entry M18); as a result, polydihy-

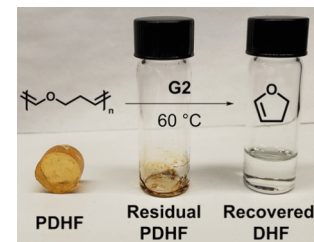
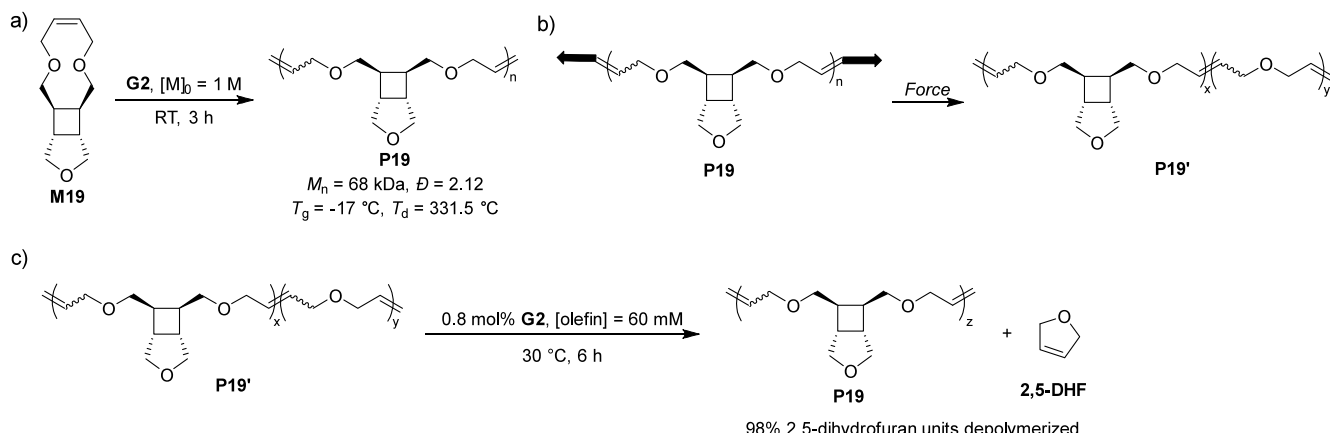


Figure 6. Bulk depolymerization of poly(2,3-dihydrofuran) (P18) in the presence of G2 (0.0001 equiv). Reproduced from ref 29. Copyright 2019 American Chemical Society.

dofuran could be depolymerized readily. This was demonstrated in the bulk state via continuous distillation of monomer to enable >90% recovery of the monomer (Figure 6). An additional feature of the enol-ether backbone was the ability of the polymer to degrade under acidic conditions.

Wang and co-workers demonstrated the synthesis of a polymer that, when subjected to mechanical force, could generate poly(2,5-dihydrofuran).⁶⁶ Note that 2,5-dihydrofuran is very challenging to polymerize due to its very low ring strain (~3.4 kcal mol⁻¹); however, this also makes poly(2,5-dihydrofuran) amenable to depolymerization to the monomer. The monomer design utilized in this work consisted of a 10-membered cyclic olefin connected with a furan ring through a cyclobutane fused ring (M19, Scheme 8a). Under ultrasonication of the corresponding polymer (P19) in solution (Scheme 8b), depending on the initial molecular weight, up to ~68% activation of the cyclobutane groups could be achieved (initial M_n = 154 kDa). When treated with 0.8 mol % G2, at $[\text{olefin}]_0 = 60 \text{ mM}$ in CDCl_3 , at 30 °C, near-quantitative (~98%) depolymerization of the mechanochemically generated poly(2,5-dihydrofuran) groups could be achieved (Scheme 8c). Bulk activation of this polymer was also attempted with bulk extrusion of P19 and compression of a network incorporating M19, resulting in very little activation, as evidenced by the very small amount (<3%) of 2,5-dihydrofuran generated upon treating the mechanically treated polymer with G2. Notable activation was achieved with ball-milling, following which treatment with G2 was found to generate a significant amount of 2,5-dihydrofuran, indicating successful mechanical activation. Degradation of the ball-milled

Scheme 8. Mechanochemical Synthesis and Depolymerization of Poly(2,5-dihydrofuran) (Ref 66)^a

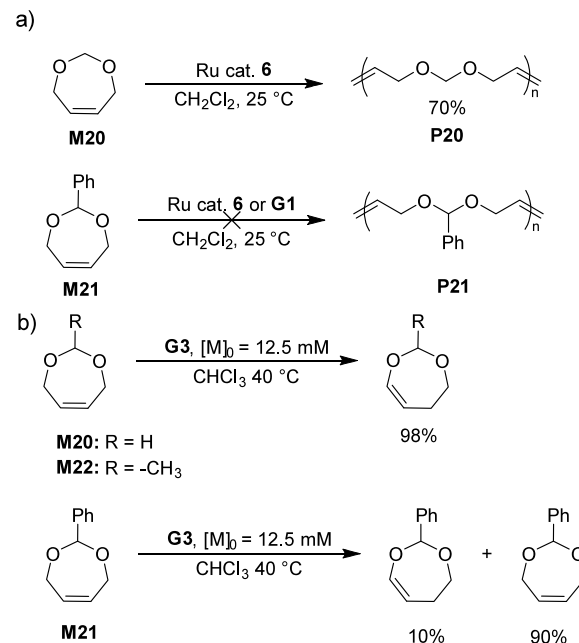
^a a) Polymerization of a THF fused cyclobutane-containing cyclic olefin (**M19**). b) The THF fused cyclobutane-containing polymer (**P19**) can generate poly(2,5-dihydrofuran) segments after mechanochemical activation. c) Depolymerization of the mechanochemically activated polymer (**P19'**) generates 2,5-dihydrofuran, together with nonactivated segments of the parent polymer.

network by hydrolysis revealed that ~17% of cyclobutane groups were activated. Interestingly, the amount of 2,5-dihydrofuran generated upon treatment was much lower (~6% with respect to mechanochemically active monomer content in the pristine network) than expected (40%, corresponding to 17% mechanochemical activation). This was ascribed to the presence of nondepolymerizable cyclooctene repeat units from the cross-linker and the distribution of the poly(2,5-dihydrofuran) segments being statistical instead of block-like as is shown in the case of the ultrasonicated polymers in solution.

2.3.2. Cycloheptene. Cycloheptene is another small cyclic olefin known to have a relatively low ring strain and ΔH_p , which makes it a potential candidate for depolymerizable polymers. However, experimental investigations of the (de)-polymerizability of cycloheptene and its polymers have been limited. In 1995, Kress demonstrated that upon treatment of cycloheptene with highly active tungsten carbene catalysts, a significant amount of cyclotetradeca-1,8-diene (cycloheptene dimer) is formed.⁶⁸ It was also seen that the equilibrium between monomer, dimer, and polyheptenamers was reversible and that increasing the temperature favored dimer and monomer formation. Interestingly, the monomer/initiator ratio at the beginning of the reaction also influenced this distribution with lower $[M]_0/[I]_0$ favoring the formation of the dimer over the polymer and the monomer over the dimer. Grubbs and co-workers also demonstrated the polymerization of cycloheptene and cyclohept-4-enone.⁶⁷ While the polymerization of cycloheptene could reach a relatively high conversion, it was nonetheless far from quantitative, with the equilibrium monomer concentration being ~0.3–0.6 M (depending on the catalyst used as the initiator and the initial monomer concentration). Similar results were obtained for the polymerization of cyclohept-4-enone. The polymerizability of these monomers is higher than that reported for cyclopentene. This is likely because of the lower entropy loss during its polymerization compared to cyclopentene.

Like cycloheptene, its heterocyclic acetal analogues, 4,7-dihydro-1,3-dioxepins, also appear to be potential candidates for depolymerizable polymers. Grubbs and co-workers could homopolymerize 4,7-dihydro-1,3-dioxepin (**M20**) at a relatively high concentration (1.1 g of **M20** in 0.21 mL of CH_2Cl_2 ,

corresponding to a concentration of ~9.1 M, assuming constant volume before and after mixing); however, they were unable to homopolymerize the 2-phenyl derivative (**M21**, Scheme 9a).⁶⁹ More recently, Sampson and co-workers employed dioxepins for alternating ROMP with bicyclo[4.2.0]-oct-1(8)-ene-8-carboxamide. While the alternating ROMP was successful, homopolymerization of the dioxepin monomers failed (Scheme 9a): when **M20** and its derivatives (**M21** and

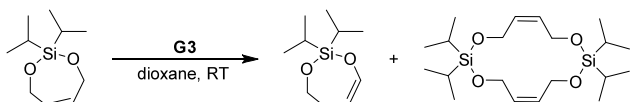
Scheme 9. Polymerization of Dioxepins^a

^a A few dioxepin structures and their polymerization conditions reported in the literature: a) At higher concentrations, 4,7-dihydro-1,3-dioxepin (**M20**) can undergo polymerization to ~70% yield ($[M]_0 = 9.1 \text{ M}$, $[M]_0/[I]_0 = 1000:1$), unlike the 2-phenyl derivative (**M21**) which remains nonpolymerizable (ref 69). b) At low monomer concentrations, dioxepins do not undergo polymerization, instead forming enol-ethers which can form stable Fischer carbenes with the metathesis catalysts or remain unreacted ($[M]_0 = 250 \text{ mM}$, $[M]_0/[I]_0 = 20:1$) (ref 71).

M22) were subjected to ROMP conditions at 0.25 M monomer concentration in the presence of 0.05 equiv of **G3** catalyst, no polymerization was observed, although **M20** and **M22** showed significant isomerization to the corresponding enol ether.⁷⁰

In their study on degradable ROMP polymers, Johnson and co-workers used a 7-membered silyl-ether-containing cycloolefin as one of the monomers (**M23**, Scheme 10).⁷¹ They

Scheme 10. Polymerization of a Diisopropyl-Siloxy-Containing Cycloheptene (M23**) Analogue from Ref 71^a**



^aMost of the monomer remained unreacted along with the formation of a cyclic enol-ether-type isomer of the monomer and trace amount of the cyclic dimer ($[M]_0 = 500$ mM, $[M]_0/[I]_0 = 500$).

found that the monomer could not be homopolymerized; upon treating with **G3** catalyst, with an initial monomer concentration of ~ 500 mM, a mixture formed, which contains the unreacted monomer (64%), a cyclic enol ether resulted from the isomerization of the monomer (32%), and a small amount of cyclic dimer.

2.3.3. Cyclooctene. Cyclooctene is known to have a relatively moderate ring strain (8.2 kcal mol⁻¹);³⁰ however, due to a relatively small loss of entropy during polymerization (-2.2 vs -18.9 cal mol⁻¹ K⁻¹ for cyclopentene), it is readily polymerizable.^{42,49,72} As a result, polycyclooctenes are not usually amenable to depolymerization to the monomer. Recently, Wang and co-workers have published a series of studies on polymers prepared from cyclooctene derivatives that can be depolymerized into monomers.³⁰ These studies all employed *trans*-fused 4- or 5-membered rings at the 5,6-positions of the cyclooctene (Figure 7–12). While these systems were the first examples of a cyclooctene-based system capable of chemical recycling to monomer, the literature does have other examples of fused rings impacting the polymerizability of cyclooctenes in a fashion that could be favorable for chemical recycling to monomer. For example, when Grubbs and co-workers attempted the polymerization of cyclooctene monomers with *cis*- and *trans*-fused acetonide rings at the 5,6-positions, they found that the monomer with the *trans*-fused acetonide had very poor polymerizability compared to the *cis*-fused monomer.⁷³ Coates and co-workers also reported the formation of significant amounts of macrocycles instead of linear polymers when they attempted polymerization of imidazolium fused cyclooctene derivatives, indicating poor polymerizability of this monomer (it should be noted, however, that in this case, there would be only a single isomer because the carbons where the rings are fused are sp^2 -hybridized).⁷⁴

In their initial report, Wang and co-workers demonstrated the synthesis and polymerization of different *trans*-cyclobutane fused cyclooctene (*t*CBCO) monomers (**M24**–**M27**) and the depolymerization of the corresponding polymers (Figure 7a).³⁰ Interestingly, the enthalpy changes of polymerization for these monomers (in the range of -1.7 to -2.8 kcal mol⁻¹, Table 2) were significantly lower than that for cyclopentene (-4.4 to -5.6 kcal mol⁻¹, Table 1). The relatively low entropy loss during polymerization offsets the small enthalpy change of

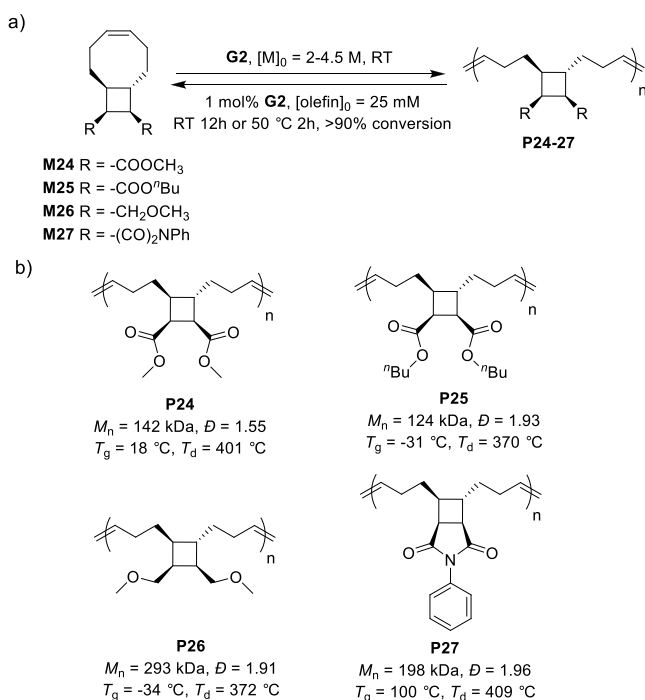


Figure 7. *trans*-Cyclobutane fused cyclooctene-based chemically recyclable polymers (ref 30). a) *t*CBCO monomers can be polymerized at high monomer concentrations to yield high-molecular-weight polymers in the presence of **G2** catalyst. The resulting polymers can be depolymerized to $>90\%$ conversion at concentrations. b) Polymers with different properties achieved by varying functional groups attached to the cyclobutane ring.

polymerization and enables high molecular weight and conversion to be obtained. Nonetheless, polymerization required relatively high initial monomer concentrations (>2 M, depending on monomer) (Figure 7a). The polymers could all be depolymerized to monomers with high conversions ($>90\%$), with the extent of depolymerization controllable by varying initial polymer concentration (expressed as the repeat unit concentration). Computational studies revealed that the low strain in the *t*CBCO monomers was made possible by the fact that the dihedral angles at the fusion site (5,6-positions on the cyclooctene ring) in the monomer and its corresponding ring-opened form are very similar. In the *cis*-cyclobutane fused cyclooctene and *cis*-cyclooctene, which had higher ring strain energies, the dihedral angles were more distorted compared with the corresponding linear dienes. The ease of functionalization of the polymers meant that they could be made to have a variety of functional groups (Figure 7b) and thermomechanical properties, with T_g ranging from ~ -34 to 100 °C. Further, this method was also used to synthesize an elastomeric polymer network by polymerizing a mixture of mono- and bifunctional *t*CBCO monomers which could be depolymerized almost quantitatively ($\sim 94\%$ total conversion to monomer and cross-linker).

This system was also expanded into the area of semi-fluorinated polymers, the chemical recycling of which has been rather limited (Figure 8).⁷⁵ Bis-heptafluorobutyl ester (**M28**), perfluorophenyl imide (**M29**), and fluorinated ladderene (**M30**) functionalized *t*CBCO monomers were synthesized, and their ROMP polymers were prepared (**P28**–**P30**, Figure 8a). The semifluorinated polymers demonstrated hydrophobicity, while the different substituents allowed tuning the

Table 2. Thermodynamics Parameters for Different Cyclooctene Analogues

Entry No.	Monomer Structure	Ring Strain Energy (kcal mol ⁻¹)	ΔH_p^a (kcal mol ⁻¹)	ΔS_p (cal mol ⁻¹ K ⁻¹)	T_c @ 1 M (°C)	Reference
M24		-	-1.7	-3.6	199	30
M27		-	-2.8	-4.9	295	30
M31		4.9	-2.1	-3.4	335	76
M32		5.3	-3.2	-3.2	614	76
M33		5.1	-2.7	-2.9	646	76
M34		4.9	-2.6	-2.7	675	76
M35		5.0	-3.2	-4.9	376	76
M36		5.0	-3.2	-5.0	380	76
M37		5.1	-2.8	-3.3	571	76
M41		-	-2.4	4.6	-	78
M45		-	0.5	1.8	5 ^a	71

T_g with P28 having the lowest T_g (-2 °C), and P29 having the highest T_g (88 °C) (Figure 8b). Post-polymerization functionalization of the perfluorophenyl imide polymer was also demonstrated by introducing a thiophenyl group on the phenyl ring, *para* to the imide group via an efficient S_NAr reaction. An amphiphilic diblock copolymer was also prepared by copolymerizing the semifluorinated diester monomer with a PEG-functionalized *t*CBCO monomer—the resulting polymer was found to self-assemble into particles with a hydrodynamic diameter D_h of 88.4 nm. Depolymerization experiments at different concentrations revealed that P28 had the highest extent of depolymerization, followed by those of P30 and P29. This is in line with previous work from Wang and co-workers where a phenyl imide-functionalized polymer (P27) was

depolymerized to a lower extent than a diester-functionalized polymer under similar conditions.

The initial work with the *t*CBCO system demonstrated that the thermodynamics of polymerization is not drastically altered when different functional groups are attached to the monomers, thus enabling a gamut of properties. Nonetheless, it is important to understand the effects of functional groups of different sizes and of other fused rings. To this end, a follow-up study compared the thermodynamics, rate of polymerization, depolymerization, and thermal properties for polymers based on cyclooctenes with *trans*-fused cyclobutane (P31), cyclopentane (P32), and 5-membered cyclic acetals (fused at the 5,6-positions, P33–P37) (Figure 9).⁷⁶ It was found that monomers M32 and M33 had a significantly higher T_c (614

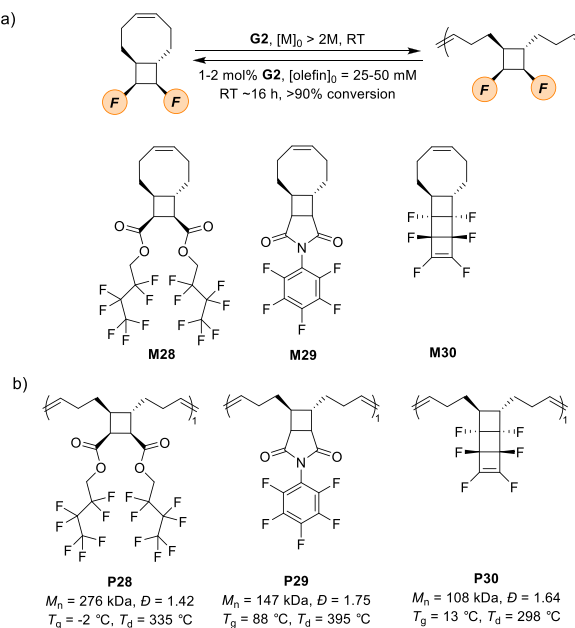


Figure 8. Depolymerizable semifluorinated olefinic polymers (ref 77).

and 646 °C, respectively) than the cyclobutane fused monomer (335 °C) (Table 2). This was attributed to the higher enthalpy changes of polymerization for these monomers compared to those of the cyclobutane fused monomer M31. When comparing the acetal fused monomers with different alkyl groups, it was observed that while the addition of a single methyl group to the acetal (M34) did not lead to a drastic change in the T_c (675 °C), the presence of geminal disubstitution on the acetal ring resulted in a significant drop in the T_c (Table 2 M35–M36), similar to the Thorpe–Ingold effect.^{51,52} The effect was driven by the larger negative entropy change of polymerization for the *gem*-disubstituted monomers (attributed to reduced rotational freedom of the polymer) with the ΔH_p of polymerization showing only slight variations. Replacing the dimethyl (M35) or di-*n*-butyl (M36) groups with a spiro cyclohexane group increased the T_c (~571 °C) (Table 2). It was unusual that these substituents were not attached on the cyclooctene ring (but rather being separated by the acetal ring), yet they demonstrated a *gem*-disubstituent effect; the effect was termed as a “remote” *gem*-disubstituent effect. Interestingly, once again, ΔH_p was smaller than the calculated ring strain energies (Table 2, M31–M37, comparing ΔH_p values with the calculated ring strain energies). This effect also seemed to affect the polymerization kinetics (Figure 9a)—while all the acetal fused monomers were slower to polymerize than M32, M35 (dimethyl-substituted) monomer had slower kinetics than M33–M34 (unsubstituted and monomethyl-substituted monomers). Depolymerization studies (Figure 9b) also demonstrated that P35 and P36 had the first and second highest degrees of depolymerization, in that order, in line with the above observations.

In another follow-up study, substituent effects were also studied for the *t*CBCO core monomer.⁷⁷ Dimethyl-ester-functionalized monomers with different stereochemistries (M24 and its epimer with the ester groups *trans* to each other; M38) and additional substituents at the cyclobutane (dimethyl and cyclohexyl fused ring; M39–M40) were prepared, and their polymerization and depolymerization were studied (Figure 10). The polymerization of these

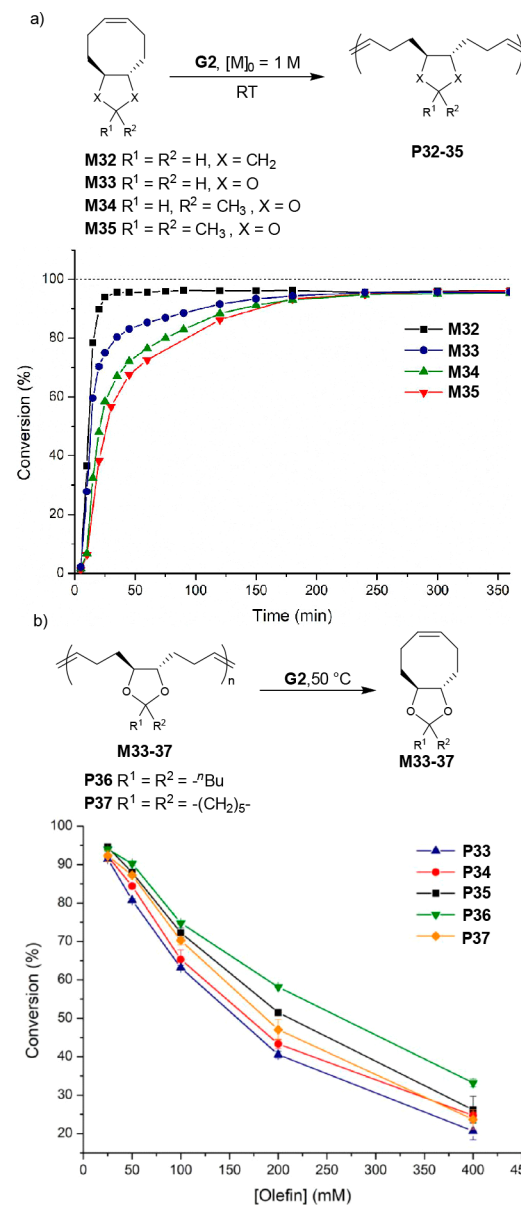


Figure 9. Understanding substituent effects on the polymerizability of chemically recyclable polyoctenamers (ref 76). a) Conversion vs time for the polymerization of cyclooctenes with cyclopentane and various 5-membered cyclic acetal fused at the 5,6-positions ($[\text{M}]_0 = 1 \text{ M}$ in xylenes, $[\text{M}]_0/[\text{G2}] = 100$). b) Depolymerization conversions of various 5-membered cyclic acetal fused polyoctenamers plotted against the concentration of olefin ($[\text{G2}] = 0.01 \text{ equiv, } \text{CDCl}_3$).

monomers (at 30 °C with initial monomer concentration $[\text{M}]_0 = 1.0 \text{ M}$) was tracked, and it was observed that while the time to reach equilibrium was largely similar, the equilibrium conversions were different. Interestingly, the substituted monomers reached higher conversion at equilibrium (~82% for M40 and ~71% for M39 vs ~66% for M24). This contrasts with the effects of geminal substituents as seen with the previous study and was speculated to arise from a higher ring strain in these monomers (thus more negative ΔH_p) which could offset an increase in the entropic loss (more negative ΔS_p) of polymerization that might arise from the presence of the substituents. M38 also showed a higher conversion than M24. These effects were also observed for the depolymerization studies, particularly at the higher polymer concentrations

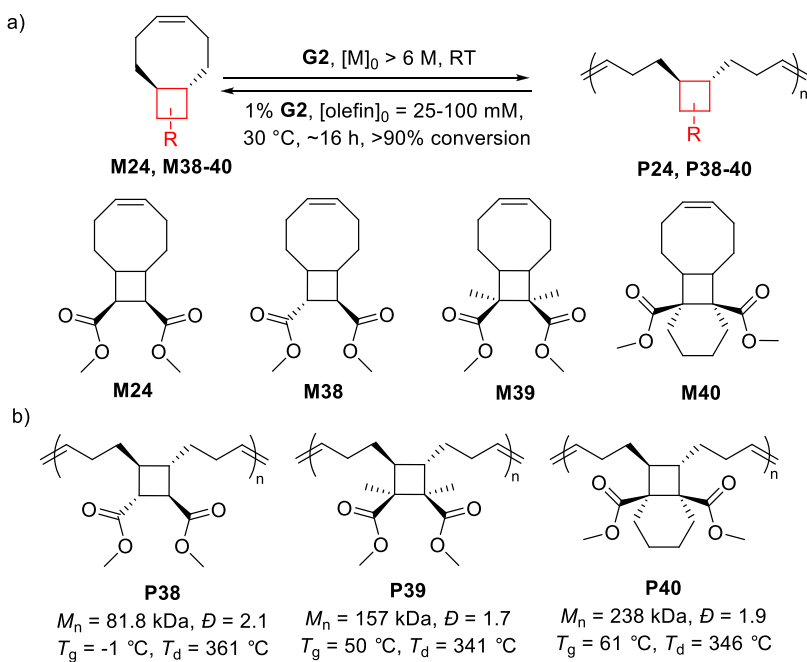


Figure 10. *trans*-Cyclobutane fused cyclooctene systems with different substituents on the cyclobutane (ref 77).

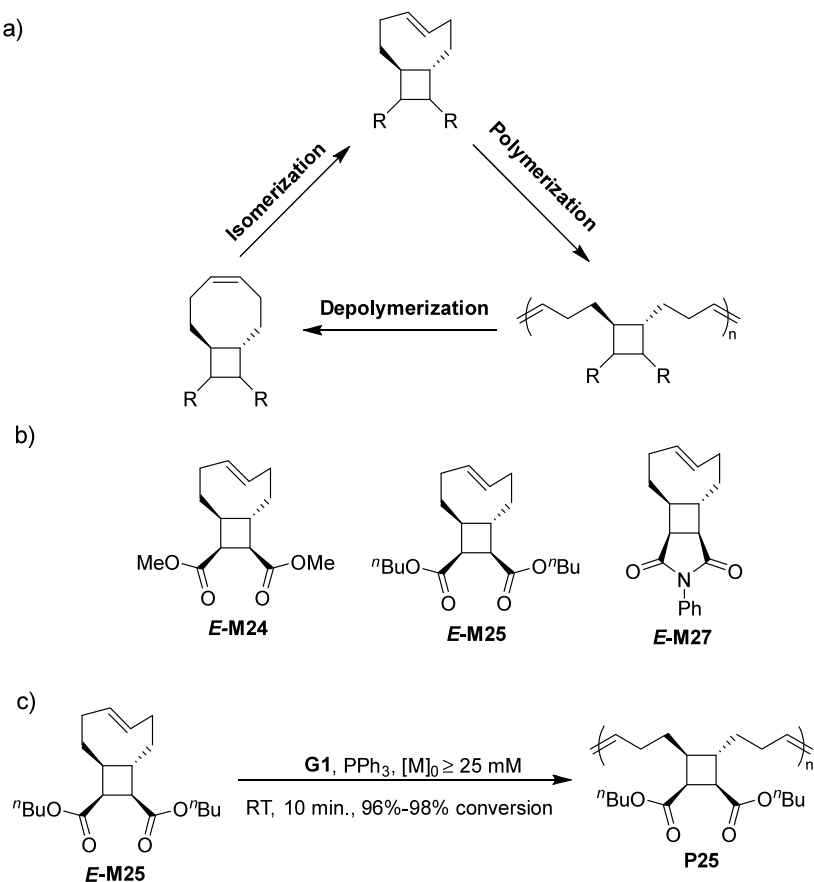


Figure 11. Living ROMP of *E*-alkene *t*CBCO-based monomers to form chemically recyclable polymers (ref 79). a) Schematic showing the conversion of *Z*-alkene-*t*CBCO monomers into their *E*-alkene isomer, polymerization of the *E*-alkene monomers, and depolymerization of the resulting polymers back to the *Z*-alkene monomers. b) Different *E*-alkene *t*CBCO monomer structures used in this study. c) Living ROMP of *E*-M25 in the presence of G1 and PPh₃ ($PPh_3/G1 \geq 20$, $[M]_0 \geq 0.025 \text{ M}$, $D = 1.17\text{--}1.23$).

($[\text{olefin}]_0 = 200$ and 400 mM). **P38**–**P40** had a lower extent of depolymerization than **P24**. The changes in the stereochemistry and additional substituents also impacted the

thermal properties of the polymers. The presence of additional methyl groups and cyclohexyl ring both resulted in higher T_g s (~ 50 and $\sim 61^\circ\text{C}$, respectively, Figure 10b) compared to **P24**

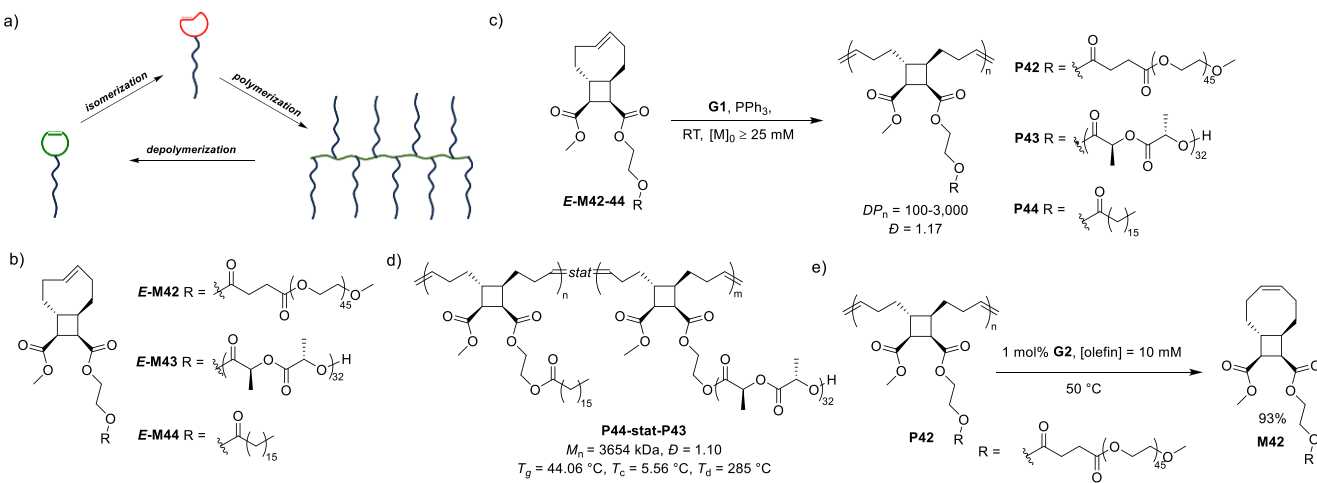


Figure 12. Chemically recyclable *trans*-cyclobutane fused cyclooctene-based graft polymers (ref 81). a) Olefin isomerization from *Z*-alkene to *E*-alkene as a route to enhance the driving force for ROMP, allowing the synthesis of chemically recyclable graft polymers with controlled molecular weight and narrow dispersity, and depolymerization of the graft copolymers yields the *Z*-alkene macromonomer. b) The macromonomers used in this work. c) The living ROMP of *E*-alkene tCBCO macromonomers in the presence of **G1** and PPh_3 ($\text{PPh}_3/\text{G1} = 30$, $[\text{M}]_0 = 0.025 \text{ M}$, $[\text{M}]_0/[\text{G1}] = 1:100\text{--}1:3000$, conversion $>96\%$). d) Statistical copolymer made from copolymerization of **E-M44** and **E-M43**. e) Depolymerization of the graft polymers ($[\text{olefin}] = 0.01 \text{ M}$ in toluene, 0.01 equiv **G2**, at 50°C).

($\sim 18^\circ\text{C}$, Figure 7b), attributed to the increased hindrance to segmental motion. Interestingly, changing the stereochemistry of the ester groups resulted in the opposite, with a lower T_g value for **P38** ($\sim -1^\circ\text{C}$). This was reasoned as arising from the relative stereochemistry of the ester group with respect to the backbone alkyl groups on the cyclobutane—having both ester groups be *trans* to the alkyl groups is expected to lower the hindrance to backbone rotation and segmental motion.

This exploration of substituent effects was further expanded with a study of the polymerization/depolymerization behavior of a system based on a cyclooctene monomer with a *trans*-fused benzocyclobutene ring (**M41**).⁷⁸ Interestingly, the thermodynamics study of this monomer (with initial monomer concentration of $\sim 0.1 \text{ M}$, Table 2, entry 10) revealed that while the ΔH_p was only slightly larger than that of the unsubstituted tCBCO monomer **M31** (-2.4 vs $-2.1 \text{ kcal mol}^{-1}$; Table 2, entry 3), its entropy of polymerization, ΔS_p , was positive ($4.6 \text{ cal mol}^{-1} \text{ K}^{-1}$, calculated for $[\text{M}]_0 = 1.0 \text{ M}$) as opposed to negative for the unsubstituted tCBCO monomer ($-3.4 \text{ cal mol}^{-1} \text{ K}^{-1}$). This behavior was also reflected in its depolymerization, with no depolymerization seen at the initial olefin concentration of 200 mM ($\Delta S_p = 1.4 \text{ cal mol}^{-1} \text{ K}^{-1}$ at $[\text{M}] = 200 \text{ mM}$). Depolymerization is feasible (although only partially, $\sim 63.7\%$) at a lower concentration (5 mM); this is enabled by a negative ΔS_p at this concentration ($-5.9 \text{ cal mol}^{-1} \text{ K}^{-1}$ at $[\text{M}] = 5 \text{ mM}$) which can offset the ΔH_p . This behavior was ascribed to a more significant gain in the rotational entropy during polymerization of **M41** vs the unsubstituted tCBCO monomer.

While tCBCO-based polymers could be readily synthesized at room temperature, the polymerization required high monomer concentrations and resulted in polymers with a broad dispersity. This also limited the accessible architectures of the polymers. To overcome these challenges, a strategy was employed where the strain of the monomer could be temporarily increased so that it could be polymerized in a controlled fashion, at low concentrations, and rapidly (Figure 11).⁷⁹ The resulting polymer could then be depolymerized to return the original low-strain tCBCO monomer. This

temporary increase in strain was realized by photoisomerization of the *cis*-alkene in the tCBCO monomer to the *trans*-alkene. A catalyst screen was performed with **G1**, **G2**, **G3**, and **HG1** and **HG2** catalysts, in the presence and absence of 60 equiv of triphenyl phosphine (PPh_3). This was inspired by the well-known approach developed by Grubbs and co-workers to perform controlled living polymerization of *trans*-cyclooctene, by introducing PPh_3 to suppress the chain transfer and backbiting reactions.⁸⁰ The best performance was observed with **G1** with 60 equiv PPh_3 with respect to **G1**, with the lowest amount of *cis*-alkene-tCBCO formation and the lowest dispersity. Further studies revealed that the polymerization could be performed with initial monomer concentration $[\text{M}]_0$ as low as 0.025 M before the dispersity started broadening and more *cis*-alkene-tCBCO monomer was formed and that a PPh_3/Ru ratio ≥ 20 was required to maintain control over the polymerization. The controlled polymerization was also utilized to prepare a diblock copolymer with a low- T_g *n*-butyl ester functionalized block (similar to **P25**) and a high- T_g *N*-phenyl-imide-functionalized block (similar to **P27**), demonstrating the potential for this strategy to be applied to different functionalized monomers and to prepare complex architectures.

The above strategy was further extended to develop depolymerizable graft polymers (Figure 12a).⁸¹ This was done by first preparing macromonomers with different side chains (poly(ethylene glycol) or PEG in **E-M42**, poly-L-lactide or PLLA in **E-M43**, and heptadecanoate ester in **E-M44**) from a hydroxyl functionalized *E*-alkene tCBCO monomer (Figure 12b). This macromonomer was then polymerized in the presence of **G1**/ PPh_3 (1:30) (an example of the grafting-through approach, Figure 12c) to yield polymers with high molecular weights ($M_n > 68 \text{ kDa}$) and narrow dispersities ($D \leq 1.17$). The PLLA-functionalized macromonomer could be polymerized at monomer/initiator ratios as high as 3000, offering controlled M_n ($14,350 \text{ kDa}$ experimental vs $13,937 \text{ kDa}$ theoretical) and narrow dispersity (1.17). Block copolymers (100:10 **P44**/**P42** blocks) and statistical copolymers (2700:300 **P44**/**P43** grafts) were also prepared (Figure

12d). The block copolymers underwent phase separation to give a lamellar morphology (domain spacing of 40.7 nm) and two melting points, 19.0 and 48.6 °C, corresponding to the hexadecanoate and PEG grafted blocks, respectively. The statistical copolymer was envisioned to have interesting mechanical properties, with the PLLA (P43) grafts acting as physical cross-links and the hexadecanoate grafts (P44) forming the soft domains bridging the hard PLLA domains. This material behaved like a thermoplastic with Young's modulus of ~130 MPa, yield stress of ~4.4 MPa, and ultimate tensile strength (at break) of ~8.5 MPa with a strain at break of ~200%. The polymers could be readily depolymerized at ~50 °C in toluene, yielding an ~93% Z-alkene *t*CBCO monomer and ~7% oligomers in 130 min (P42, Figure 12e). The statistical copolymer could also be readily depolymerized to yield the corresponding Z-alkene forms of the macro-monomers.

The examples mentioned above all deal with monomers possessing C–C cyclooctene scaffolds. Examples of depolymerizable polymers prepared from 8-membered heterocyclic olefins are rare, with the sole report coming from the Johnson group (Figure 13).⁷¹ As a part of the study with degradable

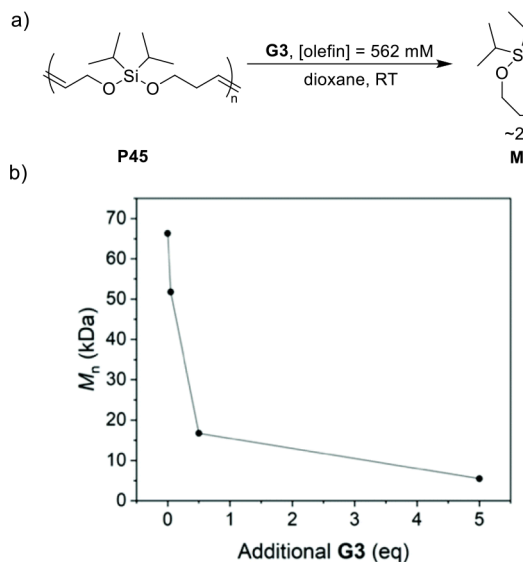


Figure 13. Chemical recycling of the ROMP polymer of a disopropyl-siloxy-containing heterocyclic cyclooctene analogue (P45) from ref 71. a) Depolymerization scheme; upon treatment with G3 catalyst, the polymer can be partially depolymerized to monomer with conversion up to ~28%. [olefin] = 562 mM. b) Decrease in molecular weight with the introduction of increasing amounts of G3. Adapted with permission from ref 71. Copyright 2022 Royal Society of Chemistry.

polymers based on silyl-ether-containing cyclic olefins discussed in the preceding subsection, a monomer with an 8-membered ring (M45) was also studied. Interestingly, the thermodynamics studies with this monomer revealed a very small enthalpy change of polymerization ($\Delta H_p = 0.5$ kcal mol⁻¹) but a positive entropy change of polymerization ($\Delta S_p = 1.9$ cal mol⁻¹ K⁻¹). The monomer was polymerized via entropy-driven ROMP (ED-ROMP) in the presence of G3 to give polymerization conversions of up to ~96% with a relatively broad dispersity ($D = 1.76$). The resulting polymers could be partially depolymerized in dilute solutions exposed to an increasing amount of G3 catalyst (Figure 14a,b). The

molecular weight reached a minimum of ~5.5 kDa (from an initial molecular weight of ~58 kDa), accompanied by a 28% conversion to a monomer (Figure 14b).

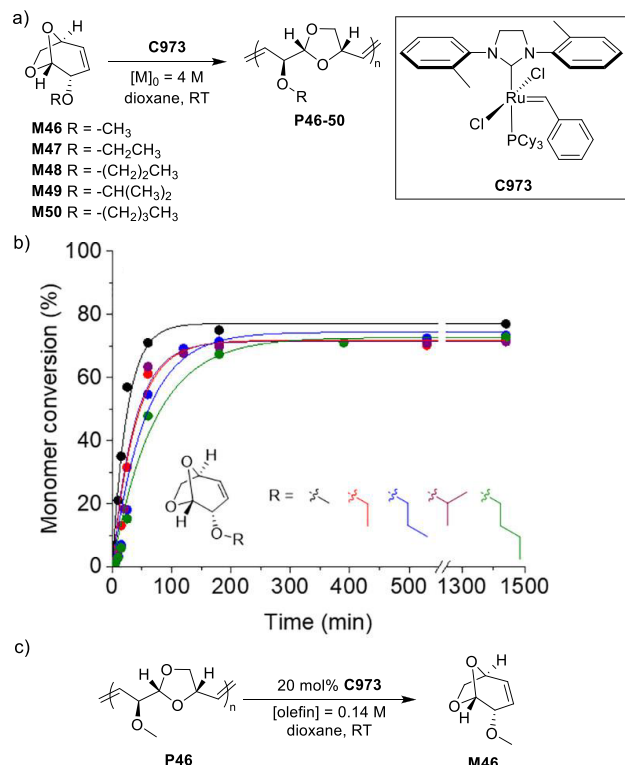
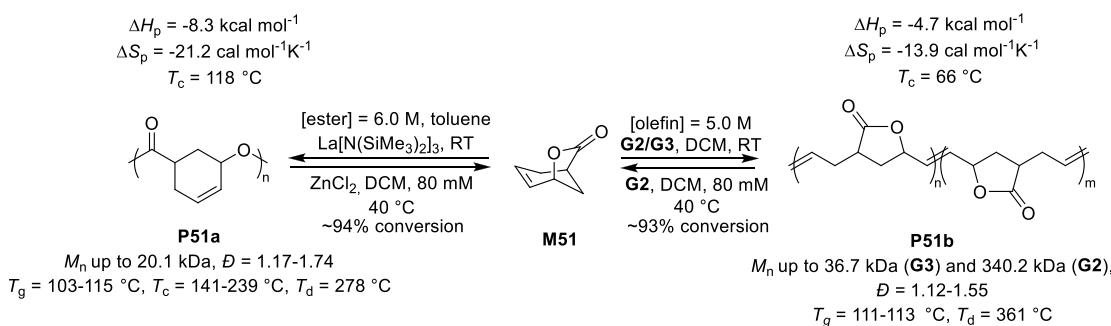


Figure 14. Biobased olefinic polymers from levoglucosan ethers. a) Polymerization of levoglucosan monomers (M46–M50) with different alkyl ether groups in the presence of a Ru benzylidene catalyst with a bis-tolyl N-heterocyclic carbene ligand. b) Monomer conversion vs time for the polymerization of different levoglucosan alkyl ether monomers ($[M]_0 = 4$ M in dioxane, 0.01 equiv of C973). c) Depolymerization of the methyl-ether-functionalized polymer ($[olefin]_0 = 0.14$ M, 0.2 equiv of C973). Adapted with permission from ref 82. Copyright 2021 The American Chemical Society.

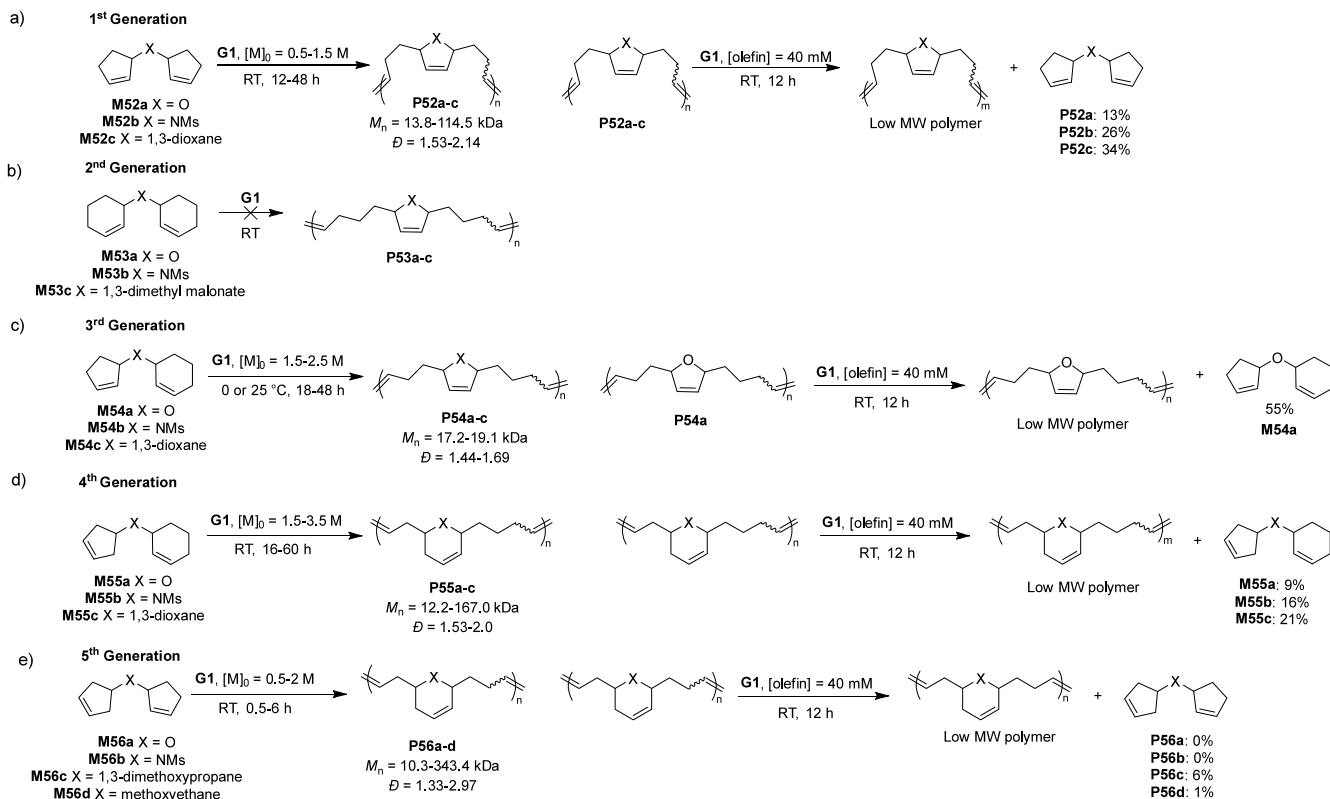
2.3.4. Bridged Bicyclic Olefins. Examples of ROMP polymers of bridged bicyclic olefins that can depolymerize into monomers are rare. The most commonly used bridged bicyclic olefins, particularly norbornene and related derivatives, are readily polymerizable, driven by their high ring strain.^{32,44} This same driving force, however, makes the depolymerization of the resulting polymers unfavorable. Here, we note two interesting examples of depolymerizable polymers prepared from the ROMP of bridged bicyclic olefins.

Recently, Schlaad and co-workers demonstrated the polymerization of levoglucosan alkyl ethers (cyclic olefins based on carbohydrate derivatives, M46–M50).⁸² To polymerize these monomers, ruthenium metathesis catalyst C973 (Figure 2, Figure 14a) with a less bulky N-heterocyclic carbene ligand compared to G2 was required. The resulting polymers possessed a range of glass transition temperatures (0–43 °C) and 5% decomposition temperatures of 240–285 °C. The monomers could be polymerized to 70–80% conversion with the methyl-ether-substituted monomer having the highest conversion. The rate of polymerization was found to be slightly slower for the monomers with larger substituents (Figure 14b). Additionally, the mechanism was understood to involve slow initiation followed by the polymerization reaching

Scheme 11. A Bridged Bicyclic Olefin/Lactone-Based Platform Possessing Orthogonal Polymerizability and Depolymerizability (Ref 83)



Scheme 12. Polymerization of Different Bis-cycloolefin Monomers via Cascade Ring-Opening/Ring-Closing Metathesis and Depolymerization of the Resulting Polymers (Refs 84, 85)^a

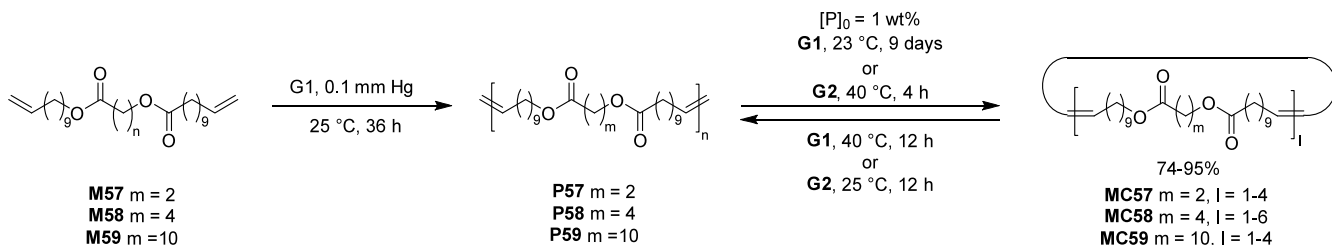


^aa)–e) 1st–5th generation of bicyclic monomers used in these studies. The ease of polymerization (and depolymerizability) is governed by the thermodynamic feasibility of ring opening of the two cyclic olefins together with that of the formation of the new cyclic olefin as the monomer forms a repeat unit.

a steady state, following which the remaining catalyst could lead to chain scission and fragmentation events. The initial increase and eventual decline of the number-average degree of polymerization observed over the course of the polymerization reaction was attributed to a combination of these events. Although the depolymerization of these polymers was not studied in detail, it was found that when the solution of the methyl-ether-substituted polymer was treated with ~0.2 equiv of catalyst, the monomer was generated and a decrease in molecular weight was observed (Figure 14c).

The Chen group also demonstrated a bicyclic unsaturated lactone (**M51**) that could be polymerized by metal-catalyzed ring-opening polymerization through the lactone moiety or by ROMP in the presence of **G2** or **G3** catalysts through the

olefin (Scheme 11).⁸³ The enthalpy and entropy changes of ROMP for this monomer were determined by conducting polymerization at different temperatures and found to be $\Delta H_p = -4.7 \text{ kcal mol}^{-1}$ and $\Delta S_p = -13.9 \text{ cal mol}^{-1} \text{ K}^{-1}$. The ROMP polymer (**P51b**) could be depolymerized at a multigram scale (~28 g) in the presence of catalyst **G2** in DCM under reflux in air to give ~93% monomer recovery. The ROP polymer (**P51a**) also had thermodynamics amenable to preparing depolymerizable polymers, with $\Delta H_p = -8.3 \text{ kcal mol}^{-1}$, $\Delta S_p = -21.2 \text{ cal mol}^{-1} \text{ K}^{-1}$, and $T_c = 118 \text{ }^\circ\text{C}$. Interestingly, despite the enthalpy change of the ROP being relatively higher than the typical depolymerizable polymers discussed earlier in Section 2.1, the larger entropy loss compensates for this and thus enables depolymerization. **P51a** could be depolymerized

Scheme 13. Chemically Recyclable Olefinic Polyesters (Ref 86)^a

^a Representative scheme for the synthesis of olefinic polyester by ADMET polymerization. The resulting polymers can be degraded to cyclic oligomers by RCM which can be subsequently repolymerized.

in the presence of a Lewis acid (ZnCl_2) in a DCM solution at 40 °C to reach ~94% conversion. Interestingly, attempting depolymerization at high temperatures was not feasible due to the side reactions of the cycloolefin group in the backbone. Polymers produced by either route possessed T_g s (111–113 °C for the ROMP polymer and 103–115 °C for the ROP polymer). The ROP polymer could also be prepared to be semicrystalline with a T_m = 141–239 °C, depending on the tacticity.

2.4. Depolymerizable Polymers via Cascade Metathesis Reactions

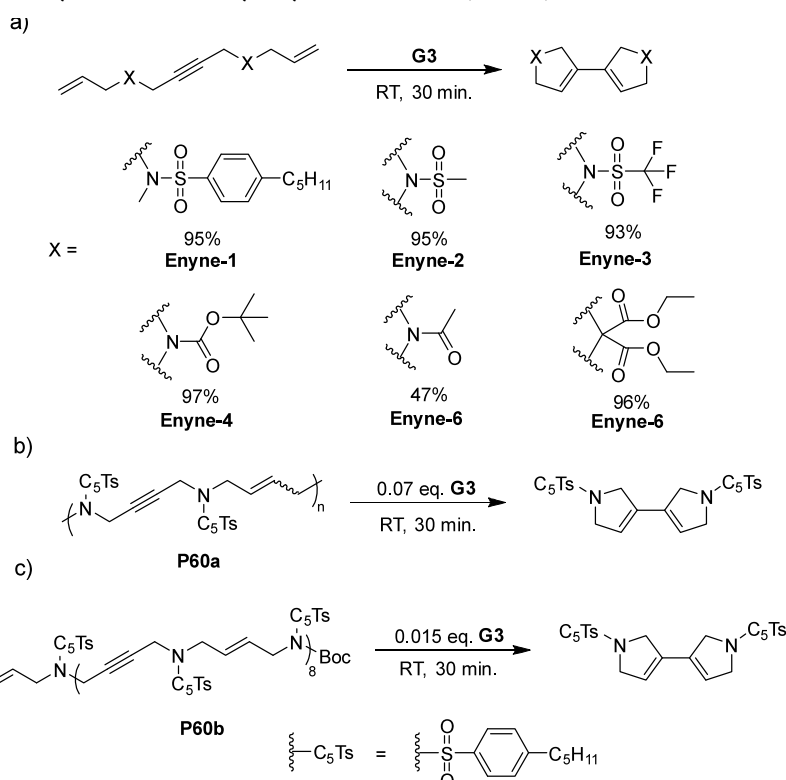
In 2015, Choi and co-workers demonstrated a new olefin-metathesis-based polymerization approach that involved a cascade of multiple metathesis events.⁸⁴ The incorporation of a monomer involved sequential ring-opening, ring-closing, and ring-opening events to lead to an olefinic polymer with a cycloolefin ring in the polymer backbone. The monomer design consisted of two cyclopentene rings connected by either an oxygen atom (**M52a**), nitrogen of a *p*-toluene sulfonamide (-NTs) group (**M52b**), or carbon atom (at position 5 of a 1,3-dioxane group, **M52c**) substituted at the allyl position of each cyclopentene (Scheme 12a). The cyclopentene ring was chosen for this design because of its ability to undergo both ring-opening and ring-closing metathesis. To avoid formation of cross-linked gels, polymerization had to be carried out at lower concentrations (below the critical monomer concentration)—only under these conditions would the intramolecular ROM/RCM cascade be thermodynamically favorable. Due to the reversible nature of this polymerization, the polymer was also expected to be depolymerizable—upon treatment of a solution of the polymers ($[\text{olefin}]_0 = 40 \text{ mM}$ in DCM) with **G1** catalyst, the polymers could be depolymerized into various degrees (~13–34% depending on the linker group between the two cyclopentenes, Scheme 12a). Interestingly, for **M52a**, a higher concentration was required for polymerization (~1.5 M), a behavior that was reflected in the higher depolymerization conversion of **P52a**. In a follow-up study, other monomer structures were studied (Scheme 12b–e).⁸⁵ The bis-cyclohexenyl monomers (**M53a–c**) could not be polymerized since that would require ring opening of two very low-strain cyclohexene rings and form a more strained cyclopentene ring (Scheme 12b). Monomers that possessed a combination of cyclohexene and cyclopentene rings could be polymerized more readily (**M54a–c**), but still the conversions achieved were rather low (30–55%) for monomers other than **M54a** (~100%) (Scheme 12c). Further changing the olefin on the cyclopentene ring to the 3,4-positions resulted in more efficient polymerization to conversions over 90%, albeit requiring long reaction times (>16 h) (Scheme 12d). In the

final step of this iterative design strategy, the cyclohexyl ring was replaced with a cyclopentene ring, resulting in monomers (Scheme 12e) that could be polymerized much faster, to high conversions, and with a range of monomer/initiator ratios. The depolymerization of all three generations of polymers was tested and appeared to follow the opposite trend of the polymerization behavior (Scheme 12c–e). Notably, the polymer prepared from **M5a–d** (Scheme 12e) showed the lowest extent of depolymerization. The depolymerization, however, was not studied in detail, and there may be room to enhance monomer recovery by further tuning the depolymerization conditions. It is interesting to note that the thermodynamics considerations must account for the multiple metathesis events that occur here—polymerization is driven by both the ease of ring-opening of the two cycloolefins and the ease of formation of the cycloolefin in the backbone.

2.5. Other Olefin-Metathesis Based Chemically Recyclable Polymers

Hodge and co-workers studied the synthesis of olefinic polyesters and polycarbonates via acyclic diene metathesis (ADMET) polymerization of α,ω -olefins with one or two ester groups in the backbone, and an α,ω -olefin-containing carbonate as well as their chemical recycling to cyclic oligomers (Scheme 13).⁸⁶ The resulting polymers had molecular weights of 5–20 kDa and had low glass transition temperatures, with some showing melting temperatures in the range of 52–85 °C. The olefin stereochemistry was 70–82% *trans* and 18–30% *cis*. These polymers could be depolymerized/degredated into cyclic oligomers when treated with ~1 mol % **G1** catalyst, in a dilute solution (~1 wt %/v). The reaction was rather slow, taking multiple days to proceed to equilibrium. The resulting products were a mixture of cyclic oligomers of various sizes, with the monomeric and dimeric species forming the majority of products. For most of these polymers, the predominant driving force for depolymerization is entropy due to the large size of monomers (≥ 15 -membered, except for 2 cases with 9- or 12-membered rings), the strain of which would be minimal. For the two polymers with the smaller repeat units (9 and 12 atoms), no monomers were formed, likely due to the strained nature of these structures, with the majority of the product being the larger cyclic dimer. These oligomer mixtures could also be recycled to make polymers in the presence of 1 mol % **G1** or **G2** catalysts, with conversions of >90% for all.

In 2021, Niu and co-workers reported polymers that could undergo head-to-tail self-immolative degradation via enyne cascade metathesis.⁸⁷ To enable monomer design, model compound studies were performed with fused 1,6-enynes with a linker between adjacent alkyne and alkene groups (i.e., an

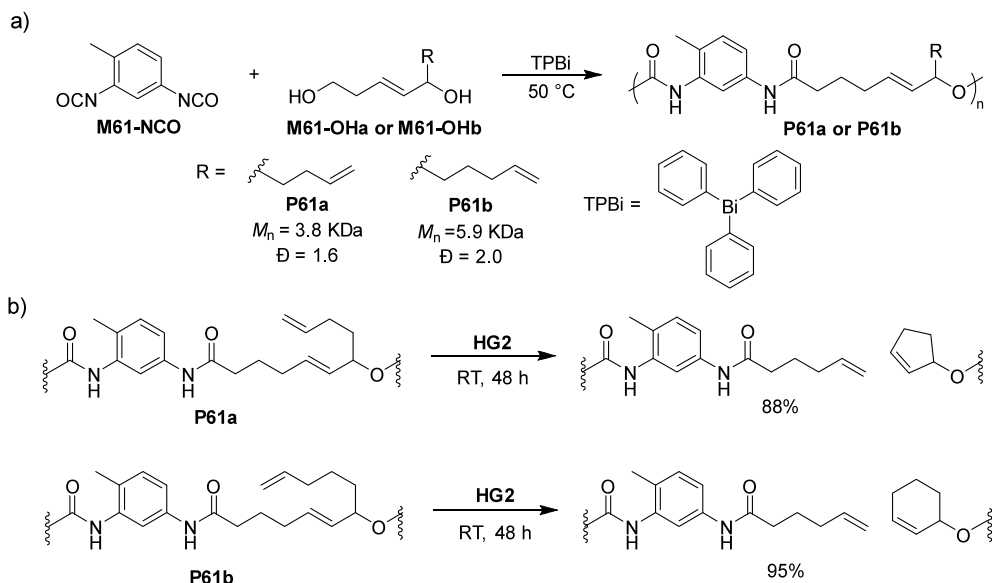
Scheme 14. Self-immolative Polymers Enabled by Enyne Metathesis (Ref 87)^a

^a a) Small-molecule enyne metathesis model studies with fused 1,6-enyne analogues with different linkers connecting the alkene and alkyne groups (0.15 M in THF or DCM, 0.03 equiv of G3). b) Degradation of 1,6-enyne polymers (60a–b) without terminal alkene groups, prepared by polycondensation of the corresponding disulfonamide alkyne and dibromobutane ($[\text{olefin}]_0 = 60 \text{ mM}$ in THF, 0.07 equiv of G3). c) Degradation of allyl-sulfonamide-terminated 1,6-enyne octamer prepared by iterative exponential growth (IEG) polymerization ($[\text{olefin}]_0 = 60 \text{ mM}$ in THF, 0.015 equiv of G3).

internal alkyne and two terminal alkenes, as shown in Scheme 14a). Enyne metathesis experiments with these model substrates revealed that having a sterically demanding functional group attached to the linker X led to the highest conversion (Scheme 14a) (reminiscent of the Thorpe–Ingold effect).^{51,52} Similar reactions with a model compound possessing two terminal alkynes and an internal alkene were much less productive with a conversion of ~10%, which was attributed to the lower reactivity of the vinyl carbene formed in this case as compared to the vinylidene carbenes formed in the previous case. A *p*-toluene sulfonamide-based linker was chosen for the monomer design due to good solubility and high enyne metathesis conversions of the corresponding model compound. Polymers with high molecular weight (P60a) could be obtained by polycondensation between A–A and B–B type monomers—a disulfonamide alkyne and *cis* and *trans*-1,4-dibromobutane in the presence of Cs_2CO_3 . Despite lacking terminal alkenes, these polymers could be degraded via enyne metathesis, albeit under high catalyst loading (~7 mol % G3 with respect to monomer repeat units) (Scheme 14b). It should be noted that the degradation here generates a bis-cyclopentene small molecule, not the monomer. To understand the role of alkene end groups, the authors prepared polymers via the iterative exponential growth method and end-capped them with an allyl-*(p*-toluene sulfonamide). Mechanistic studies indicated that the resulting polymers were depolymerized via an end-to-end process and required lower catalyst loadings (1.5 mol % G3 catalyst). This mechanism is discussed further in Section 5. On the other hand, the AA–BB

type polymers first underwent chain scission at internal alkenes to initiate depolymerization, which would result in an active chain and a dead chain, with the active chain depolymerizing in an end-to-end fashion and the dead chains undergoing another chain-scission event. To enable the AA–BB type polymers prepared by polycondensation to undergo depolymerization in a similar manner, they were end-capped with allyl bromide to install terminal alkene chain ends (~74% of the chains were successfully end-capped). The resulting polymer underwent efficient depolymerization with lower catalyst loadings (~3 mol % G3 catalyst) than the AA–BB type polymers without the alkene chain ends (Scheme 14c). Temperature-controlled depolymerization of these polymers was also studied using a metathesis catalyst inhibited with tributylphosphite which could be activated at ~100 °C—at these temperatures, the depolymerization was complete in a span of minutes. Although this material may not be perfectly self-immolative due to the partial end-capping, it nonetheless provides an interesting route toward triggered small molecule release via metathesis-based degradation.

In a strategy different from what has been discussed so far, Jones and co-workers synthesized polyurethanes which incorporated diols possessing internal and pendant olefins such that they could be cleaved via ring-closing metathesis between the pendant and internal olefins to form low-strain 5- or 6-membered cyclic olefins.⁸⁸ Initially, two different polyurethanes were prepared by a step-growth reaction between 2,4-toluene diisocyanate (M61-NCO) and either *E*-nona-3,8-diene-1,5-diol or *E*-deca-3,9-diene-1,5-diol (M61a–

Scheme 15. Metathesis-Based Degradable Polyurethanes (Ref 88)^a

^aPolymerization and metathesis degradation: a) Synthesis of polyurethanes containing moieties that can undergo cleavage via ring closing metathesis. b) Chemical recycling of polyurethanes in the presence of HG2 catalyst.

b) in the presence of triphenylbismuth (Scheme 15a, P61a–b). In the presence of ~2 mol % HG2 catalyst, these polymers could be degraded almost quantitatively to yield dicarbamate small molecules with different combinations of either allyl and/or cycloalkene groups (Scheme 15b). The authors further prepared polymer networks based on this chemistry. To this end, the diols were polymerized with two different multifunctional isocyanates, biuret of hexamethylene diisocyanate (HDIB, functionality = 3) and polymeric diphenylmethane-diisocyanate (PMDI, functionality = 2.7), to yield a flexible ($T_g = 33\text{ }^\circ\text{C}$) and a rigid ($T_g = 107\text{ }^\circ\text{C}$) network, respectively. The flexible network disintegrated and became soluble when submerged in a solution of HG2 catalyst in CHCl_3 and yielded low-molecular-weight products with NMR chemical shifts similar to those observed in the degradation of the linear polymer. On the other hand, although the rigid PMDI-based network degraded into a coarse powder in the HG2/ CHCl_3 solution, the poor solubility of the products in CHCl_3 precluded analysis. Interestingly, when the degradation was done in THF, soluble products were formed. The molecular weight distributions of the degradation products showed that the network fragmented into smaller fractions with a low molecular weight but broad molecular weight distribution. Repolymerization of these degraded networks was also attempted via thiol–ene chemistry with a trifunctional thiol, resulting in the formation of very high-molecular-weight polymers ($>10^7\text{ Da}$). This repolymerization was, however, partial, and the material was not characterized beyond size exclusion chromatography. Although the metathesis-based degradation achieved here is not truly closed-loop in nature, it introduces an interesting new approach for the chemical recycling of a commercially relevant class of materials, especially considering that approaches toward chemically recyclable polymer networks are very limited.

3. METATHESIS-BASED DEGRADATION OF COMMERCIAL POLYMERS

Olefin metathesis is a useful tool for the degradation of commercial polymers since it can effectively cleave carbon–carbon bonds in a well-controlled catalytic process under mild conditions. To the best of our knowledge, the first example was reported by the Hummel group in 1970 for the degradation of cross-linked polybutadiene (PB).⁸⁹ The metathesis-based degradation happens through intrachain cyclization when no chain transfer agent (CTA) is present or through interchain CM when a CTA is present, resulting in low-molecular-weight unstrained cyclic olefins or linear species, respectively. Compared to oxidative degradation methods, olefin metathesis retains the structural information and the properties of polymers well; it was therefore extensively used for the microstructural analysis of rubbers.^{90–92} Moreover, enabled by the excellent functional group tolerance of modern metathesis catalysts,⁸⁵ olefin metathesis was also widely used to convert olefinic commercial polymers into functional polymers, such as telechelic polymers. Olefin-metathesis-based degradation has been applied to a wide range of unsaturated and saturated polymers, serving purposes including analysis, synthesis of new polymers, and chemical recycling.

Most metathesis-based degradation studies of commercial unsaturated polymers were based on polybutadiene and polyisoprene. These studies have been summarized well in other reviews;^{89–99} thus, they will not be discussed in this review. Our focus in this section will instead be on metathesis-based degradation of polyolefins and some other commercial polymers.

3.1. Metathesis-Based Degradation of Polyolefins

Conventional polyethylene degradation methods typically involve pyrolysis and/or hydrocracking, but the adoption of these approaches has been limited.¹⁰⁰ For example, pyrolysis requires a high temperature ($>500\text{ }^\circ\text{C}$) and generates products with a wide distribution of molecular weights and a wide range

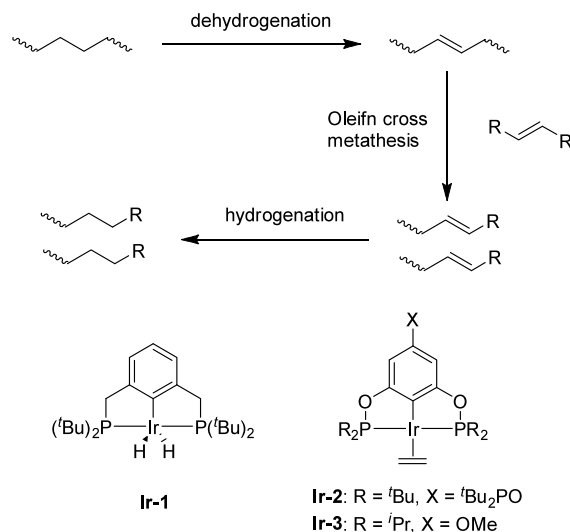
of functionalities. Hydrocracking requires reactive gases, which can pose safety concerns.

Recently, there has been growing interest in exploring the potential of olefin metathesis for the degradation of polyolefins, especially polyethylene, with the aim of developing milder and more practical chemical recycling strategies. Such methods usually involve the introduction of unsaturation, followed by olefin metathesis to convert a polyolefin into small molecules with well-defined functionality.

Polyethylene degradation based on “alkane metathesis” is one such approach. This process needs only mild temperatures and does not require a reactive gas as a reagent. The generated products are usually alkanes in the oil or wax form. This chemistry was first proposed by the Brookhart group in 2006 for the metathesis of *n*-alkanes.¹⁰¹ It utilized a combination of dehydrogenation, olefin metathesis, and hydrogenation in tandem to convert the substrates into smaller saturated hydrocarbons. The dehydrogenation step would introduce double bonds to the substrate, while cross-metathesis and isomerization of the generated olefins would lead to a change in the molecular weight and subsequent hydrogenation would lead to the formation of smaller saturated hydrocarbons.

In 2016, Guan, Huang, and co-workers applied a similar strategy, namely cross alkane metathesis (CAM), for degrading polyethylene (Scheme 16).¹⁰² It could quantitatively degrade

Scheme 16. Degradation of Polyethylene via Cross Alkane Metathesis (Ref 102)

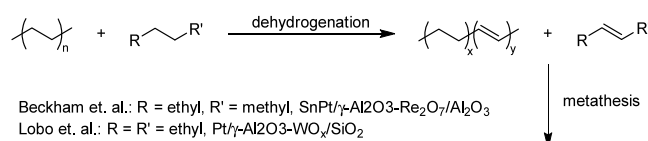


HDPE (M_w up to 3350 Da) to an oil that contains mainly C₇–C₁₂ hydrocarbons. In this process, pincer Ir catalysts (Ir-1, Ir-2, and Ir-3) (Scheme 16) were used for the dehydrogenation of polyethylene (PE) and *n*-hexane, while Re₂O₇/Al₂O₃ was used to catalyze the olefin CM to reduce the molecular weight of the dehydrogenated PE. Dehydrogenation, olefin metathesis, and hydrogenation occurred in a tandem manner in one pot. Catalyst Ir-2 was shown to be more active for (de)hydrogenation compared to Ir-1, resulting in a higher conversion of PE into oil. A similar method was then applied to high-molecular-weight commercial-grade PEs, including HDPE (M_w up to 1,740 kDa), LDPE, and LLDPE. All the studies showed complete degradation of PE as indicated by GPC and a high conversion (>50%) of polymers into fuel or wax. The CAM degradation showed good control on the

distribution, with dispersity as low as 1.3 after 4 days of degradation.

Since 2021, several other groups have developed other tandem dehydrogenation–metathesis strategies for polyethylene degradation. Beckham and co-workers developed a fully heterogeneous catalyst system, using Pt/ γ -Al₂O₃ or SnPt/ γ -Al₂O₃ for dehydrogenation and Re₂O₇/Al₂O₃ for olefin metathesis (Scheme 17). When SnPt/ γ -Al₂O₃ and Re₂O₇/

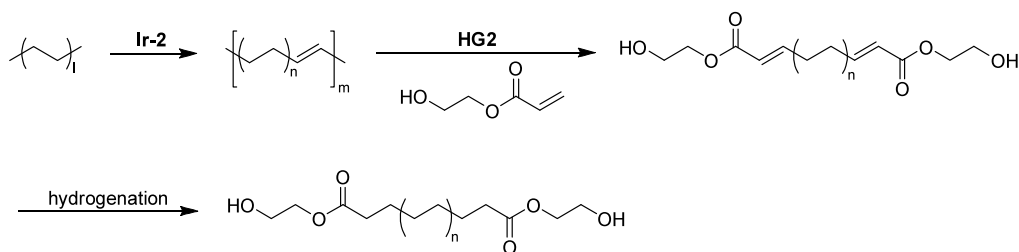
Scheme 17. Cross-Alkane Metathesis Degradation of Post-consumer PE in the Presence of Heterogeneous Catalysts (Refs 103, 104)^a



^aAlkane-metathesis-based degradation of post-consumer polyethylene in the presence of heterogeneous dehydrogenation and metathesis catalysts based on refs 103, 104. A mixture of polyethylene and short-chain alkane (pentane or *n*-decane) undergoes dehydrogenation. The resulting polyethylene with olefin functionality is degraded to smaller olefins via cross-metathesis with the dehydrogenated alkanes.

Al₂O₃ were used for degradation at 200 °C, 99 wt % of the loaded PE were recovered as alkanes in the liquid phase, and the remaining polymer showed a molecular weight reduction from 54 kDa to 31 kDa.¹⁰³ Lobo and co-workers modified the catalyst system, using WO_x/SiO₂ for olefin metathesis and Pt/ γ -Al₂O₃ for dehydrogenation (Scheme 17). Compared to Re₂O₇/Al₂O₃, WO_x/SiO₂ is less expensive and allows for higher operating temperatures, significantly reducing the reaction time. It only took 3 h to degrade LDPE from a M_w of ~75 kDa to <1 kDa, and the distribution was also narrowed significantly from $D = 8.3$ to 1.2. Interestingly, in small molecule studies, alkane metathesis still happened in the absence of Pt/ γ -Al₂O₃. It is presumably due to the WO_{3-x} species in WO_x/SiO₂, which has been reported to show (de)hydrogenation reactivity.¹⁰⁴ Coates and co-workers applied a similar strategy to recycle HDPE and make telechelic oligomers (Scheme 18).⁷ HDPE was dehydrogenated using Ir-2 as the catalyst to reach a low extent of unsaturation (<0.8%), followed by CM using HG2 with 2-hydroxyethyl acrylate to introduce 2-hydroxyethyl ester chain ends. After hydrogenation to remove unsaturation, the resulting telechelic oligomers were used as a macromonomer to make a polyester, which showed thermal properties similar to those of HDPE.

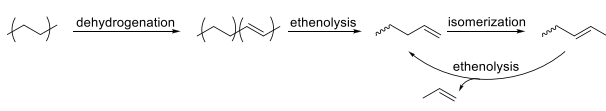
In 2020, Guironnet and Peters proposed a strategy for the degradation of PE that involves the reaction of PE with ethylene to generate propylene.¹⁰⁵ They gained inspiration from the Shell higher olefin process (SHOP) process, which is an important process to synthesize linear α -olefins in industry using olefin isomerization and olefin metathesis reactions in a tandem manner. They proposed that SHOP can be applied to degrade PE containing an olefinic group. An estimation of the thermodynamics suggested that the process was highly thermodynamically favorable in the presence of excess ethylene. Detailed calculations on the kinetics of reactions at various relative reaction rates showed that at the same rate of isomerization, faster ethenolysis would lead to higher selectivity in generating propylene and faster reduction in the molecular weight.¹⁰⁵

Scheme 18. Upcycling of Polyethylene Waste via a Dehydrogenation/Cross-Metathesis Approach (Ref 7)^a

^aPolyethylene was dehydrogenated and converted to telechelic oligomers via cross-metathesis. The oligomer after hydrogenation was used to make polyesters and poly(ester amide).

In 2022, Hartwig and co-workers demonstrated the feasibility of generating propylene by reacting partially dehydrogenated PE with ethylene (Scheme 19), and they

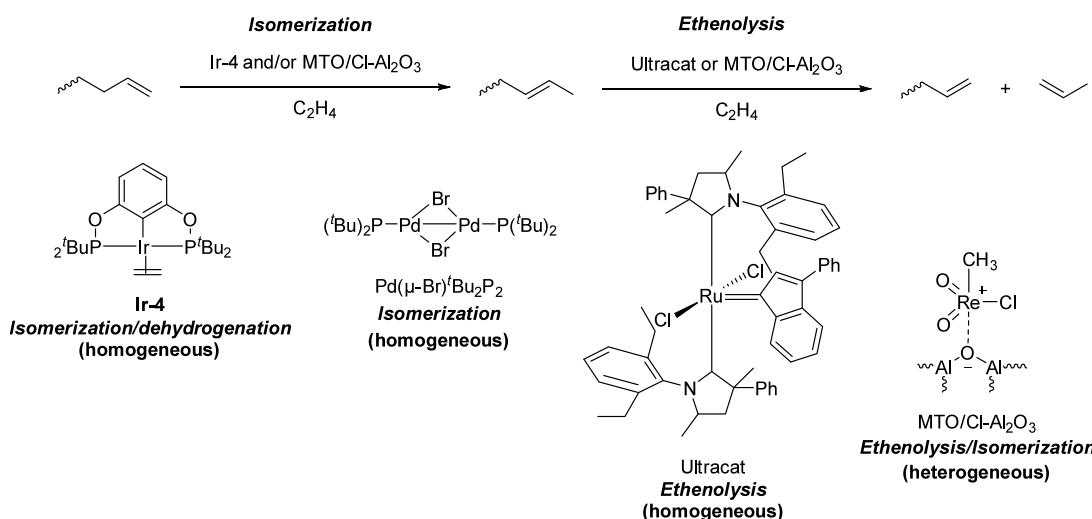
Scheme 19. Degradation of Polyethylene via Dehydrogenation and Isomerizing Ethenolysis (DIE) to Generate Propylene (Ref 6)



named the process dehydrogenation and isomerizing ethenolysis (DIE).⁶ Compared to alkane metathesis, this method selectively generates a single product—propylene, a commercially important chemical building block and monomer. The process involved dehydrogenation to introduce ~2% unsaturation, followed by isomerization and ethenolysis (I/E) to degrade the dehydrogenated polyethylene into propylene. During the I/E process, the unsaturated polyethylene was cleaved into terminal olefins, followed by isomerization from terminal olefins (1-alkenes) into 2-alkenes. The resulting 2-alkene undergoes olefin metathesis with ethylene to generate propylene and another 1-alkene. As the process progresses, the dehydrogenated HDPE would eventually be converted into

propylene. The authors tested several combinations of catalysts for the I/E process and found that the combination of $[\text{PdP}(\text{Bu})_3(\mu\text{-Br})]_2$ and HG2 showed the highest yield of over 80% from HDPE. Interestingly, DIE for dehydrogenated LDPE showed a lower yield compared to HDPE with the same degree of unsaturation, probably due to the slower isomerization of trisubstituted alkenes generated from the branches during I/E. The DIE process is also compatible with commercial HDPE and LDPE, but purification of the polymers is necessary in some cases.⁶

Notably, Guironnet and Scott also reported the chemical recycling of PE by tandem catalytic conversion into propylene (Scheme 20).¹⁰⁶ They designed a semicontinuous flow reactor for the process. Through the screening of a range of catalyst combinations, the combination of Ultracat catalyst and $[\text{PdP}(\text{Bu})_3(\mu\text{-Br})]_2$ was found to work best for the I/E process, resulting in 94% selectivity to generate propylene. The mass of collected propylene corresponded well to the weight loss of PE (24 wt % vs 27 wt % loss of PE). In the case of heterogeneous catalysts, methyltrioxorhenium/Cl-Al₂O₃ (MTO/Cl-Al₂O₃) showed the highest conversion (50%) and selectivity (95%). Interestingly, they pointed out the possibility of using ethylene as the hydrogen acceptor to introduce unsaturation on PE, allowing the DIE process to be performed in a one-pot manner. Although when this was attempted with a

Scheme 20. Degradation of Polyethylene via Dehydrogenation and Isomerizing Ethenolysis (DIE) to Generate Propylene (Ref 106)^a

^aPolyethylene was dehydrogenated and converted to telechelic oligomers via cross-metathesis. The oligomer after hydrogenation was used to make polyesters and poly(ester amide)s.

saturated PE using Pt/ γ -Al₂O₃ and MTO/Cl-Al₂O₃, it resulted in only 1 wt % conversion, it nonetheless suggested the possibility of such an intriguing process.⁹⁷

3.2. Metathesis-Based Degradation of Other Commercial Polymers

In addition to polyolefins, metathesis-based degradation has also been applied to halogenated polymers. For example, De Vos and co-workers utilized olefin metathesis as part of a process for the degradation of chlorinated polyethylene (CPE).¹⁰⁷ Dehydrochlorination of CPE ($M_w \sim 48$ kDa, 36% Cl) was performed using [P₄₄₄₂][(C₂H₅O)₂PO₂] (an ionic liquid known for catalyzing fast dehydrochlorination of lightly cross-linked PVC). This was followed by washing (neutralizing), drying, and ethenolysis using HG2, resulting in 34% conversion to α,ω -dienes and α -olefins. GC-MS showed that the reaction yielded C₅ to C₂₀ hydrocarbons, including 1,5-hexadiene (6.6%) and 1,6-heptadiene (7.3%). Although the work focused on the dehydrochlorination of both PVC and CPE, ethenolysis was not conducted on dehydrochlorinated PVC.¹⁰⁷ Similarly, Abu-Omar et al. recently reported a bromination–dehydrobromination–metathesis process for the degradation of PE. PE (<10 kDa) was first subjected to bromination using bromine under irradiation to generate brominated PE (BPE) with a high bromine content (21–32 wt %), followed by complete dehydrobromination under basic conditions to introduce unsaturation. Dehydrobromination generated unsaturated polyethylene with a few percent olefin units but also led to cross-linking in the case of a BPE with M_w of 15 kDa. Ethenolysis using ruthenium indenylidene catalyst 9 (Figure 2) resulted in a mixture of olefin-terminated oligomers with molecular weight <1 kDa.¹⁰⁸

4. EFFECTS OF EXPERIMENTAL CONDITIONS ON METATHESIS-BASED DECONSTRUCTION

In the previous sections, we looked at approaches toward new chemically recyclable polymers based on olefin metathesis and the application of olefin metathesis to chemical recycling of commercial polyolefins and polyalkenamers. In this section, we delve deeper into the effects of experimental conditions on RCM-based depolymerization and CM-based degradation processes. To be more specific, we will be looking at how concentration, temperature, pressure, catalysts, and additives (such as chain-transfer agents) affect depolymerization yields and rates in this context.

4.1. Effects of Experimental Conditions on RCM-Based Depolymerization/Degradation

4.1.1. Concentration Effects. The overall polymer concentration can affect the reaction rate and yield of depolymerization, as discussed in Section 2. One notable example that shows this phenomenon is the degradation of 1,4-polybutadiene. Wagener demonstrated the degradation of 1,4-polybutadiene in bulk through addition of G1 catalyst.¹⁰⁹ Although the 1,4-polybutadiene and the G1 catalyst were not mixed thoroughly at the beginning of the experiment, degradation at the contact surface allowed the polymer to liquefy after 2–3 h of reaction. The catalyst was then easily mixed into the polymer through mechanical agitation. The 1,4-polybutadiene with molecular weight of 2000–3000 kDa was degraded into smaller 1,4-polybutadiene fragments with molecular weights of ~7.2 kDa after 48 h of reaction at ambient temperature. Sels and co-workers conducted the degradation of 1,4-polybutadiene with G1 catalyst in DCM at

35 °C and lower concentration of [olefin]₀ = 0.17 M for 8 h.¹¹⁰ They achieved 83% conversion of degradation, turning a 250 kDa 1,4-polybutadiene into cyclic oligomers with molecular weight <1 kDa. The difference between the results of these two studies suggests that lower concentration led to a greater extent of degradation.

Further details about the effects of feed concentration on the extent of degradation at equilibrium are discussed in Thorn-Csányi's investigation of polymerization/degradation equilibrium in the 1,4-polybutadiene system.¹¹¹ It has been reported that regardless of the starting material for the reaction, such as *cis*-1,4-polybutadiene, 1,5-cyclooctadiene (COD), or *ttt*-cyclododecatriene (CDT), the resulting product in polymerization/degradation equilibrium is a mixture of polymers and cyclic oligomers. Chauvin and co-workers reported that the polymerization/degradation equilibrium of 1,4-polybutadiene system is in between the polymer and the cyclic oligomers, and, therefore, COD does not participate in the product mixture.¹¹² Specifically, in Thorn-Csányi's report, it was confirmed that cyclic oligomers are mostly trihexameric rings.^{111,113} When the feed concentration was less than 0.455 M, complete degradation into cyclic oligomers was observed, and a linear increase in the cyclic oligomer concentration was observed as the feed concentration increased. When the feed concentration was above 0.455 M, the polymer concentration was found to increase and the cyclic oligomer concentration as a function of feed concentration to deviate from a linear trend, with the cyclic oligomer concentration eventually reaching a plateau. The concentration at this plateau was defined as the saturation concentration, which was 0.445 M at 25 °C (this is similar to the “critical concentration” as defined by Grubbs, Kornfield, and co-workers⁴³ and discussed earlier in this review). Interestingly, the cyclic oligomer concentration increased above the saturation concentration when the feed concentration was above 1.8 M, which was also observed in Chauvin's report.¹¹² The saturation concentration of the cyclic trimer was the greatest among the cyclic oligomers. The “turning point concentration”, which is the feed concentration at which the polymer concentration became nonzero, showed a linear relationship with the degree of polymerization.¹¹² This can be explained by the increased translational entropy gain from depolymerization/fragmentation at lower concentrations, favoring oligomers with a smaller degree of polymerizations. The trend of saturation concentration and turning point concentration of *ttt*-CDT and *ctt*-CDT supports this explanation. Since *ttt*-CDT has lower ring strain energy, it has a higher saturation concentration than *ctt*-CDT. However, since the number of repeat units and the translational entropy for both *ttt*-CDT and *ctt*-CDT are the same, their turning point concentrations are the same.

Polymers of fused-ring cyclooctenes also show a decrease in the extent of depolymerization as the concentration increases. Wang and co-workers reported the depolymerization of poly(*trans*-cyclobutane-fused cyclooctene) at various concentrations and temperatures (P24–27, Figure 7).³⁰ When the depolymerization was conducted at 50 °C and up to 200 mM olefin concentration with G2 catalyst, the change in conversion with concentration was insignificant. However, when the concentration was increased above 200 mM, the conversion dropped more significantly. The depolymerization conversion consistently stayed above 90% at concentrations below 200 mM and dropped to 84% and 66% at 400 mM and 600 mM, respectively. A follow-up study that investigated the

depolymerization of other fused-ring cyclooctene polymers reported similar trends in depolymerization (Figure 9).⁷⁴ Polymers based on cyclooctenes with *trans*-fused 5-membered-ring acetals at the 5,6-positions (P33–37) exhibited a decrease in the extent of depolymerization as the concentration increased. It was suggested that a rise in concentration leads to a smaller gain in translational entropy during depolymerization, thus disfavoring depolymerization. Additionally, polymers prepared from monomers with a lower T_c (Table 2, M31–37) showed a smaller decrease in the extent of depolymerization at increased olefin concentration. RCM-based depolymerization was accompanied by a decrease in rotational entropy, and the constrained conformation of the *gem*-disubstituted system was thought to lower this loss of rotational entropy compared to other monomers. Hence, since the effect of translational entropy is less significant at higher concentrations, the smaller decrease in rotational entropy of the *gem*-disubstituted system led to a higher depolymerization conversion at high concentrations.

The effect of the olefin concentration on depolymerization has also been investigated for polypentenamers. The extent of depolymerization of polypentenamers also appears to be negatively correlated to the feed concentration of the olefinic repeat units.⁵⁷ Kennemur's report on the depolymerization of polypentenamer-based bottlebrush polymers (P13-g-PS) also shed light on the influence of concentration on the depolymerization kinetics (Scheme 7, Figure 5).²⁸ In their report, a higher concentration led to a faster depolymerization. When the olefin concentration was consistent, the polymers with different backbone lengths or side chain lengths had similar depolymerization kinetics. When the overall olefin concentration is the same and the backbone length is different, the concentration of the terminal olefin is also different. This suggests that the depolymerization rate is zeroth order with respect to terminal olefins. Overall, a higher olefin concentration results in faster depolymerization but lower conversion of depolymerization.

4.1.2. Temperature Effects. Temperature often influences the depolymerization/degradation conversion by affecting the Gibbs free energy change for the reaction. One of the first reports discussing the influence of reaction temperature on the RCM-based degradation of olefinic polymers is the work on 1,4-polybutadiene by Chauvin and co-workers.¹¹² Interestingly, the equilibrium oligomer concentration was consistently ~44% as the reaction temperature was raised from 5 to 40 °C. In contrast, Thorn-Csányi's report shows dramatic change in equilibrium oligomer concentration across a temperature range from 4 to 50 °C.¹¹¹ It was shown that a lower temperature led to a higher rate of conversion of degradation. When the concentration of each oligomer was tracked to obtain the thermodynamic data, only the cyclic trimer had significant enthalpy loss for degradation, while other oligomers had no enthalpy change. This suggests that only the equilibrium concentration of the cyclic trimer is affected by the temperature change. In Chauvin's report, the cyclic trimer was only ~2% of the total oligomer content (as a result of the catalyst used in that study); this would explain why conversion did not seem to change with temperature in that work.¹¹² The temperature dependence of the degradation conversion changes at a lower temperature range.¹¹⁴ When the temperature used for the degradation decreased to below the precipitation temperature of 1,4-polybutadiene in the reaction solvent (studied below 3 °C for a reaction in toluene), the

degradation conversion decreased with temperature. This is mostly due to the changed enthalpy and entropy for the formation of *ttt*-CDT from 1,4-polybutadiene since *ttt*-CDT is the dominant product of degradation. *cis*-1,4-Polybutadiene undergoes isomerization into *trans*-1,4-polybutadiene at the precipitation point, resulting in a crystalline chain accompanied by a negative enthalpy change. As a result, the enthalpy change for the degradation process into *ttt*-CDT becomes positive. Hence, when *ttt*-CDT is the major product for the degradation of *cis*-1,4-polybutadiene, the extent of degradation is maximized at 3 °C.

Due to the positive enthalpy and entropy changes for the depolymerization of polypentenamer, many investigations have reported that increased temperature favors depolymerization.^{28,52,57,60,115,116} When cyclopentene was copolymerized with high-strain monomers such as norbornene, it was found that equilibrium cyclopentene concentration increased as the temperature rose, regardless of the presence of the comonomer and the type of metathesis catalyst used.^{52,57,116} It was also shown that although the T_c of polypentenamer derivatives changes as the attached functional groups change (Table 1), the trend of depolymerization conversion increasing with temperature was observed for all derivatives.⁶⁰ Additionally, since the boiling points of the cyclopentene derivatives are low, the equilibrium of the depolymerization could be easily affected. Tuba et al. showed that increasing the temperature of depolymerization of polypentenamer to 50 °C resulted in complete depolymerization since the continuous removal of cyclopentene (boiling point ~44 °C) fully shifted the equilibrium to depolymerization.^{57,59} Similarly, Schrock et al. reported that lower pressure facilitates depolymerization by removing cyclopentene and shifting the equilibrium to full depolymerization.¹¹⁵

In the case of *trans*-cyclobutane-fused cyclooctene systems (Figure 7, P24–27), the influence of temperature at the conversion of depolymerization is less significant.³⁰ The difference between the depolymerization conversions at 50 and 19 °C was negligible. This is because of the lower gain in translational entropy and higher loss in rotational entropy for depolymerization, which resulted in a smaller magnitude of the entropy change and a smaller temperature effect on the depolymerization conversion. Although the temperature did not affect the conversion of depolymerization significantly, the effect of temperature on kinetics was clearly observed, as faster consumption of polymer was observed at higher temperature. At the initial stage of depolymerization, a mixture of cyclic oligomers and monomers was produced, followed by the further transformation of oligomers into the monomer. While most of the product after 10 min of depolymerization was the monomer when the depolymerization was conducted at 45 °C, more oligomers were produced than monomers after 10 min of depolymerization at 19 °C. These results suggested that the formation of cyclic oligomers was kinetically favored (10 min at 19 °C), but the formation of the monomer was thermodynamically favored (10 min at 45 °C). Hence, the influence of temperature on depolymerization of *trans*-cyclobutane-fused cyclooctenes system is more significant at the early stage of depolymerization but almost negligible at equilibrium.

4.1.3. Effects of Catalysts and Catalyst Loading. The nature of the metathesis catalyst and its loading has been shown to have a significant impact on not only the rate of

degradation but also the degradation products in some instances.

Degradation of 1,4-polybutadiene via RCM results in the formation of oligomers of various sizes. The type of catalyst and its loading can affect the conversion of degradation and the ratio of the resulting product. According to Chauvin's degradation study of 1,4-polybutadiene, when **1**/TiCl₄ (activated by UV light) or **2**/TiCl₄ was used, only 2% of the product at equilibrium was found to contain CDT.¹¹² In Thorn-Csányi's study where **3** or **4** was used, most of the product at equilibrium was CDT.¹¹¹ Sels and co-workers presumed that the degradation of 1,4-polybutadiene involves the formation of C₁₆–C₄₄ oligomers followed by the transformation of oligomers into CDT.¹¹⁰ Taken together, it is likely that Chauvin's catalysts could not convert the C₁₆–C₄₄ cyclic oligomers into CDT while those used by Thorn-Csányi could. Ru(Pcy₃)₂ complexes, such as **G1**, gave a higher conversion of degradation than did W- or Mo-based Schrock complexes did. However, in the presence of these catalysts, the C₁₆–C₄₄ cyclic oligomers could not be converted into CDT either. Sels and co-workers have demonstrated that the low yield of CDT with Ru(Pcy₃)₂ complexes (first generation) is not due to the deactivation of the catalyst, since increasing catalyst loading or sequential addition of catalyst increased neither the overall conversion nor the fraction of CDT among the produced oligomers. **HG1** catalyst and indenylidene Schiff base Ru complex **16** resulted in slower degradation and a slightly lower degradation conversion than when catalyst **5** or **7** was used, but comparable degradation conversion was obtained after prolonged reaction time. Ru complexes with N-heterocyclic carbene (NHC) ligands (second generation) led to a high yield of CDT in the degradation of 1,4-polybutadiene. Additionally, the formation of C₁₆–C₄₄ oligomers when using Ru-NHC complexes as the catalyst is much faster than that when Ru(Pcy₃)₂ is used as the catalyst. The difference was attributed to the different energy barriers in forming the metallacyclobutane transition states when different catalysts were used. This hypothesis could be verified by further studies with Ru(Pcy₃)₂ catalysts at elevated temperatures. When catalyst **17** was utilized, the steric hindrance from the bulky adamanyl NHC ligand led to lower reactivity and, therefore, a lower degradation conversion compared to other second-generation catalysts. Interestingly, while the ligand steric effect in catalyst **17** did not affect the fraction of CDT among the produced oligomers, *tcc*-CDT was found to be the major product, while most of the second-generation catalysts mainly produced *ttt*-CDT. Lastly, utilizing the **G3** catalyst for degradation gave mostly C₁₆–C₄₄ cyclic oligomers due to fast deactivation of the catalyst. As described above, the choice of metathesis catalyst for the degradation of 1,4-polybutadiene not only affects the conversion of the degradation but also the ratio of the produced oligomers and the stereoselectivity.

Polypentenamer and the fused-ring cyclooctene-based polymers are less affected by the catalyst choice for RCM depolymerization due to their high tendency to depolymerize. Multiple W- and Mo-based catalysts show no difference in affecting the thermodynamics of depolymerization of polypentenamer.^{55,115,116} Ru catalysts only showed slightly better performance in depolymerizing the polypentenamer. Moreover, the resulting thermodynamics of the depolymerization of polypentenamer are identical with different generations of Grubbs catalysts. In the case of depolymerization of polypentenamer-based bottlebrush polymers (Figure 4),

depolymerization with **G3** showed the fastest depolymerization rate among various Grubbs catalysts.²⁸ Interestingly, while **G1** is typically less active than **HG2** for RCM, the depolymerization of these bottlebrush polymers proceeded more rapidly with **G1** than with **HG2**. This phenomenon was attributed to the fast reuptake of the *o*-isopropoxystyrene ligand by the growing chain end in the case of **HG2**, thus interrupting the depolymerization of the chain. Depolymerization of *t*CBCO-based polymers also did not show any difference in the equilibrium depolymerization conversion with different Grubbs catalysts.^{30,79} Moreover, *t*CBCO-based block copolymers can also undergo complete depolymerization with both **G1** and **G2**. However, when PPh₃ was added as an additive to suppress secondary metathesis, a notable difference in the polymerization activity of the different catalysts was observed. In their work involving living ROMP of *t*CBCO-based monomers (Figure 11), Wang and co-workers demonstrated that the depolymerization of *t*CBCO-based polymers in the presence of catalyst **G1** could be inhibited by PPh₃.⁷⁹ Interestingly, when catalyst **G2** was used with PPh₃, the depolymerization was suppressed to a much lesser extent. This could be attributed to the preferential coordination of the Ru-NHC complex to olefin over phosphine.

4.2. Effects of Experimental Conditions on Cross-Metathesis-Based Degradation

4.2.1. Concentration Effects.

Competing reaction pathways typically exist in the case of the CM-based degradation of unsaturated polymers. While CM degradation requires olefins along the backbone of the polymer, metathesis catalysts, and chain transfer agents (CTAs), RCM depolymerization requires only backbone olefins and metathesis catalysts. Hence, RCM can occur concurrently with CM. However, the influence of the polymer concentration on the depolymerization/degradation via each pathway is different. As discussed earlier, a lower concentration of polymers leads to greater depolymerization conversion at the equilibrium of the reaction in most RCM depolymerizations. Sadaka and co-workers reported that the degradation of polyisoprene in toluene with *cis*-1,4-diacetoxy-2-butene (DAB) as the CTA and with **G2** as the catalyst was enhanced at higher concentrations of polyisoprene (as indicated by lower molecular weight of the products at higher feed concentrations).¹¹⁷ Furthermore, a report by Mouawia and co-workers showed a similar trend for the CM degradation of PI by DAB in the presence of **G2** with a phosphonium ionic liquid (Cyphos I) as the solvent.¹¹⁸ In these cases, the enhanced CM degradation at higher concentrations of polymers can be attributed to the promoted bimolecular reaction at higher concentrations.

4.2.2. Effects of Catalysts and Catalyst Loading.

It has been shown in CM degradation of polyisoprene or polybutadiene that fast degradation occurred at the early stage of the reaction, and the degradation then suddenly slowed down or stopped.^{117,119,120} Moreover, it was observed that increasing catalyst amount led to further degradation of unsaturated polymers.^{117,119–122} These results suggest that the deactivation of the catalysts took place during CM degradation. Additionally, Fontaine, Pilard, and co-workers demonstrated that with different catalyst concentrations, while the degradation rate was slowed down after a similar reaction time, the resulting molecular weight right before a decrease in the reaction rate was lower in the case where catalyst loading was higher.¹¹⁹ Pilard and co-workers reported that in the

presence of *cis*-butene-1,4-diol as CTA, the degradation of polyisoprene slowed down drastically after 30 min.¹²⁰ Further, their studies involving degradation of low-molecular-weight hydroxytelechelic polyisoprene ($M_n = 5000$) showed no reduction in molecular weight. Increasing the temperature or CTA equivalences also did not lead to any decrease in molecular weight. The lack of molecular weight reduction could be due to catalyst poisoning caused by the hydroxyl groups.

Since **G1** catalyst shows low efficacy toward metathesis of trisubstituted olefins, the CM degradation of polyisoprene is less effective when **G1** is utilized. Since catalyst deactivation also takes place, degradation using the **G1** catalyst often leads to incomplete degradation before deactivation of the catalyst. **G2** catalyst, on the other hand, has better performance toward trisubstituted olefins. Hence, **G2** shows faster CM degradation on polyisoprene, and, therefore, leading to lower molecular weight of the degraded polymer before the slowdown of reaction rate.¹²⁰ The greater reactivity of **G2** catalyst is further highlighted in the investigation of CM degradation of polybutadiene containing vinyl, *cis*, and *trans* olefins by Thompson, Khosravi, and co-workers.¹²³ It has been proposed that *cis* olefins have the highest reactivity for CM among the three types of alkenes. When CM was investigated with **G1** and **G2** catalysts, the resulting degraded polymer contained a smaller fraction of *cis* olefins when the **G2** catalyst was utilized. This suggests that the greater activity of the **G2** catalyst led to greater consumption of *cis* olefins during degradation. Although the superior activity of the **G2** catalyst compared to the **G1** catalyst led to enhanced degradation, the deactivation of the catalyst was still a problem. The low stability of the **G2** catalyst at high temperatures led to incomplete degradation of polybutadiene in the work by Wagener and co-workers.¹²⁴ Since no evidence for the presence of a hydroxyl group at the polymer chain end was reported, and the reaction took place at 50 °C under argon, it was suggested that the low thermal stability was the main cause for inhibited degradation. On the other hand, utilization of **HG2** catalyst (known to have higher thermal stability than **G2**) for CM degradation led to complete degradation where every unsaturated repeating unit was reacted. Finally, degradation using a mixture of **G2** catalyst and CuI showed degradation conversions comparable to those obtained using **HG2** catalyst and much greater than what was obtained using **G2** catalyst; the improved degradation using CuI as the cocatalyst was attributed to the stabilization effect of CuI on **G2**.¹²⁵ These results indicate that the thermal stability of the metathesis catalyst is the major factor determining the extent of degradation in this case.

4.2.3. Effects of Chain-Transfer Agents and Their Loading. Chain-transfer agents are essential reagents for CM degradation since the metathesis between CTA and alkenes along the polymer backbone results in chain scission. The structure of CTAs can often affect this process, since the metathesis catalysts can interact with the CTAs, even leading to catalyst deactivation in some cases. DAB is one of the CTAs that has been often utilized due to its high activity for CM.^{117,118,120,126} However, similar structures such as dimethyl fumarate and dimethyl maleate show poor performance for CM degradation.^{123,126} Gutiérrez and Tlenkopatchev have shown that while DAB and *cis*-1,4-dichloro-2-butene can be utilized to degrade polyisoprene via CM to produce well-defined telechelic oligomers, dimethyl maleate does not

degrade polyisoprene as well as other CTAs.¹²⁶ The degradation using dimethyl maleate results in products with molecular weights much higher than theoretical molecular weight. Thompson, Khosravi, and co-workers demonstrated that dimethyl fumarate has even lower activity toward CM than dimethyl maleate.¹²³ Gutiérrez and Tlenkopatchev reasoned that the carbonyl oxygen of dimethyl maleate coordinates with the 14-electron Ru center of the catalyst, resulting in deactivation of the catalyst, while the carbonyl oxygen of DAB does not. Similarly, carbonyl oxygen can deactivate tungsten-based Schrock catalyst.¹²⁷ Computational calculations at the B3LYP/LACVP* level of theory showed that the nonproductive complex in which the carbonyl oxygen of DAB coordinates to the Ru center is higher in energy than the productive complex in which the double bond of DAB coordinates to the Ru center; however, the nonproductive complex of **G2** catalyst and dimethyl maleate is lower in energy than the productive complex.¹²⁷ Similar effects have been observed in the investigation of Jiang and co-workers.¹¹⁸ While the CM degradation with α -olefins like 1-octene, 1-dodecene, or 1-tetradecene can efficiently degrade polybutadiene in a controlled manner, that with methacrylates (such as cyclohexyl methacrylate or isobornyl methacrylate) is challenging. Degradation using cyclohexyl methacrylate or isobornyl methacrylate requires high catalyst loading and long reaction times to achieve meaningful reduction of molecular weight, which is still much higher than what one can achieve with other CTAs. Similar to the case of dimethyl maleate and dimethyl fumarate, the carbonyl oxygen in methacrylates coordinates to the Ru center to form nonproductive complexes and inhibits polymer degradation. Wagener has reported that when two or more methylene spacers are utilized to separate the olefin from the carbonyl, the formation of a nonproductive complex can be avoided.^{127,128} Therefore, when diethyl 4-octene-1,8-dioate was used for the CM degradation of 1,4-polybutadiene, the degradation led to efficient formation of difunctional telechelic ester oligomers. Additionally, Wagener showed that 3-hexene-1,6-diol was a poor CTA since the alcohol functionality deactivates the catalysts. Hence, when the silyl-ether-protected CTA was utilized instead, a difunctional telechelic monomer and dimer were obtained. However, the silyl-ether-protected CTA did not give purely telechelic oligomers, which was attributed to the oxygen β to the alkylidene causing deactivation of the catalyst before complete degradation. However, degradation using 2-butene-1,4-diylbis(phthalimide), (which contains one spacer between the olefin and imide) as the CTA was nearly quantitative. This was attributed to the weaker coordination of nitrogen of the imide functionality to the Ru center due to a sterically shielded lone pair and electron delocalization in the imide nitrogen atom. Overall, although certain structural features can cause CTAs to interact with metathesis catalysts and to deactivate them during CM degradation, several measures can be used to obviate such effects.

It has been reported multiple times that increasing the CTA equivalence often facilitates the CM degradation.^{119–121,130} Increased concentrations of CTA lead to enhanced CM degradation. Furthermore, since the molecular weight is decreased to approach the minimum value, the molecular weight dispersity tends to decrease as the CTA concentration is increased. Additionally, Fontaine, Pilard, and co-workers demonstrated that increasing the amount of CTA with respect to polymer resulted in improved chain-end functionaliza-

tion.¹¹⁹ This is also because of more abundant CM that is taking place due to the increased concentration of the reagent. Another study by Pilard and co-workers showed that the deceleration of the reaction rate due to the deactivation of the catalyst was slower when a higher concentration of CTA was utilized.¹²⁰ This suggests that the coordination of CTA to the catalyst is competing with the deactivation of the catalyst. Since the amount of CTA is increased, the coordination of the olefins in the CTA is favored over the deactivation to suppress the deceleration of the degradation rate. An extensively used CTA is ethylene since it has superior reactivity toward CM and produces unique products with alkene chain ends. Such CM degradation is often named retro-ADMET since it generates the small molecules which, when polymerized by ADMET polymerization, would yield the starting polymer backbone. Wagener has reported that increasing ethylene pressure favors the ethenolysis over the intramolecular reaction of polybutadiene.¹³¹ However, increasing the ethylene pressure above 400 psi resulted in decreased conversion of degradation because the high ethylene concentration can allow self-metathesis of ethylene to compete with the CM between ethylene and polybutadiene. Furthermore, decomposition of the catalyst can take place to lower the conversion. Bazan and co-workers also reported that the degradation conversion increased up to certain point then decreased significantly when the ethylene pressure was increased.¹²² Hence, there is an optimal amount of CTAs that maximizes the degradation, since the self-metathesis reactions of the polymer and CTAs compete with the CM of each other.

4.2.4. Influence of Metathesis Catalyst on Tandem Dehydrogenation and Olefin Cross-Metathesis Degradation. Since the dehydrogenation of saturated polyolefins requires high temperatures, when the degradation reaction is conducted with both the dehydrogenation catalyst and metathesis catalyst, the stability of both catalysts is crucial to maintaining the catalyst activity during the reaction. One of the initial investigations by Goldman, Brookhart, and co-workers showed that utilizing Schrock-type catalyst 4 as the metathesis catalyst resulted in the suppressed degradation of polyethylene.¹⁰¹ It was suggested that the thermal deactivation of catalyst 4 suppressed the degradation. The deactivation of the catalyst was consistent with the observation that the product concentration plateaued with prolonged reaction times. Also, supplementing additional catalyst 4 resulted in the further production of low-molecular-weight alkanes. Hence, the supported Re metathesis catalyst $\text{Re}_2\text{O}_7/\text{Al}_2\text{O}_3$, which exhibited a high thermal stability, was utilized to achieve improved degradation. Silica-supported tungsten oxide (WO_x/SiO_2) is another candidate to be used as a metathesis catalyst for the degradation of saturated polymers. However, during the activation process of the catalyst, aldehydes and ketones can be produced. The presence of such species can deactivate the tungsten oxide species and suppress the degradation of the polymer after dehydrogenation. Zeolite 4A was therefore utilized as an absorbent for polar species in the study by Kim and co-workers (Scheme 17).¹⁰⁴ It was shown that the addition of zeolite 4A indeed promoted degradation significantly, while degradation without zeolite 4A failed. When the tungsten oxide catalyst was utilized with zeolite 4A and a Pt-based dehydrogenation catalyst, the degradation of LDPE was achieved with efficiency comparable to those in other works on the degradation of PE with Re catalysts. Since the tungsten oxide catalyst is more affordable compared to Re

catalysts but showed similar performance in the degradation of saturated polymers, the authors proposed tungsten oxide as a promising catalyst candidate for chemical degradation/upcycling of PE. In conclusion, the major challenge with tandem dehydrogenation and CM degradation is the deactivation of the catalyst. Since there are multiple factors that can lead to the deactivation of known metathesis catalysts, it is crucial to identify those factors to obviate deactivation and develop improved catalyst systems suitable for degradation.

4.2.5. Influence of Short-Length Alkane on Tandem Dehydrogenation and Olefin Cross-Metathesis Degradation. Since the tandem dehydrogenation and olefin CM degradation involves dehydrogenation of both polymer and short alkane followed by CM degradation, the selection of short alkane can affect factors such as heat/mass transfer, solubility of the polymer, and the substrate–catalyst interaction. Guan, Huang, and co-workers reported that the hydrogenolysis reactivity of HDPE was significantly increased when hexane was used compared to when pentane was used (Scheme 16).¹⁰² It was proposed that the physical state of the short alkane in the reaction affects the solubility of PE and, therefore, degradability since hexane was utilized as a liquid while pentane was utilized as a supercritical fluid. According to the study by Lobo and co-workers, the degradation of PE in the presence of decane showed slower reduction in molecular weight than the degradation in the presence of heptane (Scheme 17).¹⁰⁴ However, although decane resulted in slower molecular weight reduction, the relative reaction rate of decane with the polymer was higher than that of heptane with the polymer. The slower reduction in molecular weight of the polymer in the case of decane was ascribed to the incorporation of decane, which has a higher molecular weight than heptane. Interestingly, the prolonged reaction with heptane resulted in an increased fraction of low-molecular-weight alkanes, while the prolonged reaction with decane resulted in an increased fraction of high-molecular-weight alkanes. This is also possibly due to the short length of the polyethylene analogue utilized for this part of the study (C_{16}). Similar to Guan and Huang's work, the higher reactivity of decane, compared with that of heptane, could be attributed to their different states—decane was in the liquid state while heptane was in the supercritical state. It was also suggested that the high solubility of the intermediates and products in the liquid alkanes facilitated the degradation.

4.2.6. Influence of Dehydrogenation Catalyst on Tandem Dehydrogenation and Olefin Cross-Metathesis Degradation. Although the dehydrogenation catalysts do not directly deconstruct the polymer during tandem (de)-hydrogenation and olefin CM processes, they set up the foundation for metathesis degradation by the generation of olefins. Since the location and concentration of olefins affect the CM degradation, the reactivity and selectivity of the dehydrogenation catalyst can affect the overall degradation behavior. The study by Guan, Huang, and co-workers (Scheme 16) highlights the influence of the regioselectivity of dehydrogenation catalysts on degradation.¹⁰² It was demonstrated that the utilization of regioselective iridium catalysts Ir-2 and Ir-3 that selectively form internal alkenes led to higher yield of low-molecular-weight alkanes compared to when iridium catalyst Ir-1 was utilized. Interestingly, Ir-2 and Ir-3 exhibited greater efficiency in PE degradation and produced more long-chain alkanes as the products than did Ir-1. These results support the hypothesis that catalysts that selectively

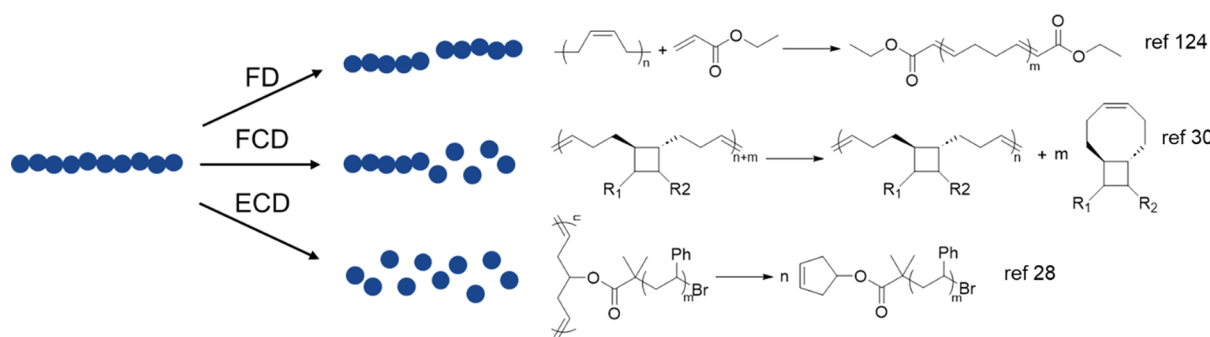


Figure 15. Three general mechanisms of olefin-metathesis-based polymer deconstruction with literature examples.

generate internal alkenes can promote tandem dehydrogenation and olefin CM degradation.

Beckham et al. demonstrated the viability of using $\text{Pt}/\gamma\text{-Al}_2\text{O}_3$ and $\text{SnPt}/\gamma\text{-Al}_2\text{O}_3$ as dehydrogenation catalysts (Scheme 17).¹⁰³ It was shown that the catalytic activity of $\text{SnPt}/\gamma\text{-Al}_2\text{O}_3$ was much higher than that of commercially available $\text{Pt}/\gamma\text{-Al}_2\text{O}_3$, while both catalysts showed similar product selectivity. Although the synthesized $\text{Pt}/\gamma\text{-Al}_2\text{O}_3$ catalysts showed greater activity than commercial $\text{Pt}/\gamma\text{-Al}_2\text{O}_3$, the activity of $\text{SnPt}/\gamma\text{-Al}_2\text{O}_3$ was still higher. This was attributed to the stabilization effect of Sn on Pt, which decreased the deactivation rate of Pt. However, the dehydrogenation catalyst and metathesis catalyst were still susceptible to deactivation, and, therefore, the conversion of degradation was not improved significantly by the addition of Sn. In addition, the influence of the pretreatment procedure of $\text{SnPt}/\gamma\text{-Al}_2\text{O}_3$ with $\text{Re}_2\text{O}_7/\gamma\text{-Al}_2\text{O}_3$ was investigated. It was shown that when the catalysts were mixed before the pretreatment, polymer degradation was facilitated, likely because mixing of the catalysts before pretreatment results in the coexistence of multiple metals in one particle. However, when the catalysts were synthesized so that either the Re_2O_7 was on $\text{SnPt}/\gamma\text{-Al}_2\text{O}_3$ or SnPt was on $\text{Re}_2\text{O}_7/\gamma\text{-Al}_2\text{O}_3$, the performance of the catalysts decreased significantly, although the reactive surface area was comparable to $\text{SnPt}/\gamma\text{-Al}_2\text{O}_3$. This was ascribed to the reduced support for the Re catalyst and therefore the decreased number of metathesis sites as the alloy was formed. Therefore, when additional $\text{Re}_2\text{O}_7/\gamma\text{-Al}_2\text{O}_3$ was added to the alloy catalysts, a higher degradation conversion was observed. Hence, it was concluded that the closer proximity of the metathesis catalyst to the dehydrogenation catalysts could enhance polymer degradation, but the two catalysts on the same support led to failed metathesis reactions.

5. MECHANISMS OF OLEFIN-METATHESIS-BASED DECONSTRUCTION

As discussed in previous sections, unsaturated polymers (and saturated polymers that can be converted into unsaturated polymers) can be chemically recycled by means of olefin metathesis. In this section, we will establish a classification of different depolymerization/degradation mechanisms observed in some of the above systems and the metathesis processes involved therein.

An appropriate classification is desired for better understanding and differentiating various olefin-metathesis-enabled depolymerization/degradation processes. The defining features for this categorization are (a) where the initiation of the reaction occurs and (b) whether the polymers are fragmented into well-defined small-molecule products in a continuous

fashion. Therefore, we categorize the olefin-metathesis-based depolymerization/degradation processes in the literature based on their characteristics, and each will be discussed below.

5.1. Fragmentation Degradation

Fragmentation degradation (FD) involves random chain scissions along the unsaturated polymer backbone, leading to polymer fragments with reduced molecular weight (Figure 15). In this classification, the metathesis reaction involved is typically an intermolecular CM reaction between the backbone olefins and other alkene species. Due to the random fashion of the cleavage and the differences in the nature of the other alkene species, it is helpful to further divide the mechanism into two subcategories: alkenolysis and alkane metathesis.

5.1.1. Alkenolysis. This involves CM between internal olefins along the polymer backbone and external small-molecule olefins as CTAs. As discussed in Section 4.2.3, changing the structure of the concentration of CTAs results in different activities toward CM degradation. The mechanism behind them is basically the same. Analogous to hydrolysis/alcoholysis of polyesters, CM reactions between a CTA and a polymer backbone alkene lead to degradation of the molecular weight by fragmentation of the polymer chains (Scheme 3). Increasing the concentration of CTAs relative to the polymer concentration favors the formation of metal alkylidene species, shifting the equilibrium in the direction of degradation products.^{119,120} Ethylene is the simplest olefinic CTA, and the CM between ethylene and internal olefins leads to the cleavage of the latter to give 1-olefins. This specific type of CM was first dubbed “ethenolysis” by Bradshaw et al.¹³² The mechanism of ethenolysis follows the general Chauvin mechanism proposed for the olefin metathesis reactions catalyzed by metal alkylidene complexes, and is a special case of the cross-metathesis mechanism (Scheme 3).³⁷

In the 1990s, Wagener and co-workers reported a series of CM-based degradation studies of 1,4-polybutadiene using monoenes, including terminal alkenes and symmetric internal alkenes, as CTAs via an alkenolysis mechanism which they termed acyclic diene metathesis (ADMET) degradation.^{129,131,133,134} Dienes are produced in ADMET degradation of polymers, which is the reverse process of ADMET polymerization, where dienes condense to form polymers. Precise difunctional telechelic oligomers ($f = 2.0$) were synthesized from ADMET degradation of 1,4-polybutadiene with α,ω -allylsilanes using well-defined Schrock’s catalyst.¹³³ Following this report, they went on to employ various functionalized monoenes to prepare telechelics with diverse functionalities, including ester, silyl ether, and imide groups.¹²⁹

Supported by the data reported in Hummel's and Wagener's respective work,^{129,135} Wagener proposed a mechanism scheme for the ADMET degradation.¹²⁹ The excess monoene CTA first reacts with a metal alkylidene catalyst to dimerize into a symmetric olefin, driven by the evolution of ethylene gas that was evidenced by NMR spectroscopy, along with the formation of a new metal alkylidene derived from the CTA. In the meantime, polybutadiene intramolecularly metathesizes to generate macrocyclic polybutadiene. The macrocycle is then ring-opened by the CTA-based alkylidene, through a metalocyclobutane intermediate, to generate an oligobutadiene with the metal center at the α -position and the monoene from CTA at the ω -position. The metal alkylidene chain end and the CTA dimer then undergo CM to produce the telechelic product and regenerate the CTA-derived metal alkylidene.

CM between electron-rich olefins (Type I) and electron-deficient olefins (Type II) is essentially irreversible.³⁹ Wagener and co-workers introduced the idea of insertion metathesis depolymerization by utilizing the irreversible CM between acrylates as CTAs and polybutadiene.¹²⁴ Once thought to impede productive metathesis,^{128,129} electron-deficient olefins possess high selectivity in metathetic degradation of polybutadiene into largely butadiene diester. However, the degradation was not complete, as evidenced by the presence of butadiene dimer diesters. There was also a small population of diethyl fumarate from homodimerized acrylate and butadiene monoester, the latter of which was believed to be the product of insertion metathesis and ethenolysis as a result of ethylene being generated as the CM byproduct. Utilizing this selective metathesis reaction, a polymer-to-polymer transformation was realized when acryloyl chloride was used as the CTA, to afford a polyamide after hexamethylenediamine was introduced to the difunctional acyl chloride. Insertion metathesis depolymerization has recently been employed by Coates and co-workers to prepare telechelic isotactic polypropylene from CM between propylene–butadiene copolymer and 2-hydroxyethyl acrylate.¹³⁶ The hydroxyl and ester functionalities enabled the repolymerization of the initially metathetically depolymerized polypropylene and subsequent degradation through transesterification using a Lewis acid and a Lewis base, respectively. This chemistry was also applied to post-consumer polyethylene from a water jug, where the unsaturation was introduced to the hydrocarbon backbone via dehydrogenation using an iridium-based catalyst.⁷

Alkenolysis has not only been utilized to depolymerize rubber polymers for recycling,⁹⁰ microstructure analysis,^{92,94} and synthesis of telechelics,^{120,95,129,96} which have been discussed in detail in several reviews,^{93,87–99} but has also been recently employed together with dehydrogenation and isomerization to turn polyethylene into value-added propylene monomer.^{7,105} The mechanism is discussed in Section 3.2 (Schemes 16–20).

Without externally added CTAs, alkenolysis of unsaturated polymers is also possible to occur, through intra- and/or intermolecular CM and/or RCM, driven by the entropic gain. Initially observed by Hummel et al., vulcanizates, or cross-linked rubbers, could be depolymerized with the catalyst system $\text{WCl}_6/\text{AlC}_2\text{H}_5\text{Cl}_2/\text{C}_2\text{H}_5\text{OH}$ with or without low-molecular-weight olefins as CTAs.⁸⁹ They reasoned that such a polymer network swollen in a solvent underwent metathesis to form completely soluble products, driven by a gain in entropy.

Watson and Wagener first observed the complete degradation of high-molecular-weight polybutadiene into lower-molecular-weight oligomers using G1 in the absence of any solvents or CTAs.¹⁰⁹ Due to the inevitable amounts of vinyl content in commercial *cis*-1,4-polybutadiene, the degradation is entropically driven by the extrusion of vinyl cyclohexene from RCM reactions along the backbone olefins of a 1,4–1,2–1,4 triad. The generated vinyl cyclohexene molecule then serves as a CTA via CM with polymer backbone olefins. RCM within a tail-to-head 1,4–1,2 diad, CM between metathesis catalyst, or vinyl cyclohexene and polymer backbone all lead to the reduction of the molecular weight. When a polybutadiene sample with a higher vinyl content from 1,2-insertion was used, lower-molecular-weight degradation products were obtained, verifying the mechanism associated with the pendent vinyl acting as CTA. The degradation products possessed a dispersity of 2.0 in both high- and low-vinyl-content polymers, suggesting a random fashion of the chain scission. Despite being more reactive, complex 4 (Figure 2) failed to liquefy the solid polymers, due to a much higher crystalline *trans* content that hindered the diffusion kinetics. Owing to the presence of 1,2-insertion in any 1,4-polybutadiene, cross-linked polybutadiene networks could also be depolymerized into a mobile liquid in the presence of ruthenium catalysts.¹¹⁰

Degradation of polybutadiene with low 1,2-linkages at low concentrations ($[\text{C}_2\text{H}_4] < 0.3 \text{ M}$) was shown to favor the formation of large cyclic oligomers (C_{16} to C_{44}).¹⁰¹ As the concentration of macrocyclic oligobutadienes decreased, following an initial spike, that of cyclododecatriene (C_{12}) saw a concomitant increase. This observation, therefore, suggested a rapid backbiting of the polymer to form the kinetic products, macrocycles, succeeded by their conversion into the thermodynamically favored cyclododecatriene via consecutive ring-opening and ring-closing metathesis events. When polybutadiene samples with a higher amount of vinyl were used, more linear oligomers were generated from RCM within the 1,4–1,2–1,4 triad, similar to the results in the bulk degradation study.¹³⁷

5.1.2. Alkane Metathesis. As mentioned above, dehydrogenation can be used to introduce carbon–carbon double bonds on the saturated polymer backbone, allowing for the degradation of the resulting unsaturated polymers through subsequent alkene metathesis. Pioneered by Brookhart and co-workers,^{101,138} catalytic alkane metathesis by dehydrogenation–olefin-metathesis–hydrogenation catalysis has proven to be a powerful tool to transform saturated polymers, more specifically, polyethylene, into short alkanes.^{102,103} The mechanism is discussed in Section 3.2 (a representative example is shown in Scheme 16).

5.2. Fragmentation Followed by Continuous Depolymerization

Section 2 gave a comprehensive discussion on metathesis-based depolymerizable polycycloalkenes, the depolymerization of which is consistent with the reversible nature of the polymerization.^{28–30,42,55,57,59,60,66,76,83} While the depolymerizability and depolymerization thermodynamics are determined by the ring size, substituents, concentration, etc., the depolymerization mechanisms through different systems are quite similar. Investigation into the depolymerization mechanisms of various polyalkenamers all revealed a similar depolymerization profile,^{28,30,56,83} in line with a depolymerization mechanism that we term fragmentation followed by

continuous depolymerization (FCD), as the depolymerization involves an initial fragmentation of the backbone before continuous depolymerization occurs (Figure 15). While the reversibility of metathesis polymerization/depolymerization had already been confirmed in certain cycloalkenes, cyclopentene, and bicyclo[4.3.0]nona-3,7-diene⁵² in 1972, the depolymerization mechanism was not known until a decade later.⁵⁶ Badamshina et al. investigated the depolymerization characteristics of polypentenamer with a tungsten catalyst by studying the changes in the molecular weight distribution during depolymerization. While cyclopentene was continuously generated as the depolymerization product, the dispersity (D) of the polypentenamer decreased from 5.1 to 1.8, and the relative molecular weight $\frac{M_n}{M_n^0}$ throughout the depolymerization was below what would be expected if the polymer undergoes an end-to-end depolymerization fashion. These results match well with the theoretical predictions for random depolymerization, when a parent chain cleaves into two daughter chains, with one being stable and the other depolymerizing into the monomer.¹³⁹ No significant influence of the initial catalyst concentration on the depolymerization profile was found, indicating a slow initiation process using this catalytic system. Kennemur and co-workers also investigated the depolymerization of a low-dispersity polypentenamer sample ($D = 1.2$) prepared from variable-temperature ROMP.²⁸ Gradual reduction in the molecular weight and broadening of distribution was observed. Despite the divergent observations in the relative change in dispersity in the above-mentioned two studies, the mechanism behind them is essentially the same, as the dispersities of both studies approached $D = 2$, which is a feature of random chain scission.

The depolymerization mechanism of the chemically recyclable *t*CBCO-based polycetenamers (Figure 7) was investigated by Wang and co-workers.³⁰ The depolymerization of this type of polymer using G2 led to the formation of the original monomer along with some cyclic oligomers of different ring sizes due to RCM in the form of backbiting. Rapid reduction in the molecular weight (below the diagonal of the $\frac{M_n}{M_n^0}$ vs conversion plot, which is expected for end-to-end depolymerization) confirmed the random chain scission mechanism.

It should be noted that while these above-mentioned polymers all depolymerize via a fragmentation–depolymerization two-step process, the depolymerization is reversible, the extent of which is governed by the thermodynamic conditions, e.g., concentration and temperature. There are examples of polymers that depolymerize through the FCD mechanism but are not prepared through equilibrium metathesis polymerization.⁶⁶ Wang et al. designed an unsaturated polyether that contains cyclobutane-fused tetrahydrofuran in each repeating unit, which upon mechanochemical activation of the cyclobutane moiety, each repeating unit is converted into three units of poly(2,5-dihydrofuran) (Scheme 8).⁶⁶ The latter polymer is not readily accessible because of the extremely low ceiling temperature, while the parent polymer before the mechanochemical transformation can be obtained at a high molecular weight. In the presence of G2, the mechanochemically generated poly(2,5-dihydrofuran) component depolymerized into 2,5-dihydrofuran, accompanied by a large decrease in the molecular weight.

5.3. End-to-End Continuous Depolymerization

Depolymerization often occurs through random chain scissions along the backbone, regardless of the chemistry on which the depolymerization is based; an end-to-end continuous depolymerization (ECD) occurs from one end to the other in an unzipping fashion (Figure 15). Shabat and co-workers demonstrated an early example of such depolymerizable polymers in the form of a polyurethane that unzipped from the chain ends through 1,6-elimination and decarboxylation reactions along the urethane backbone.¹⁴⁰ Such polymers that depolymerize continuously from head to tail were referred to as self-immolative polymers in some literature.^{81,140–145} The depolymerization of these self-immolative polymers is usually inhibited by kinetic stabilization of the chain ends and is triggered only when exposed to the stimuli of interest, including acid/base, light, heat, or an appropriate catalyst.

Most of these polymers are prepared through polycondensation and usually rely on nucleophilic depolymerization mechanisms. Few polymers depolymerize metathetically in an end-to-end manner.^{28,81,87} The first example was reported by Kennemur et al., in which they demonstrated depolymerizable bottlebrush polypentenamers (Scheme 7, Figure 5).²⁸ In contrast to linear polypentenamers, the depolymerization of which using G1 catalyst in chloroform occurs rapidly (85% after 4 min) and randomly along the polymer chains, as discussed in detail in Section 5.2, the bottlebrush counterparts depolymerized at a much slower rate (18% after 20 min) with no molecular-weight reduction or broadening observed by SEC. The absence of polymeric species with molecular weights between the initial bottlebrush and macromonomer suggests no chain scission occurred on the backbone and that the ruthenium benzylidene catalyst bound to one terminal olefin and continuous RCM proceeded all the way to the other end. The little change in molecular weight throughout the depolymerization also suggests that the initiation is much slower than the depolymerization and that once a ruthenium complex finds an olefinic chain end, the depolymerization occurs very rapidly to disintegrate the bottlebrush into the macromonomer. This is intriguingly analogous to the inverse of conventional radical polymerization. One might hypothesize that the depolymerization rate is dependent on the initial concentration of the terminal olefins since the initiation seems to be the rate-determining step. However, two depolymerizations conducted with different chain-end concentrations (0.10 and 0.06 μ M) using G1 showed very similar rates. Although it might be specific for G1, the kinetics of depolymerization of these bottlebrushes might be more dependent on the dissociation of the phosphine ligand from G1.

More recently, Wang and co-workers reported depolymerizable graft polymers synthesized from grafting-through polymerization of *E*-alkene-*t*CBCO-based macromonomers (Figure 12).⁸¹ These graft polymers exhibited a depolymerization mechanism similar to that of the polypentenamer bottlebrush polymers discussed previously; however, several characteristic differences were observed. Although there was little reduction in the molecular weight throughout the major course of the depolymerization, oligomeric species were observed from SEC evolution. The oligomers were determined to be star-like macromolecules with a cyclic oligocyclooctene core (i.e., lacking benzylidene or methylidene end groups) by matrix-assisted laser desorption/ionization time-of-flight mass spectrometry, resulting from backbiting RCM crossing multiple repeating units. The macrooligomers formed rapidly at the

very beginning stage of the depolymerization before they were gradually consumed as more macromonomer formed. This phenomenon resembles the depolymerization of 1,4-polybutadiene in dilute conditions, as mentioned in Section 5.1.1, that the depolymerization generates a mixture of oligomers as the kinetic products, which was eventually converted into the thermodynamically more stable monomer through a series of metathesis reactions.

All the above-mentioned depolymerization pathways occur through alkene-metathesis-based CM and/or RCM reactions. In Niu and co-workers' work discussed earlier (Section 2.5, Scheme 14),⁸⁷ their polymers contain a backbone of repeating 1,6-enynes, and the ruthenium-coordinated chain ends can continuously undergo consecutive *S*-*exo*-*dig* and *S*-*exo*-*trig* cyclizations to release 1,1'-bicyclopentene as the depolymerization product. Unlike the depolymerization of polymers synthesized from ROMP,^{30,59} which is based on the reversibility of such polymerization, the depolymerization of these enyne polymers is irreversible. The as-synthesized polymers lack alkene chain ends and thus depolymerize through an FCD mechanism with a characteristic reduction in molecular weight. Alkene chain ends can be conveniently introduced through end-capping with an allyl group. These alkene-terminated enyne polymers depolymerized much more efficiently than the analogues without olefin chain ends due to the presence of mobile chain ends via a head-to-tail ECD mechanism.

6. CONCLUSION AND OUTLOOK

The low cost, light weight, and high strength of polymers make them desirable materials compared with other structural solids, such as metals and ceramics. However, the durability and lack of recycling of polymers have caused societal concerns. To continue enjoying the use of polymeric materials, a sustainable polymer economy needs to be established. Efforts in this regard include recycling of current polymers and the redesign of new polymers that can be more efficiently recycled. Olefin metathesis, as an enabling chemistry for many fields, has found applications in both fronts. In this review, we discuss how olefin metathesis has been applied to the development of new chemically recyclable polymers and to the deconstruction of commercial polymers, how structural features and experimental conditions affect (de)polymerizability, and the mechanisms behind the deconstruction processes. Historically, it has been applied to the degradation and depolymerization of commercial olefinic polymers. More recently, there has been growing interest in new monomer designs for chemically recyclable polymers, as well as the use of olefin metathesis in tandem with other alkene chemistries to enable chemical recycling of saturated polyolefins. Nonetheless, several challenges remain to be addressed if these approaches are to be adopted as scalable real-world solutions.

Replacement of commodity polymers is challenging since any new materials would have to match the economic feasibility as well as properties offered by the currently used ones. Since there is a gap in the thermomechanical properties between most polymers discussed here and the commercial polymers (e.g., crystallinity), further development in this regard requires diversification of the material properties. While many of the studies discussed in this review utilize different functional groups to tune material properties, an important future direction would be the development of stereo- and regioregular depolymerizable ROMP polymers. It

has been shown that the position of substituents relative to the olefin group can control the regiochemistry (head–tail vs head–head) of monomer addition. This was demonstrated on cyclooctenes by Hillmyer and co-workers¹⁴⁶ and on cyclopentenes by Sita¹⁴⁷ and Kennemur and co-workers.¹⁴⁸ Additionally, catalyst choice can also affect the stereochemistry of olefin groups in ROMP polymers.^{149,150} Chemically recyclable olefinic polymers with such controlled microstructures could lead to more attractive material properties, especially the rather elusive semicrystallinity in current depolymerizable ROMP polymers.^{151,152}

Monomer design for such chemically recyclable polymers also stands to benefit from new computer-aided predictive techniques. Traditionally, such advances have been driven by slow iterations over well-understood systems, often with a slow trial-and-error approach. However, improvements in predictive modeling coupled with large monomer libraries rapidly screened through ab initio computational methods could lead to improved design processes toward better closed-loop materials. New works from Kennemur^{153,154} and Gutekunst¹⁵⁵ have contributed to interesting approaches for computational evaluation and prediction of the enthalpies of polymerization for different cyclic monomers. Approaches that do the same for entropies of polymerization could further aid in the rapid evaluation and prediction of the thermodynamics of polymerization for large libraries of monomers.

The cost of monomers is also a major hurdle that precludes the commercialization of most metathesis-based polymers. For example, polydicyclopentadiene is a rare commercial ROMP polymer owing to the low cost of the cyclopentadiene monomer. Most of the monomers discussed in this review are based on fossil fuels; designing monomers based on more environmentally friendly feedstocks, such as biobased materials and CO₂ can alleviate the reliance on finite natural resources. While closed-loop recycling and multiple usage would reduce the ultimate cost, technoeconomic analysis and life-cycle assessment need to be conducted to guide the optimization of the production processes.

The cost of catalysts is another important consideration for metathesis-based polymer deconstruction, which is involved in the chemical recycling of both newly designed and current commodity polymers. As a matter of fact, most metathesis-based deconstruction work discussed in this review has been conducted using catalysts based on transition metals, such as Ru, Mo, and W, which are much more expensive than the monomers and feedstocks recovered from the deconstruction of polymers. We envision two strategies that can be used to reduce the cost of the catalysts. First, the catalysts used for polymer deconstruction are typically unrecovered after the reaction. If they can be recycled and reused multiple times, then the cost associated with catalysts will be reduced. The recycling of metathesis catalysts can be facilitated by using supported catalysts and a continuous flow reaction setup, as they can enable economic feasibility, scalability, and ease of catalyst removal. The recycling of metathesis catalyst has been realized in Choi and Grubbs's recent work, where they demonstrated the synthesis of high-molecular-weight cyclic polypentenamer using a well-defined silica-supported ruthenium catalyst using a flow process.⁵⁸ This work indicates the feasibility of recycling metathesis catalysts for the deconstruction of polymers in a similar fashion. Another strategy to reduce the cost of metathesis catalysts is to develop inexpensive, alternative metathesis catalysts, such as those

based on abundant transition metals^{156–158} and those without a metal.^{159,160}

To make a significant dent in the plastic waste problem, chemical recycling of polyolefins is essential, since these polymers occupy >60% of the plastic market. The approaches of using olefin metathesis to deconstruct commercial polymers will continue to be developed. Many of the current approaches use large amounts of unrecoverable, expensive metathesis catalysts and do not necessarily generate high-value products. It is important that such chemical recycling approaches yield either monomers or other useful/high-value chemical building blocks in an economically feasible manner if the end-goal is utilization of polymer waste as chemical feedstocks. In this regard, approaches that allow depolymerization of polyolefins into olefinic monomers hold great promise. If made scalable and economically competitive with hydrocarbon feedstocks, such processes could potentially enable large-scale adoption of commodity plastic waste as chemical feedstock while also reducing the chemical industry's dependence on fossil fuels.

AUTHOR INFORMATION

Corresponding Author

Junpeng Wang – School of Polymer Science and Polymer Engineering, University of Akron, Akron, Ohio 44325, United States;  orcid.org/0000-0002-4503-5026; Email: jwang6@uakron.edu

Authors

Devavrat Sathe – School of Polymer Science and Polymer Engineering, University of Akron, Akron, Ohio 44325, United States

Seiyoung Yoon – School of Polymer Science and Polymer Engineering, University of Akron, Akron, Ohio 44325, United States;  orcid.org/0000-0002-2961-1505

Zeyu Wang – School of Polymer Science and Polymer Engineering, University of Akron, Akron, Ohio 44325, United States;  orcid.org/0000-0002-6343-0548

Hanlin Chen – School of Polymer Science and Polymer Engineering, University of Akron, Akron, Ohio 44325, United States

Complete contact information is available at:
<https://pubs.acs.org/10.1021/acs.chemrev.3c00748>

Notes

The authors declare no competing financial interest.

Biographies

Devavrat Sathe received a Bachelor of Technology degree in Polymer Engineering and Technology from the Institute of Chemical Technology in Mumbai in 2018. That same year, he moved to the Rubber Capital of the world, Akron, Ohio, USA, and started his doctoral studies in Polymer Science at the University of Akron. There, he worked in Prof. Junpeng Wang's lab, studying chemically recyclable polymers and bulk polymer mechanochemistry, receiving his Ph.D. in the fall of 2023. He has been selected to present in the Excellence in Graduate Polymer Research Symposium at the ACS Spring 2022 meeting and has won a Professor Harwood Award and an Eastman Travel Award.

Seiyoung Yoon is originally from Daejeon, South Korea. He earned his Bachelor of Arts degree in Chemistry from Grinnell College (Grinnell, IA) in 2020, where he investigated electrochemical impedance spectroscopy of silicon-based electrolytes for lithium-ion

batteries under the guidance of Professor Leslie J Lyons. He is currently pursuing his doctoral studies in Polymer Science at University of Akron, under the supervision of Prof. Junpeng Wang. His current research interests include sustainable polymers and polymer mechanochemistry. He has won a Maurice Morton Award and a Goodyear Fellowship.

Zeyu Wang received his B.E. in Polymer Materials and Engineering from Donghua University in 2018 and his M.S. in Polymer Science from University of Akron. He is currently a Ph.D. student in the lab of Prof. Junpeng Wang at University of Akron, where his research interest lies in chemically recyclable graft polymers and mechanochemically responsive polymer networks. He has received an Eastman Travel Award and a Darrell H. Reneker Scholarship.

Hanlin Chen, originally from Guangdong, China, received his B.E. in Macromolecular Materials and Engineering at University of Science and Technology of China, where he conducted research under the guidance of Prof. Changle Chen and Prof. Tongwen Xu. He was awarded his Ph.D. in Polymer Science from University of Akron in October 2023, focusing his research on polymer recycling and mechanochemistry in Prof. Junpeng Wang's lab. He has been awarded a Robert E. Helm Fellowship and a Polymer Modifier & Additives Division Scholarship. He is currently a Senior Research Associate at Brewer Science, where his work is concentrated on the development of materials for the advanced packaging and processing of semiconductors.

Junpeng Wang received a B.S. in Chemistry from University of Science and Technology of China (2010) and a Ph.D. from Duke University under the guidance of Prof. Stephen Craig. From 2016 to 2018, he worked as a postdoctoral fellow with Prof. Luping Yu at University of Chicago and Prof. Jeremiah Johnson at Massachusetts Institute of Technology. In 2019, he started his independent career at University of Akron, where he is now an Assistant Professor of Polymer Science. He has received a Sloan Research Fellowship and an NSF CAREER award. His research aims to address challenges in materials science by applying physical organic chemistry approaches.

ACKNOWLEDGMENTS

This material is based on work supported by the National Science Foundation under grant DMR-2042494. Acknowledgement is also made to the donors of the American Chemical Society Petroleum Research Fund (65048-DNI7) for partial support of this work. J. W. acknowledges the Alfred P. Sloan Foundation for a Sloan Research Fellowship (FG-2023-20341).

ABBREVIATIONS

OECD, Organization for Economic Co-operation and Development; ROP, ring-opening polymerization; CM, cross-metathesis; RCM, ring-closing metathesis; ROM, ring-opening metathesis; ROMP, ring-opening metathesis polymerization; ADMET, acyclic diene metathesis; RSE, ring strain energy; G1, Grubbs first-generation catalyst; G2, Grubbs second-generation catalyst; G3, Grubbs third-generation catalyst; HG1, Hoveyda–Grubbs first-generation catalyst; HG2, Hoveyda–Grubbs second-generation catalyst; DFT, density functional theory; T_g , glass transition temperature; T_d , decomposition onset temperature corresponding to 5% weight loss; DSC, differential scanning calorimetry; DFT, density functional theory; VT, variable temperature; NMR, nuclear magnetic resonance; PS, polystyrene; PMMA, poly(methyl methacrylate); tCBO, *trans*-cyclobutane fused cyclooctene; PEG,

poly(ethylene glycol); D_h , hydrodynamic diameter; PLLA, poly-L-lactide; DCM, dichloromethane; HDIB, hexamethylene diisocyanate; CAM, cross alkane metathesis; CTA, chain transfer agent; HDPE, high density polyethylene; M_n , number-average molecular weight; M_w , weight-average molecular weight; DP, degree of polymerization; DIE, dehydrogenation and isomerizing ethenolysis; I/E, isomerizing ethenolysis; CPE, chlorinated polyethylene; PVC, polyvinyl chloride; GC-MS, gas chromatography-mass spectrometry; BPE, brominated polyethylene; COD, 1,5-cyclooctadiene; CDT, cyclododeca- triene; NHC, *N*-heterocyclic carbene; DAB, *cis*-1,4-diacetoxy-2-butene; FD, fragmentation degradation; FCD, fragmentation followed by continuous depolymerization; ECD, end-to-end continuous depolymerization

REFERENCES

- (1) *Current Plastics Lifecycle Is Far from Circular*. Organisation for Economic Co-operation and Development. 2022. <https://www.oecd.org/environment/plastics/plastics-lifecycle-is-far-from-circular.htm> (accessed 2023 5–5–2023).
- (2) Hundertmark, T.; Mayer, M.; McNally, C.; Simons, T. J.; Witte, C. How plastics-waste recycling can transform the chemical industry. McKinsey & Company. 2018. <https://www.mckinsey.com/industries/chemicals/our-insights/how-plastics-waste-recycling-could-transform-the-chemical-industry#/> (accessed 1–26–2024).
- (3) Schyns, Z. O. G.; Shaver, M. P. Mechanical Recycling of Packaging Plastics: A Review. *Macromol. Rapid Commun.* **2021**, *42*, 2000415.
- (4) Kosloski-Oh, S. C.; Wood, Z. A.; Manjarrez, Y.; de los Rios, J. P.; Fieser, M. E. Catalytic Methods for Chemical Recycling or Upcycling of Commercial polymers. *Mater. Horiz.* **2021**, *8*, 1084–1129.
- (5) Yeung, C. W. S.; Teo, J. Y. Q.; Loh, X. J.; Lim, J. Y. C. Polyolefins and Polystyrene as Chemical Resources for a Sustainable Future: Challenges, Advances, and Prospects. *ACS Mater. Lett.* **2021**, *3*, 1660–1676.
- (6) Conk, R. J.; Hanna, S.; Shi, J. X.; Yang, J.; Ciccia, N. R.; Qi, L.; Bloomer, B. J.; Heuvel, S.; Wills, T.; Su, J.; et al. Catalytic Deconstruction of waste polyethylene with Ethylene to form Propylene. *Science* **2022**, *377*, 1561–1566.
- (7) Arroyave, A.; Cui, S.; Lopez, J. C.; Kocen, A. L.; LaPointe, A. M.; Delferro, M.; Coates, G. W. Catalytic Chemical Recycling of Post-Consumer Polyethylene. *J. Am. Chem. Soc.* **2022**, *144*, 23280–23285.
- (8) Fazekas, T. J.; Alty, J. W.; Neidhart, E. K.; Miller, A. S.; Leibfarth, F. A.; Alexanian, E. J. Diversification Of Aliphatic C-H Bonds In Small Molecules And Polyolefins Through Radical Chain Transfer. *Science* **2022**, *375*, 545–550.
- (9) Oh, S.; Stache, E. E. Chemical Upcycling of Commercial Polystyrene via Catalyst-Controlled Photooxidation. *J. Am. Chem. Soc.* **2022**, *144*, 5745–5749.
- (10) Huang, Z.; Shanmugam, M.; Liu, Z.; Brookfield, A.; Bennett, E. L.; Guan, R.; Vega Herrera, D. E.; Lopez-Sanchez, J. A.; Slater, A. G.; McInnes, E. J. L.; et al. Chemical Recycling of Polystyrene to Valuable Chemicals via Selective Acid-Catalyzed Aerobic Oxidation under Visible Light. *J. Am. Chem. Soc.* **2022**, *144*, 6532–6542.
- (11) Xu, Z.; Pan, F.; Sun, M.; Xu, J.; Munyanze, N. E.; Croft, Z. L.; Cai, G.; Liu, G. Cascade Degradation and Upcycling of Polystyrene waste to High-Value Chemicals. *Proc. Natl. Acad. Sci. U. S. A.* **2022**, *119*, No. e2203346119.
- (12) Zakharyan, E. M.; Petrukhina, N. N.; Maksimov, A. L. Pathways of Chemical Recycling of Polyvinyl Chloride: Part 1. *Russ. J. Appl. Chem.* **2020**, *93*, 1271–1313.
- (13) Zakharyan, E. M.; Petrukhina, N. N.; Dzhabarov, E. G.; Maksimov, A. L. Pathways of Chemical Recycling of Polyvinyl Chloride. Part 2. *Russ. J. Appl. Chem.* **2020**, *93*, 1445–1490.
- (14) Chazovachii, P. T.; Somers, M. J.; Robo, M. T.; Collias, D. I.; James, M. I.; Marsh, E. N. G.; Zimmerman, P. M.; Alfaro, J. F.; McNeil, A. J. Giving Superabsorbent Polymers a Second Life as Pressure-Sensitive Adhesives. *Nat. Commun.* **2021**, *12*, 4524.
- (15) Jones, G. R.; Wang, H. S.; Parkatzidis, K.; Whitfield, R.; Truong, N. P.; Anastasaki, A. Reversed Controlled Polymerization (RCP): Depolymerization from Well-Defined Polymers to Monomers. *J. Am. Chem. Soc.* **2023**, *145*, 9898–9915.
- (16) Xu, G.; Wang, Q. Chemically Recyclable Polymer Materials: Polymerization and Depolymerization cycles. *Green Chem.* **2022**, *24*, 2321–2346.
- (17) Zheng, N.; Xu, Y.; Zhao, Q.; Xie, T. Dynamic Covalent Polymer Networks: A Molecular Platform for Designing Functions beyond Chemical Recycling and Self-Healing. *Chem. Rev.* **2021**, *121*, 1716–1745.
- (18) Coates, G. W.; Getzler, Y. D. Y. L. Chemical Recycling to Monomer for an Ideal, Circular Polymer Economy. *Nat. Rev. Mater.* **2020**, *5*, 501–516.
- (19) Zhu, J.-B.; Watson, E. M.; Tang, J.; Chen, E. Y.-X. A Synthetic Polymer System with Repeatable Chemical recyclability. *Science* **2018**, *360*, 398–403.
- (20) Hong, M.; Chen, E. Y. X. Completely Recyclable Biopolymers with Linear and Cyclic Topologies via Ring-Opening Polymerization of γ -Butyrolactone. *Nat. Chem.* **2016**, *8*, 42–49.
- (21) Häußler, M.; Eck, M.; Rothauer, D.; Mecking, S. Closed-Loop Recycling of Polyethylene-like Materials. *Nature* **2021**, *590*, 423–427.
- (22) Xiong, W.; Chang, W.; Shi, D.; Yang, L.; Tian, Z.; Wang, H.; Zhang, Z.; Zhou, X.; Chen, E. Q.; Lu, H. Gemini Dimethyl Substitution Enables Controlled Polymerization of Penicillamine-Derived β -Thiolactones and Reversed Depolymerization. *Chem.* **2020**, *6*, 1831–1843.
- (23) Yuan, J.; Xiong, W.; Zhou, X.; Zhang, Y.; Shi, D.; Li, Z.; Lu, H. 4-Hydroxyproline-Derived Sustainable Polythioesters: Controlled Ring-Opening Polymerization, Complete Recyclability, and Facile Functionalization. *J. Am. Chem. Soc.* **2019**, *141*, 4928–4935.
- (24) Shi, C.; McGraw, M. L.; Li, Z.-C.; Cavallo, L.; Falivene, L.; Chen, E. Y. X. High-Performance Pan-Tactic Polythioesters with Intrinsic Crystallinity and Chemical Recyclability. *Sci. Adv.* **2020**, *6*, No. eabc0495.
- (25) Abel, B. A.; Snyder, R. L.; Coates, G. W. Chemically Recyclable Thermoplastics from Reversible-Deactivation Polymerization of Cyclic Acetals. *Science* **2021**, *373*, 783–789.
- (26) Hester, H. G.; Abel, B. A.; Coates, G. W. Ultra-High-Molecular-Weight Poly(Dioxolane): Enhancing the Mechanical Performance of a Chemically Recyclable Polymer. *J. Am. Chem. Soc.* **2023**, *145*, 8800–8804.
- (27) Liu, Y.; Jia, Y.; Wu, Q.; Moore, J. S. Architecture-Controlled Ring-Opening Polymerization for Dynamic Covalent Poly(disulfide)s. *J. Am. Chem. Soc.* **2019**, *141*, 17075–17080.
- (28) Neary, W. J.; Isaia, T. A.; Kennemur, J. G. Depolymerization of Bottlebrush Polypentenamers and their Macromolecular Metamorphosis. *J. Am. Chem. Soc.* **2019**, *141*, 14220–14229.
- (29) Feist, J. D.; Xia, Y. Enol Ethers Are Effective Monomers for Ring-Opening Metathesis Polymerization: Synthesis of Degradable and Depolymerizable Poly(2,3-dihydrofuran). *J. Am. Chem. Soc.* **2020**, *142*, 1186–1189.
- (30) Sathe, D.; Zhou, J.; Chen, H.; Su, H.-W.; Xie, W.; Hsu, T.-G.; Schrage, B. R.; Smith, T.; Ziegler, C. J.; Wang, J. Olefin Metathesis-Based Chemically Recyclable Polymers Enabled by Fused-Ring Monomers. *Nat. Chem.* **2021**, *13*, 743–750.
- (31) Grubbs, R. H. Olefin metathesis. *Tetrahedron* **2004**, *60* (34), 7117–7140.
- (32) Slugovc, C. Synthesis of Homopolymers and Copolymers. *Handbook of Metathesis* **2015**, 1–23.
- (33) Jenkins, A.; Kratochvíl, P.; Stepto, R.; Suter, U. Glossary of Basic Terms in Polymer Science (IUPAC Recommendations 1996). *Pure Appl. Chem.* **1996**, *68*, 2287–2311.
- (34) Sun, H.; Liang, Y.; Thompson, M. P.; Gianneschi, N. C. Degradable Polymers via Olefin Metathesis Polymerization. *Prog. Polym. Sci.* **2021**, *120*, 101427.

(35) Zhang, L.-J.; Deng, X.-X.; Du, F.-S.; Li, Z.-C. Chemical Synthesis of Functional Poly (4-hydroxybutyrate) with Controlled Degradation via Intramolecular Cyclization. *Macromolecules* **2013**, *46*, 9554–9562.

(36) Cederholm, L.; Wohlert, J.; Olsen, P.; Hakkarainen, M.; Odelius, K. "Like Recycles Like": Selective Ring-Closing Depolymerization of Poly(L-Lactic Acid) to L-Lactide. *Angew. Chem., Int. Ed.* **2022**, *61* (33), No. e202204531.

(37) Jean-Louis Hérisson, P.; Chauvin, Y. Catalyse de Transformation des Oléfines par les Complexes du Tungstène. II. Téromérisation des Oléfines Cycliques en Présence d'oléfines Acycliques. *Makromol. Chem.* **1971**, *141*, 161–176.

(38) Odian, G. Ring-Opening Polymerization. In *Principles of Polymerization*, 4 ed.; John Wiley & Sons, Inc., 2004; pp 544–618.

(39) Chatterjee, A. K.; Choi, T.-L.; Sanders, D. P.; Grubbs, R. H. A General Model for Selectivity in Olefin Cross Metathesis. *J. Am. Chem. Soc.* **2003**, *125*, 11360–11370.

(40) Duda, A.; Kowalski, A. Thermodynamics and Kinetics of Ring-Opening Polymerization. *Handbook of Ring-Opening Polymerization* **2009**, 1–51.

(41) Dainton, F. S.; Devlin, T. R. E.; Small, P. A. The Thermodynamics of Polymerization of Cyclic Compounds by Ring Opening. *Trans. Faraday Soc.* **1955**, *51*, 1710–1720.

(42) Neary, W. J.; Kennemur, J. G. Polypentenamer Renaissance: Challenges and Opportunities. *ACS Macro Lett.* **2019**, *8*, 46–56.

(43) Chen, Z.-R.; Claverie, J. P.; Grubbs, R. H.; Kornfield, J. A. Modeling Ring-Chain Equilibria in Ring-Opening Polymerization of Cycloolefins. *Macromolecules* **1995**, *28*, 2147–2154.

(44) Schleyer, P. v. R.; Williams, J. E.; Blanchard, K. R. Evaluation of Strain in Hydrocarbons. The Strain in Adamantane and its Origin. *J. Am. Chem. Soc.* **1970**, *92*, 2377–2386.

(45) Allinger, N. L.; Sprague, J. T. Conformational Analysis. LXXXIV. Study of the Structures and Energies of Some Alkenes and Cycloalkenes by the Force Field Method. *J. Am. Chem. Soc.* **1972**, *94*, 5734–5747.

(46) Patton, P. A.; Lillya, C. P.; McCarthy, T. J. Olefin Metathesis of Cyclohexene. *Macromolecules* **1986**, *19*, 1266–1268.

(47) Anslyn, E. V.; Dougherty, D. A. *Modern Physical Organic Chemistry*; University Science Books, 2005.

(48) Monfette, S.; Fogg, D. E. Equilibrium Ring-Closing Metathesis. *Chem. Rev.* **2009**, *109*, 3783–3816.

(49) Ivin, K. J.; Mol, J. C. *Olefin Metathesis and Metathesis Polymerization*; Academic Press, 1997.

(50) Strandman, S.; Gautrot, J. E.; Zhu, X. X. Recent Advances in Entropy-Driven Ring-Opening Polymerizations. *Polym. Chem.* **2011**, *2*, 791–799.

(51) Jung, M. E.; Piuzzi, G. gem-Disubstituent Effect: Theoretical Basis and Synthetic Applications. *Chem. Rev.* **2005**, *105*, 1735–1766.

(52) Forbes, M. D. E.; Patton, J. T.; Myers, T. L.; Maynard, H. D.; Smith, D. W., Jr.; Schulz, G. R.; Wagener, K. B. Solvent-Free Cyclization of Linear dienes using Olefin Metathesis and the Thorpe-Ingold Effect. *J. Am. Chem. Soc.* **1992**, *114*, 10978–10980.

(53) Ofstead, E. A.; Calderon, N. Equilibrium ring-opening Polymerization of Mono- and Multicyclic Unsaturated Monomers. *Makromol. Chem.* **1972**, *154*, 21–34.

(54) Kranz, V. D.; Beck, M. Polymerisationsenthalpie der Ring-öffnenden Polymerisation von Cyclopenten (CPE) zu Trans-Polypentenamer (TPR). *Angew. Makromol. Chem.* **1972**, *27*, 29–35.

(55) Korshak, Y. V.; Tlenkopatchev, M. A.; Dolgoplosk, B. A.; Avdeikina, E. G.; Kutepov, D. F. Intra- and Intermolecular Metathesis Reactions in the Formation and Degradation of Unsaturated Polymers. *J. Mol. Catal.* **1982**, *15*, 207–218.

(56) Badamshina, E. R.; Timofeyeva, G. I.; Korshak, Y. V.; Berlin, A. A.; Vdovin, V. M.; Kutepov, D. F.; Pavlova, S. S. A. Investigation of the Mechanism of Polypentenamer Degradation in the Presence of Metathesis Catalysts. *Polym. Sci. (U.S.S.R.)* **1982**, *24*, 164–170.

(57) Tuba, R.; Grubbs, R. H. Ruthenium Catalyzed Equilibrium Ring-Opening Metathesis Polymerization of Cyclopentene. *Polym. Chem.* **2013**, *4*, 3959–3962.

(58) Yoon, K.-Y.; Noh, J.; Gan, Q.; Edwards, J. P.; Tuba, R.; Choi, T.-L.; Grubbs, R. H. Scalable and Continuous Access to Pure Cyclic Polymers Enabled by 'Quarantined' Heterogeneous Catalysts. *Nat. Chem.* **2022**, *14*, 1242–1248.

(59) Tuba, R.; Balogh, J.; Hlil, A.; Barlög, M.; Al-Hashimi, M.; Bazzi, H. S. Synthesis of Recyclable Tire Additives via Equilibrium Ring-Opening Metathesis Polymerization. *ACS Sus. Chem. Eng.* **2016**, *4*, 6090–6094.

(60) Liu, H.; Nelson, A. Z.; Ren, Y.; Yang, K.; Ewoldt, R. H.; Moore, J. S. Dynamic Remodeling of Covalent Networks via Ring-Opening Metathesis Polymerization. *ACS Macro Lett.* **2018**, *7*, 933–937.

(61) Neary, W. J.; Fultz, B. A.; Kennemur, J. G. Well-Defined and Precision-Grafted Bottlebrush Polypentenamers from Variable Temperature ROMP and ATRP. *ACS Macro Lett.* **2018**, *7*, 1080–1086.

(62) Neary, W. J.; Kennemur, J. G. Variable Temperature ROMP: Leveraging Low Ring Strain Thermodynamics To Achieve Well-Defined Polypentenamers. *Macromolecules* **2017**, *50*, 4935–4941.

(63) Guillory, G. A.; Kennemur, J. G. Investigating the Effects of Bulky Allylic Substituents on the Regioregularity and Thermodynamics of ROMP on Cyclopentene. *Eur. Polym. J.* **2019**, *120*, 109251.

(64) Hilf, S.; Kilbinger, A. F. M. Functional End Groups for Polymers Prepared using Ring-Opening Metathesis Polymerization. *Nat. Chem.* **2009**, *1*, 537–546.

(65) Schwab, P.; Grubbs, R. H.; Ziller, J. W. Synthesis and Applications of RuCl₂(CH₃)₂(PR₃)₂: The Influence of the Alkylidene Moiety on Metathesis Activity. *J. Am. Chem. Soc.* **1996**, *118*, 100–110.

(66) Hsu, T.-G.; Liu, S.; Guan, X.; Yoon, S.; Zhou, J.; Chen, W.-Y.; Gaire, S.; Seylar, J.; Chen, H.; Wang, Z.; et al. Mechanochemically Accessing a Challenging-to-Synthesize Depolymerizable Polymer. *Nat. Commun.* **2023**, *14*, 225.

(67) Hejl, A.; Scherman, O. A.; Grubbs, R. H. Ring-Opening Metathesis Polymerization of Functionalized Low-Strain Monomers with Ruthenium-Based Catalysts. *Macromolecules* **2005**, *38*, 7214–7218.

(68) Kress, J. Cyclization of Living Polyalkenamers via Intramolecular Secondary Metathesis. Dimerization of Cycloheptene into Cyclotetradeca-1,8-diene Initiated by well-defined tungsten-carbene catalysts. *J. Mol. Catal. A Chem.* **1995**, *102*, 7–21.

(69) Fraser, C.; Hillmyer, M. A.; Gutierrez, E.; Grubbs, R. H. Degradable Cyclooctadiene/Acetal Copolymers: Versatile Precursors to 1,4-Hydroxytelechelic Polybutadiene and Hydroxytelechelic Polyethylene. *Macromolecules* **1995**, *28*, 7256–7261.

(70) Boadi, F. O.; Zhang, J.; Yu, X.; Bhatia, S. R.; Sampson, N. S. Alternating Ring-Opening Metathesis Polymerization Provides Easy Access to Functional and Fully Degradable Polymers. *Macromolecules* **2020**, *53*, 5857–5868.

(71) Johnson, A. M.; Husted, K. E. L.; Kilgallon, L. J.; Johnson, J. A. Orthogonally Deconstructable and Depolymerizable Polysilylethers via Entropy-Driven Ring-Opening Metathesis Polymerization. *Chem. Commun.* **2022**, *58*, 8496–8499.

(72) Martinez, H.; Ren, N.; Matta, M. E.; Hillmyer, M. A. Ring-Opening Metathesis Polymerization of 8-Membered Cyclic Olefins. *Polym. Chem.* **2014**, *5*, 3507–3532.

(73) Scherman, O. A.; Walker, R.; Grubbs, R. H. Synthesis and Characterization of Stereoregular Ethylene-Vinyl Alcohol Copolymers Made by Ring-Opening Metathesis Polymerization. *Macromolecules* **2005**, *38*, 9009–9014.

(74) You, W.; Hugar, K. M.; Coates, G. W. Synthesis of Alkaline Anion Exchange Membranes with Chemically Stable Imidazolium Cations: Unexpected Cross-Linked Macrocycles from Ring-Fused ROMP Monomers. *Macromolecules* **2018**, *51*, 3212–3218.

(75) Sathe, D.; Zhou, J.; Chen, H.; Schrage, B. R.; Yoon, S.; Wang, Z.; Ziegler, C. J.; Wang, J. Depolymerizable Semi-Fluorinated Polymers for Sustainable Functional Materials. *Polym. Chem.* **2022**, *13*, 2608–2614.

(76) Zhou, J.; Sathe, D.; Wang, J. Understanding the Structure-Polymerization Thermodynamics Relationships of Fused-Ring Cyclo-

octenes for Developing Chemically Recyclable Polymers. *J. Am. Chem. Soc.* **2022**, *144*, 928–934.

(77) Sathe, D.; Chen, H.; Wang, J. Regulating the Thermodynamics and Thermal Properties of Depolymerizable Polyclooctenes through Substituent Effects. *Macromol. Rapid Commun.* **2023**, *44*, 2200304.

(78) Su, H.-W.; Zhou, J.; Yoon, S.; Wang, J. Evaluating Trans-Benzocyclobutene-Fused Cyclooctene as a Monomer for Chemically Recyclable Polymer. *Chem.—Asian J.* **2023**, *18*, No. e202201133.

(79) Chen, H.; Shi, Z.; Hsu, T. G.; Wang, J. Overcoming the Low Driving Force in Forming Depolymerizable Polymers through Monomer Isomerization. *Angew. Chem. Int. Ed.* **2021**, *60*, 25493–25498.

(80) Walker, R.; Conrad, R. M.; Grubbs, R. H. The Living ROMP of trans-Cyclooctene. *Macromolecules* **2009**, *42*, 599–605.

(81) Wang, Z.; Yoon, S.; Wang, J. Breaking the Paradox between Grafting-Through and Depolymerization to Access Recyclable Graft Polymers. *Macromolecules* **2022**, *55*, 9249–9256.

(82) Debsharma, T.; Schmidt, B.; Laschewsky, A.; Schlaad, H. Ring-Opening Metathesis Polymerization of Unsaturated Carbohydrate Derivatives: Levoglucosetyl Alkyl Ethers. *Macromolecules* **2021**, *54*, 2720–2728.

(83) Shi, C.; Clarke, R. W.; McGraw, M. L.; Chen, E. Y. X. Closing the “One Monomer-Two Polymers-One Monomer” Loop via Orthogonal (De)polymerization of a Lactone/Olefin Hybrid. *J. Am. Chem. Soc.* **2022**, *144*, 2264–2275.

(84) Lee, H.-K.; Bang, K.-T.; Hess, A.; Grubbs, R. H.; Choi, T.-L. Multiple Olefin Metathesis Polymerization That Combines All Three Olefin Metathesis Transformations: Ring-Opening, Ring-Closing, and Cross Metathesis. *J. Am. Chem. Soc.* **2015**, *137*, 9262–9265.

(85) Lee, H.-K.; Lee, J.; Kockelmann, J.; Herrmann, T.; Sarif, M.; Choi, T.-L. Superior Cascade Ring-Opening/Ring-Closing Metathesis Polymerization and Multiple Olefin Metathesis Polymerization: Enhancing the Driving Force for Successful Polymerization of Challenging Monomers. *J. Am. Chem. Soc.* **2018**, *140*, 10536–10545.

(86) Kamau, S. D.; Hodge, P.; Hall, A. J.; Dad, S.; Ben-Haida, A. Cyclo-Depolymerization of Olefin-Containing Polymers to Give Macroyclic Oligomers by Metathesis and the Entropically-driven ROMP of the Olefin-Containing Macroyclic Esters. *Polymer* **2007**, *48*, 6808–6822.

(87) Yuan, J.; Giardino, G. J.; Niu, J. Metathesis Cascade-Triggered Depolymerization of Enyne Self-Immulative Polymers. *Angew. Chem. Int. Ed.* **2021**, *60*, 24800–24805.

(88) Jones, B. H.; Staiger, C.; Powers, J.; Herman, J. A.; Román-Kustas, J. Selectively Depolymerizable Polyurethanes from Unsaturated Polyols Cleavable by Olefin Metathesis. *Macromol. Rapid Commun.* **2021**, *42*, 2000571.

(89) Hummel, K.; Streck, R.; Weber, H. Abbau von Vulkanisaten mit Isomerisierungs-Katalysatoren. *Naturwissenschaften* **1970**, *57*, 194–195.

(90) Hummel, K. Polymer Degradation by Cross Metathesis. *Pure Appl. Chem.* **1982**, *54*, 351–364.

(91) Streck, R. Some Applications of the Olefin Metathesis Reaction to Polymer Synthesis. *J. Mol. Catal.* **1982**, *15*, 3–19.

(92) Hummel, K. Application of Olefin Metathesis to the Investigation of Polymer Structures. *J. Mol. Catal.* **1985**, *28*, 381–392.

(93) Soares, F. A.; Steinbüchel, A. Natural Rubber Degradation Products: Fine Chemicals and Reuse of Rubber Waste. *Eur. Polym. J.* **2022**, *165*, 111001.

(94) Thorn-Csányi, E.; Perner, H. Quantitative Microstructure Determination of Diene Polymers by Means of Metathesis Degradation. *J. Mol. Catal.* **1986**, *36*, 187–199.

(95) Lapinte, V.; Fontaine, L.; Montembault, V.; Campistron, I.; Reyx, D. Ring-Opening Metathesis Polymerization (ROMP) of Isomerically Pure Functional Monomers and Acyclic Diene Metathesis Depolymerization (retro-ADMET) of Functionalized Poly-alkenamers. *J. Mol. Catal. A Chem.* **2002**, *190*, 117–129.

(96) Fainleib, A.; Pires, R. V.; Lucas, E. F.; Soares, B. G. Degradation of non-Vulcanized Natural Rubber - renewable resource for fine chemicals used in polymer synthesis. *Polímeros* **2014**, *23*, 441.

(97) Leimgruber, S.; Trimmel, G. Olefin Metathesis Meets Rubber Chemistry and Technology. *Monstsh. Chem.* **2015**, *146*, 1081–1097.

(98) Bidange, J.; Fischmeister, C.; Bruneau, C. Ethenolysis: A Green Catalytic Tool to Cleave Carbon-Carbon Double Bonds. *Chem.—Eur. J.* **2016**, *22*, 12226–12244.

(99) Liu, P.; Ai, C. Olefin Metathesis Reaction in Rubber Chemistry and Industry and Beyond. *Ind. Eng. Chem. Res.* **2018**, *57*, 3807–3820.

(100) Hassanian-Moghaddam, D.; Asghari, N.; Ahmadi, M. Circular Polyolefins: Advances toward a Sustainable Future. *Macromolecules* **2023**, *56*, 5679–5697.

(101) Goldman, A. S.; Roy, A. H.; Huang, Z.; Ahuja, R.; Schinski, W.; Brookhart, M. Catalytic Alkane Metathesis by Tandem Alkane Dehydrogenation-Olefin Metathesis. *Science* **2006**, *312*, 257–261.

(102) Jia, X.; Qin, C.; Friedberger, T.; Guan, Z.; Huang, Z. Efficient and Selective Degradation of Polyethylenes into Liquid Fuels and Waxes under Mild Conditions. *Sci. Adv.* **2016**, *2*, No. e1501591.

(103) Ellis, L. D.; Orski, S. V.; Kenlaw, G. A.; Norman, A. G.; Beers, K. L.; Román-Leshkov, Y.; Beckham, G. T. Tandem Heterogeneous Catalysis for Polyethylene Depolymerization via an Olefin-Intermediate Process. *ACS Sus. Chem. Eng.* **2021**, *9*, 623–628.

(104) Kim, D.; Hinton, Z. R.; Bai, P.; Korley, L. T. J.; Epps, T. H.; Lobo, R. F. Metathesis, Molecular Redistribution of Alkanes, and the Chemical Upgrading of Low-Density Polyethylene. *Appl. Catal., B* **2022**, *318*, 121873.

(105) Guirionnet, D.; Peters, B. Tandem Catalysts for Polyethylene Upcycling: A Simple Kinetic Model. *J. Phys. Chem. A* **2020**, *124* (19), 3935–3942.

(106) Wang, N. M.; Strong, G.; DaSilva, V.; Gao, L.; Huacuja, R.; Konstantinov, I. A.; Rosen, M. S.; Nett, A. J.; Ewart, S.; Geyer, R.; et al. Chemical Recycling of Polyethylene by Tandem Catalytic Conversion to Propylene. *J. Am. Chem. Soc.* **2022**, *144*, 18526–18531.

(107) Glas, D.; Hulsbosch, J.; Dubois, P.; Binnemans, K.; De Vos, D. E. End-of-Life Treatment of Poly(Vinyl Chloride) and Chlorinated Polyethylene by Dehydrochlorination in Ionic Liquids. *ChemSusChem* **2014**, *7*, 610–617.

(108) Zeng, M.; Lee, Y.-H.; Strong, G.; LaPointe, A. M.; Kocen, A. L.; Qu, Z.; Coates, G. W.; Scott, S. L.; Abu-Omar, M. M. Chemical Upcycling of Polyethylene to Value-Added α,ω -Divinyl-Functionalized Oligomers. *ACS Sus. Chem. Eng.* **2021**, *9*, 13926–13936.

(109) Watson, M. D.; Wagener, K. B. Solvent-Free Olefin Metathesis Depolymerization of 1,4-Polybutadiene. *Macromolecules* **2000**, *33*, 1494–1496.

(110) Dewaele, A.; Renders, T.; Yu, B.; Verpoort, F.; Sels, B. F. Depolymerization of 1,4-Polybutadiene by Metathesis: High Yield of Large Macroyclic Oligo(Butadiene)s by Ligand Selectivity Control. *Cata. Sci. Technol.* **2016**, *6*, 7708–7717.

(111) Thorn-Csányi, E.; Ruhland, K. Quantitative Description of the Metathesis Polymerization/Depolymerization Equilibrium in the 1,4-Polybutadiene System, 1. Influence of Feed Concentration and Temperature. *Macromol. Chem. Phys.* **1999**, *200*, 1662–1671.

(112) Chauvin, Y.; Commereuc, D.; Zaborowski, G. Catalysis of Olefin Transformation by Tungsten Complexes, 6. Equilibrium Oligomer Concentration in the Polymerization of 1,5-Cyclooctadiene. *Makromol. Chem.* **1978**, *179*, 1285–1290.

(113) Thorn-Csányi, E.; Ruhland, K. ROMP of COD Under Equilibrium Conditions: the Turning Point Concept. *Macromol. Symp.* **2000**, *153*, 145–150.

(114) Thorn-Csányi, E.; Ruhland, K. Quantitative Description of the Metathesis Polymerization/Depolymerization Equilibrium in the 1,4-Polybutadiene System, 2. Unusual Behaviour at Lower Temperature. *Macromol. Chem. Phys.* **1999**, *200*, 2245–2249.

(115) Schrock, R. R.; Yap, K. B.; Yang, D. C.; Sitzmann, H.; Sita, L. R.; Bazan, G. C. Evaluation of Cyclopentene-Based Chain-Transfer Agents for Living Ring-Opening Metathesis Polymerization. *Macromolecules* **1989**, *22*, 3191–3200.

(116) Torre, M.; Mulhearn, W. D.; Register, R. A. Ring-Opening Metathesis Copolymerization of Cyclopentene Above and Below Its Equilibrium Monomer Concentration. *Macromol. Chem. Phys.* **2018**, *219*, 1800030.

(117) Sadaka, F.; Campistron, I.; Laguerre, A.; Pilard, J.-F. Telechelic Oligomers Obtained by Metathetic Degradation of both Polyisoprene and Styrene-Butadiene Rubbers. Applications for Recycling Waste Tyre Rubber. *Polym. Degrad. Stab.* **2013**, *98*, 736–742.

(118) Mouawia, A.; Nourry, A.; Gaumont, A.-C.; Pilard, J.-F.; Dez, I. Controlled Metathetic Depolymerization of Natural Rubber in Ionic Liquids: From Waste Tires to Telechelic Polyisoprene Oligomers. *ACS Sus. Chem. Eng.* **2017**, *5*, 696–700.

(119) Saetung, N.; Campistron, I.; Pascual, S.; Pilard, J.-F.; Fontaine, L. One-Pot Synthesis of Natural Rubber-Based Telechelic cis-1,4-Polyisoprenes and Their Use To Prepare Block Copolymers by RAFT Polymerization. *Macromolecules* **2011**, *44*, 784–794.

(120) Solanky, S. S.; Campistron, I.; Laguerre, A.; Pilard, J.-F. Metathetic Selective Degradation of Polyisoprene: Low-Molecular-Weight Telechelic Oligomer Obtained from Both Synthetic and Natural Rubber. *Macromol. Chem. Phys.* **2005**, *206*, 1057–1063.

(121) Jiang, B.; Wei, T.; Zou, T.-T.; Rempel, G. L.; Pan, Q.-M. A Novel Approval for Degradation of Polybutadiene and Synthesis of Diene-Based Telechelic Oligomers via Olefin Cross Metathesis. *Macromol. React. Eng.* **2015**, *9*, 480–489.

(122) Patil, V. B.; Saliu, K. O.; Jenkins, R. M.; Carnahan, E. M.; Kramer, E. J.; Fredrickson, G. H.; Bazan, G. C. Efficient Synthesis of α,ω -Divinyl-Functionalized Polyolefins. *Macromol. Chem. Phys.* **2014**, *215*, 1140–1145.

(123) Smith, R. F.; Boothroyd, S. C.; Thompson, R. L.; Khosravi, E. A Facile Route for Rubber Breakdown via Cross Metathesis Reactions. *Green Chem.* **2016**, *18*, 3448–3455.

(124) Schulz, M. D.; Ford, R. R.; Wagener, K. B. Insertion metathesis depolymerization. *Polym. Chem.* **2013**, *4*, 3656–3658.

(125) Voigttritter, K.; Ghorai, S.; Lipshutz, B. H. Rate Enhanced Olefin Cross-Metathesis Reactions: The Copper Iodide Effect. *J. Org. Chem.* **2011**, *76*, 4697–4702.

(126) Gutiérrez, S.; Tlenkopatchev, M. Degradation of Natural Rubber via Cross-Metathesis with Functionalized Olefins Using Ruthenium Alkylidene Catalysts. *Revista Latinoamerica de Metalurgia y Materiales* **2009**, *1463*–1467.

(127) Feldman, J.; Murdzek, J. S.; Davis, W. M.; Schrock, R. R. Reaction of Neopentylidene Complexes of the Type M(CH-t-Bu)(N-2,6-C6H3-i-Pr2)(OR)2 (M = W, Mo) with Methyl Acrylate and N,N-dimethylacrylamide to give Metallacyclobutane Complexes. *Organometallics* **1989**, *8*, 2260–2265.

(128) Patton, J. T.; Boncella, J. M.; Wagener, K. B. Acyclic Diene Metathesis (ADMET) Polymerization: the Synthesis of Unsaturated Polyesters. *Macromolecules* **1992**, *25*, 3862–3867.

(129) Marmo, J. C.; Wagener, K. B. ADMET Depolymerization. Synthesis of Perfectly Difunctional ($f = 2.0$) Telechelic Polybutadiene Oligomers. *Macromolecules* **1995**, *28*, 2602–2606.

(130) Gutiérrez, S.; Tlenkopatchev, M. A. Metathesis of Renewable Products: Degradation of Natural Rubber via Cross-metathesis with β -pinene using Ru-alkylidene catalysts. *Polym. Bull.* **2011**, *66*, 1029–1038.

(131) Watson, M. D.; Wagener, K. B. Acyclic Diene Metathesis (ADMET) Depolymerization: Ethenolysis of 1,4-polybutadiene using a Ruthenium Complex. *J. Polym. Sci. A Polym. Chem.* **1999**, *37*, 1857–1861.

(132) Bradshaw, C.; Howman, E.; Turner, L. Olefin Dismutation: Reactions of Olefins on Cobalt Oxide-Molybdenum Oxide-Alumina. *J. Catal.* **1967**, *7*, 269–276.

(133) Marmo, J.; Wagener, K. Acyclic Diene Metathesis (ADMET) Depolymerization. Synthesis of Mass-Exact Telechelic Polybutadiene Oligomers. *Macromolecules* **1993**, *26*, 2137–2138.

(134) Wagener, K. B.; Marmo, J. C. Acyclic Diene Metathesis (ADMET) Depolymerization: The Synthesis of 1, 4-Polybutadiene Telechelics. *Macromol. Rapid Commun.* **1995**, *16*, 557–561.

(135) Lorber, F.; Hummel, K. Ein Kinetischer Effekt bei der Metathese-Reaktion von Ungesättigten Polymeren mit Niedermolekularen Olefinen. *Makromol. Chem.* **1973**, *171*, 257–260.

(136) Kocen, A. L.; Cui, S.; Lin, T.-W.; LaPointe, A. M.; Coates, G. W. Chemically Recyclable Ester-Linked Polypropylene. *J. Am. Chem. Soc.* **2022**, *144*, 12613–12618.

(137) Herman, J. A.; Seazzo, M. E.; Hughes, L. G.; Wheeler, D. R.; Washburn, C. M.; Jones, B. H. Depolymerization of Cross-Linked Polybutadiene Networks in situ using Latent Alkene Metathesis. *ACS Appl. Polym. Mater.* **2019**, *1*, 2177–2188.

(138) Haibach, M. C.; Kundu, S.; Brookhart, M.; Goldman, A. S. Alkane Metathesis by Tandem Alkane-Dehydrogenation-olefin-metathesis catalysis and related Chemistry. *Acc. Chem. Res.* **2012**, *45*, 947–958.

(139) Berlin, A. A.; Volfson, S. A.; Enikolopian, N. S. Kinetics of Polymerization Processes in. *Polymerization Processes* **1981**, *38*, 89–140.

(140) Sagi, A.; Weinstein, R.; Karton, N.; Shabat, D. Self-Immulative Polymers. *J. Am. Chem. Soc.* **2008**, *130*, 5434–5435.

(141) Peterson, G. I.; Larsen, M. B.; Boydston, A. J. Controlled Depolymerization: Stimuli-Responsive Self-Immulative Polymers. *Macromolecules* **2012**, *45*, 7317–7328.

(142) Roth, M. E.; Green, O.; Gnaim, S.; Shabat, D. Dendritic, Oligomeric, and Polymeric Self-Immulative Molecular Amplification. *Chem. Rev.* **2016**, *116*, 1309–1352.

(143) Xiao, Y.; Li, H.; Zhang, B.; Cheng, Z.; Li, Y.; Tan, X.; Zhang, K. Modulating the Depolymerization of Self-Immulative Brush Polymers with Poly (benzyl ether) Backbones. *Macromolecules* **2018**, *51*, 2899–2905.

(144) Gnaim, S.; Shabat, D. Self-immulative Chemiluminescence Polymers: Innate Assimilation of Chemiexcitation in a Domino-like Depolymerization. *J. Am. Chem. Soc.* **2017**, *139*, 10002–10008.

(145) Wong, A. D.; DeWit, M. A.; Gillies, E. R. Amplified Release through the Stimulus Triggered Degradation of Self-Immulative Oligomers, Dendrimers, and Linear Polymers. *Adv. Drug Delivery Rev.* **2012**, *64*, 1031–1045.

(146) Kobayashi, S.; Pitet, L. M.; Hillmyer, M. A. Regio- and Stereoselective Ring-Opening Metathesis Polymerization of 3-Substituted Cyclooctenes. *J. Am. Chem. Soc.* **2011**, *133*, 5794–5797.

(147) Sita, L. R. Main-Chain Chiral Polymers from beta-Citronellene via Tandem Diene Metathesis Cyclization/Ring-Opening Metathesis Polymerization. *Macromolecules* **1995**, *28*, 656–657.

(148) Brits, S.; Neary, W. J.; Palui, G.; Kennemur, J. G. A New Echelon of Precision Polypentenamers: Highly Isotactic Branching on Every Five Carbons. *Polym. Chem.* **2018**, *9*, 1719–1727.

(149) Khan, R. K. M.; Torker, S.; Hoveyda, A. H. Readily Accessible and Easily Modifiable Ru-Based Catalysts for Efficient and Z-Selective Ring-Opening Metathesis Polymerization and Ring-Opening/Cross-Metathesis. *J. Am. Chem. Soc.* **2013**, *135*, 10258–10261.

(150) Montgomery, T. P.; Grandner, J. M.; Houk, K. N.; Grubbs, R. H. Synthesis and Evaluation of Sterically Demanding Ruthenium Dithiolate Catalysts for Stereoretentive Olefin Metathesis. *Organometallics* **2017**, *36*, 3940–3953.

(151) Osawa, K.; Kobayashi, S.; Tanaka, M. Synthesis of Sequence-Specific Polymers with Amide Side Chains via Regio-/Stereoselective Ring-Opening Metathesis Polymerization of 3-Substituted cis-Cyclooctene. *Macromolecules* **2016**, *49*, 8154–8161.

(152) Li, M.; Cui, F.; Li, Y.; Tao, Y.; Wang, X. Crystalline Regio-/Stereoregular Glycine-Bearing Polymers from ROMP: Effect of Microstructures on Materials Performances. *Macromolecules* **2016**, *49*, 9415–9424.

(153) Coia, B. M.; Werner, S. E.; Kennemur, J. G. Conformational Bias in Density Functional Theory Ring Strain Energy Calculations of Cyclopentene Derivatives: Towards Predictive Design of Chemically Recyclable Elastomers. *J. Polym. Sci.* **2022**, *60*, 3391–3403.

(154) Coia, B. M.; Hudson, L. A.; Specht, A. J., III; Kennemur, J. G. Substituent Effects on Torsional Strain in Cyclopentene Derivatives: A Computational Study. *J. Phys. Chem. A* **2023**, *127*, 5005–5017.

(155) Toland, A.; Tran, H.; Chen, L.; Li, Y.; Zhang, C.; Gutekunst, W.; Ramprasad, R. Accelerated Scheme to Predict Ring-Opening Polymerization Enthalpy: Simulation-Experimental Data Fusion and Multitask Machine Learning. *J. Phys. Chem. A* **2023**, *127*, 10709–10716.

(156) Yang, B.; Truhlar, D. G. Computational Design of an Iron Catalyst for Olefin Metathesis. *Organometallics* **2018**, *37*, 3917–3927.

(157) Belov, D. S.; Mathivathanan, L.; Beazley, M. J.; Martin, W. B.; Bukhryakov, K. V. Stereospecific Ring-Opening Metathesis Polymerization of Norbornene Catalyzed by Iron Complexes. *Angew. Chem., Int. Ed.* **2021**, *60*, 2934–2938.

(158) Takebayashi, S.; Iron, M. A.; Feller, M.; Rivada-Wheelaghan, O.; Leitus, G.; Diskin-Posner, Y.; Shimon, L. J. W.; Avram, L.; Carmieli, R.; Wolf, S. G.; et al. Iron-Catalysed Ring-Opening Metathesis Polymerization of Olefins and Mechanistic Studies. *Nat. Catal.* **2022**, *5*, 494–502.

(159) Ogawa, K. A.; Goetz, A. E.; Boydston, A. J. Metal-Free Ring-Opening Metathesis Polymerization. *J. Am. Chem. Soc.* **2015**, *137*, 1400–1403.

(160) Quach, P. K.; Hsu, J. H.; Keresztes, I.; Fors, B. P.; Lambert, T. H. Metal-Free Ring-Opening Metathesis Polymerization with Hydrazonium Initiators. *Angew. Chem., Int. Ed.* **2022**, *61*, No. e202203344.